

# When to Screen, When to Bypass: LLM-Judges in Resource-Scarce AI-Human Workflow

Ruihan Lin, Jiheng Zhang

Hong Kong University of Science and Technology, Hong Kong  
rlinah@connect.ust.hk, jiheng@ust.hk

---

**Abstract.** AI systems can generate outputs at scale, but most outputs require human approval before release. This creates a bottleneck: humans cannot keep pace with AI-generated volume. A natural response is to insert an LLM-judge that screens outputs before they reach humans, filtering errors and amplifying effective review capacity. But judges are imperfect. False rejections send correct outputs back for unnecessary rework; false acceptances consume judge capacity without relieving humans. When should outputs be routed through the judge, and when should they bypass it directly to human review? We model this workflow as a queueing network with three resource pools and use a fluid approximation to characterize optimal judge allocation. The analysis reveals that optimal allocation depends critically on which resource is the current bottleneck: screening amplifies human capacity when reviewers are scarce, yet generates a rework trap that crowds out new production when workers are stretched thin. For heterogeneous task classes with different error profiles, optimal priority can reverse across operating regimes, and classes with complementary error structures can be mixed to achieve throughput that neither class attains alone. We propose a policy that uses the fluid-optimal allocation fractions for routing and the fluid-optimal service levels for admission control, and establish its asymptotic optimality as system scale grows. Extensions incorporate human feedback that improves rework quality and joint capacity planning under budget constraints. Numerical experiments confirm rapid convergence to the fluid optimum and demonstrate that the policy significantly outperforms benchmarks that either always screen or never screen.

**Key words:** Stochastic control, Queueing network, AI-Human collaboration

---

## 1. Introduction

The path toward AI automation runs through human oversight. Organizations are rapidly deploying AI systems to handle tasks at scale: generating marketing visuals, drafting customer service responses, running automated analysis pipelines, producing code with test suites, and much more. These systems can operate continuously, process requests in parallel, and produce outputs at a pace no human team could match. Yet for all this speed, a fundamental constraint remains: most AI outputs do not go directly to end users. Instead, they pass through human reviewers who decide what gets released.

This pattern is pervasive across domains. Whether the task involves visual content creation, software development, or data analysis, the workflow follows a consistent structure: AI systems generate candidate outputs, while domain experts (designers, engineers, analysts) serve as gatekeepers who authorize final release. This division of labor reflects a basic reality of delegation: when outputs carry the organization's

name, affect customer relationships, or have downstream consequences, principals verify the work of agents before committing to it (Susarla et al. 2023).

In high-stakes domains, this human oversight becomes not just common practice but a strict requirement. Legal documents must be reviewed for compliance and liability. Medical summaries require clinician sign-off before entering patient records. Financial reports need auditor verification. Security-critical code demands human inspection before deployment. For these applications, human review is mandated by regulation, professional standards, or risk management. Yet even in routine applications without such mandates, organizations typically maintain human review as a quality gate, recognizing that AI outputs are not yet reliable enough for autonomous release.

This creates a bottleneck. AI workers can generate outputs at a pace that far exceeds human review capacity, though their own throughput remains bounded by computational resources, execution environments, or service limits. A team of human reviewers that could comfortably handle a manual workflow becomes overwhelmed when AI multiplies the volume of content requiring their attention. The promise of AI-driven productivity gains stalls at the human review stage.

A natural architectural response is to insert an LLM-judge between AI workers and human reviewers. The judge screens each worker output, rejecting those it deems low-quality back to the worker for revision, and forwarding the rest to human review. When functioning well, this intermediate layer filters out errors before they reach humans, effectively amplifying human review capacity.

However, automated judges are imperfect. They make two types of errors. A *false rejection* (Type I error) sends a correct output back to the worker for unnecessary revision, wasting worker capacity on rework. A *false acceptance* (Type II error) lets an incorrect output pass through, consuming judge capacity without actually reducing the human burden. Recent benchmarks document how different models exhibit these two types of errors across task types (Tan et al. 2025, Zheng et al. 2023, Bavaresco et al. 2025). These error channels interact with resource constraints in ways that are not obvious. More screening can amplify human capacity when reviewers are scarce, yet trap the system in unproductive rework when workers are stretched thin. This raises a fundamental operational question: ***When should outputs be routed through the judge for screening, and when should they bypass the judge and go directly to human review?***

We study this question by modeling the AI-human workflow as a queueing network with three resource pools: AI workers, LLM-judges, and human reviewers. Tasks arrive continuously and queue for worker processing. Upon completion, a routing decision determines whether each output goes to the judge for screening or directly to the human review queue. Outputs approved by the judge also proceed to human review. A task is completed only after passing human review; outputs that fail at either the judge or the human stage return for rework.

The decision-maker controls two levers. First, a *routing policy* sets the fraction of outputs sent through the judge versus directly to humans. Second, an *admission policy* regulates how tasks flow into service at

---

each station, preventing unbounded queue buildup. The objective is to maximize long-run throughput: the rate at which tasks successfully complete human review.

The key modeling feature is that judge errors create feedback loops. False rejections generate rework that competes with new arrivals for worker capacity. When workers have spare capacity, this rework is easily absorbed. When workers are already busy, rework crowds out new production. This interaction between error rates and capacity constraints produces the structural phenomena we characterize.

Existing research on LLM-as-a-judge focuses on evaluation quality: accuracy, consistency, bias, and calibration. This literature treats the judge as a standalone measurement instrument and asks whether it can reliably approximate human judgments. Studies document failure modes such as non-transitivity in pairwise comparisons, rating instability across prompts, and susceptibility to adversarial manipulation. These findings have motivated work on training better judges, calibrating outputs, and designing robust evaluation protocols.

This perspective overlooks the *system context* in which the judge operates. In a resource-constrained workflow, the value of judge screening depends not only on error rates but also on which resource is currently the bottleneck. The same judge with the same error rates can be beneficial when humans are scarce (because filtering amplifies effective human capacity) and harmful when workers are scarce (because filtering generates rework that crowds out new production). This observation suggests that judge deployment decisions cannot be made by examining judge accuracy alone. They require understanding how judge errors propagate through the system and interact with capacity constraints.

While the queueing literature provides tools for analyzing rework and routing in service networks, these tools have not yet been applied to the specific structure of AI-human workflows with automated screening. Similarly, the human-AI collaboration literature emphasizes workflow design but does not provide quantitative guidance on when to use versus bypass an automated filter. We bridge this gap by developing a tractable model that yields explicit allocation rules.

Our approach is to develop a fluid model that approximates the stochastic queueing network when all resource pools are large. The fluid model replaces random arrivals and service completions with their deterministic mean rates, yielding a system of flow-balance equations. We focus on steady-state behavior, which corresponds to solving a linear program whose constraints encode capacity limits and flow conservation.

This formulation enables direct analysis of optimal judge allocation. By examining how optimal solutions change as parameters vary, we characterize how the allocation shifts when different capacity constraints become binding. The analysis proceeds in two steps. First, we study a single task class to isolate the fundamental trade-off between the filtering benefit and the rework cost of judge screening. Second, we extend to multiple task classes with different error profiles, revealing how optimal priority depends on which resource is currently the bottleneck.

For implementation, we translate the optimization solution into a policy that operates in the original stochastic system. The policy uses capacity-based thresholds for admission control and optimized fractions

for routing decisions. We establish that this policy is asymptotically optimal: as the system scale grows, the throughput it achieves converges to the theoretical maximum.

Our main contribution is a unified analytical framework that connects judge error rates to system-level throughput through the lens of capacity constraints. The central insight is that judge screening has two faces: it *amplifies* human capacity by filtering errors, but it also *consumes* worker capacity by generating rework. Which effect dominates depends on which resource is the current bottleneck. This bottleneck-dependent logic drives all of our structural results, which address two fundamental questions.

*When should the judge be used, and how intensively?* We show that optimal judge usage is not monotone in judge quality or availability. Instead, it undergoes sharp transitions as the system bottleneck shifts among humans, judges, and workers. When humans are scarce, the system should maximize judge usage because filtering amplifies effective human capacity. When the judge itself becomes the constraint, the system should use all available judge capacity while routing excess flow directly to humans. A less obvious regime arises when workers become the bottleneck. Here, the system should actively *reduce* judge usage even if judge capacity sits idle. The reason is that each false rejection sends a task back for rework, and when workers are stretched thin, this rework crowds out new arrivals. In this regime, more screening makes throughput worse, not better, because rework from false rejections displaces new production. Finally, when human capacity is abundant, the judge should be bypassed entirely because its filtering benefit no longer justifies its rework cost. We derive closed-form capacity thresholds that determine exactly when to maximize, throttle, or bypass judge usage (Proposition 1).

*How should judge capacity be allocated across heterogeneous tasks?* When tasks differ in their error profiles, importance, or judge characteristics, the question shifts from “how much” to “which tasks.” We show that optimal allocation depends on the bottleneck and can exhibit *priority reversal*: the task class that should receive judge priority when humans are scarce may be the opposite of the class that should receive priority when workers are scarce. Consider tasks with a strict judge (rarely lets bad outputs through, but frequently rejects good ones) versus tasks with a lenient judge (opposite profile). When humans are scarce, the strict-judge tasks should receive priority because their approved outputs are higher quality, making the best use of limited human attention. When workers are scarce, the lenient-judge tasks should receive priority because they generate less rework, preserving worker capacity. Between these extremes, we identify *complementarity zones* where mixing task types outperforms specializing in either: the strict-judge tasks contribute quality while the lenient-judge tasks contribute efficiency, and the combination achieves throughput that neither can reach alone. All priority thresholds are computable in closed form from system parameters (Proposition 3).

*Implementation and extensions.* We translate these structural insights into a policy for the stochastic system. The policy has two components: an admission rule that uses the optimal service levels from the fluid analysis as capacity thresholds, and a routing rule that sends each completed task to the judge with

---

the probability prescribed by the fluid-optimal allocation. We establish that this policy is asymptotically optimal: as the system scales up, its throughput converges to the theoretical maximum (Theorem 2). We further extend the model to incorporate human feedback that improves rework success rates (Section 6.1) and to jointly optimize AI worker and judge capacities under a budget constraint (Section 6.2).

### 1.1. Related Literature and Positioning

Our work connects three streams: (i) human–AI workflow design, (ii) LLM-as-a-judge as a screening and evaluation primitive, and (iii) queueing control for resource-constrained service networks. Our central positioning is that LLM-judge performance cannot be assessed in isolation. The same judge error rates can be helpful or harmful depending on where the bottleneck sits and how rework feeds back into upstream queues.

*Human–AI collaboration.* A growing body of work argues that the value of AI depends on process design, not only model accuracy. In particular, when and how AI advice is injected can change decisions and outcomes (Yin et al. 2025). At a higher level, delegation and task allocation can introduce cognitive frictions that limit realized gains from AI assistance (Fügener et al. 2022). Field evidence further shows that collaboration outcomes depend on how humans respond to AI output, for example through reliance and disagreement management (Wang et al. 2026, Yang et al. 2026). These findings motivate a workflow view in which routing rules and intermediate checks are part of the system design, rather than implementation details.

Two additional themes are especially relevant for our setting. First, role framing clarifies that AI can automate, augment, or restructure human work, which changes the effective demand placed on scarce human attention (Fügener et al. 2026). Second, reliance on algorithmic output responds to incentives and information, so the same technical system can generate different downstream workloads under different behavioral regimes, and resource pooling can even backfire when agents respond strategically (Greiner et al. 2026, Balakrishnan et al. 2026, Wang et al. 2023). At a conceptual level, reciprocal learning between humans and machines emphasizes that the interaction is dynamic and can create feedback loops (Te’eni et al. 2026). In the context of generative AI, recent work highlights explicit Type I and Type II style trade-offs in integrating humans, machines, and GenAI (Zhong 2025).

Our model focuses on a common architecture that has recently emerged in practice: an AI worker produces outputs, an automated screen filters them, and humans provide the final verification. We formalize the screening step as an LLM-judge, and study when it is optimal to route outputs through the judge versus bypassing it.

*LLM judges for screening and evaluation.* LLM-based evaluation has become a standard component in benchmarking pipelines and leaderboards, scaling assessment beyond what human labeling can cover (Zheng et al. 2023, Gu et al. 2024). However, the judge itself introduces structured failures that matter for screening: non-transitivity in pairwise comparisons challenges ranking-based decisions (Xu et al. 2025), rating indeterminacy under fixed rubrics complicates threshold-based accept/reject policies (Guerdan et al. 2025), and adversarial manipulation can invert the intended filtering logic (Tong et al. 2025). These concerns have motivated work on training and calibrating judges as first-class objects, including fine-tuned judges as scalable substitutes for human evaluation (Ye et al. 2025, Zhu et al. 2025), automated judge construction (Garipov et al. 2025), and benchmarking judge reliability across text and multimodal settings (Zhou et al. 2025, Chen et al. 2024). Many alignment pipelines further depend on judge-like signals through preference-based learning (Rafailov et al. 2023) and self-rewarding mechanisms (Yuan et al. 2024), making judge reliability a first-order concern for downstream conclusions (Liu et al. 2025b,a). When human oversight is scarce, judge deployment naturally couples to limited human capacity (Ao et al. 2026).

We incorporate these insights through a simple but operational abstraction: judge errors are Type I and Type II errors. A false rejection creates rework and increases upstream load; a false acceptance consumes judge capacity without reducing downstream human workload. This makes reliability a system-level parameter, not only a metric-level concern.

*Queueing control under bottlenecks and rework.* Queueing models provide the core language for analyzing how capacity constraints and routing decisions shape throughput and delay. Fluid approximations for many-server systems are particularly useful for identifying capacity-driven regime changes (Whitt 2006, Zhang 2013). Heavy-traffic and control results show that optimal scheduling structure depends on which constraint binds and can change sharply across regimes (Harrison and Zeevi 2004, Atar et al. 2010). These tools are directly relevant because our system has three interacting resource pools, and routing and screening decisions shift load among them (Ata 2006, Gurvich and Ward 2014, Dong et al. 2024). When tasks are heterogeneous, the structure of optimal matching policies depends on which constraints bind (Hu and Zhou 2022).

A particularly relevant structural feature in our model is that judge errors induce *feedback*: rejected work returns upstream and competes with new work for scarce capacity. Feedback and rework have been studied in classical single-station models, where the performance impact can depend sharply on the return mechanism and service-time variability (Adve and Nelson 1994), and in applied production designs that incorporate explicit feedback buffers (Lee and Seo 1997). In manufacturing and logistics settings, re-entrant and rework flows are central in semiconductor wafer fabrication, circulatory shipping networks, and related systems; queueing-network models can predict cycle-time and congestion propagation with useful accuracy (Chen et al. 1988, Hu and Zhang 2023). At the control level, when a bottleneck alternates between regular processing and rework, optimal operating policies can exhibit threshold structure (So and Tang 1995). In

---

service systems, returns can interact subtly with congestion-management levers such as temporary speedup, slowdowns, or strategic idling (Chan et al. 2014, Dong et al. 2015, Goh et al. 2025), and re-entrant customers in time-varying environments motivate staffing and approximation methods that explicitly account for repeated returns (Yom-Tov and Mandelbaum 2014, Furman et al. 2021).

Several complementary queueing results inform our modeling choices. For capacity planning, fluid models can be accurate enough to guide sizing decisions in systems with impatience (Bassamboo and Randhawa 2010). For diffusion-scale justification, state space collapse results formalize why low-dimensional bottleneck descriptions can be valid in many-server limits (Dai and Tezcan 2011). For operational control under overload, tutorial treatments synthesize structural scheduling insights for many-server systems with impatience (Puha and Ward 2019). For real-time operations, delay estimation and information sharing provide routes to implement congestion-aware policies (Ibrahim and Whitt 2009, Ibrahim 2018). Multiclass scheduling results that highlight how rework-like flows interact with priority and service allocation motivate our focus on bottleneck-dependent structure (Long et al. 2020, 2024). Recent work on deferral decisions under congestion in AI-human systems further demonstrates the relevance of queueing-theoretic analysis to human-AI collaboration (Lykouris and Weng 2024).

Our work sits at the intersection of these three streams. From the collaboration perspective, we formalize routing decisions that determine when outputs pass through automated screening versus proceeding directly to humans. From the LLM-judge perspective, we translate Type I and Type II errors into operational consequences: false rejections generate rework load, while false acceptances consume judge capacity without relieving human reviewers. From the queueing perspective, we analyze how these error-induced flows interact with capacity constraints across three resource pools. The central finding is that optimal judge usage depends on which resource is the current bottleneck, generating phase transitions in allocation policy and priority reversals across task classes. This perspective aligns with recent calls to use operations research as the orchestration layer for generative AI systems (Dai et al. 2025).

## 1.2. Paper Organization

The remainder of this paper is organized as follows. Section 2 formulates the stochastic queueing network, defines the quality and error model, and states the control objective. Section 3 develops the fluid approximation and derives the steady-state linear program. Section 4 characterizes phase transitions in optimal judge allocation: first for a single-class system (four phases, including a regime where screening reduces throughput), then for a two-class system (priority reversal, complementarity zones). Section 5 presents the Fluid-Tracking policy and establishes its asymptotic optimality. Section 6 extends the model to incorporate human feedback and joint capacity planning. Section 7 validates the policy through numerical experiments. Section 8 concludes. Proofs of all main results appear in the Electronic Companion.

## 2. Problem Formulation

This section formulates an AI–human collaborative workflow as a multiclass service network with rework and abandonment at the worker queue. We proceed in three steps. Section 2.1 describes the workflow architecture and highlights the trade-offs created by judge errors. Section 2.2 introduces a probabilistic abstraction for worker quality and judge Type I/II errors. Section 2.3 embeds these primitives into a stochastic queueing network, specifies the state and flow processes, and states the control objective.

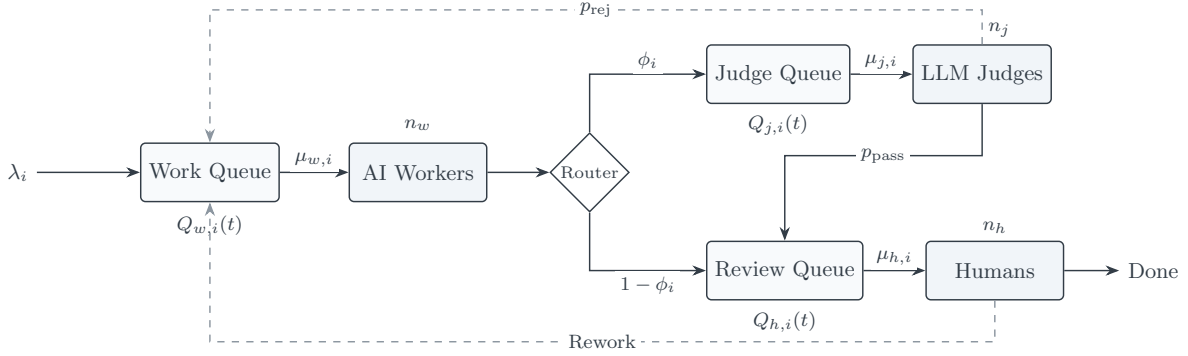


**Figure 1** Workflow architecture. Solid arrows indicate forward flow; dashed arrows indicate rework.

### 2.1. Workflow Architecture

*Workflow overview.* We consider an AI-human collaborative workflow with three resource pools. Figure 1 illustrates the architecture. Tasks arrive exogenously and enter the *Work Queue*, where they wait for processing by AI-Workers. Upon service completion, the *Router* directs each output to one of two paths: the *Judge Queue* for automated screening by the LLM-Judge, or directly to the *Review Queue*. Outputs that pass the judge screening also enter the Review Queue. Finally, human reviewers provide the ultimate verification: a task is *completed* only after passing human review.

*Rework and the judge trade-off.* Two rework channels exist (dashed red arrows in Figure 1): (i) the judge may reject an output, returning it to the Work Queue; (ii) human review may find the output unsatisfactory, also triggering rework. Routing through the LLM-Judge can reduce the load on scarce human reviewers by filtering out low-quality outputs before they reach humans. However, the judge is imperfect: false rejections (Type I errors) create unnecessary rework by sending correct outputs back to workers, while false acceptances (Type II errors) consume judge capacity without improving what humans ultimately see. These two error channels interact with the scarcity of worker, judge, and human capacity, and are the source of the phase-transition behavior we later characterize.

## 2.2. Quality and Error Model

Consider  $I$  task classes indexed by  $i \in \mathcal{I} := \{1, \dots, I\}$ . An AI-Worker output for class  $i$  is *correct* with probability  $(1 - \alpha_i)$  and *incorrect* otherwise; that is,  $\alpha_i \in [0, 1]$  is the raw error probability of a worker output. On the direct path (no judge), a human reviewer rejects an output with probability  $\alpha_i$ . On the judge path, conditional on judge acceptance, the human rejection probability is  $(1 - q_{\text{acc},i})$ , which differs from  $\alpha_i$  when the judge improves quality. Each worker attempt is independent: when a task returns for rework, the new output has the same error probability  $\alpha_i$ , regardless of previous rejection history. Section 6.1 relaxes this assumption by modeling how human feedback improves success probability on rework.

Conditional on the (latent) correctness of the output, the LLM-Judge makes classification errors:

- Type I error (false rejection):  $\beta_i^{(I)}$  is the probability that the judge rejects a correct output.
- Type II error (false acceptance):  $\beta_i^{(II)}$  is the probability that the judge accepts an incorrect output.

Therefore the judge accept/reject probabilities are

$$p_{\text{pass},i} := (1 - \alpha_i)(1 - \beta_i^{(I)}) + \alpha_i \beta_i^{(II)}, \quad (1)$$

$$p_{\text{rej},i} := (1 - \alpha_i)\beta_i^{(I)} + \alpha_i(1 - \beta_i^{(II)}). \quad (2)$$

When the judge accepts an output, the posterior probability that it is correct is

$$q_{\text{acc},i} := \mathbb{P}(\text{correct} \mid \text{judge accepts}) = \frac{(1 - \alpha_i)(1 - \beta_i^{(I)})}{p_{\text{pass},i}}. \quad (3)$$

The quantities  $(p_{\text{pass},i}, p_{\text{rej},i}, q_{\text{acc},i})$  will repeatedly appear in the fluid model and the steady-state optimization:  $p_{\text{pass},i}$  determines how much *judge-routed* flow proceeds to humans, while  $p_{\text{rej},i}$  determines how much judge usage induces rework back to workers.

*When does the judge improve quality?* The judge improves the quality of tasks sent to humans if and only if  $q_{\text{acc},i} > (1 - \alpha_i)$ . To see this, compare the two pathways:

- **Direct path (no judge):** A worker output sent directly to humans is correct with probability  $(1 - \alpha_i)$ .
- **Judge path:** Among worker outputs accepted by the judge and sent to humans, the fraction that is correct is  $q_{\text{acc},i}$ .

Therefore, if  $q_{\text{acc},i} < (1 - \alpha_i)$ , the judge is *counterproductive*: it degrades the average quality of tasks reaching humans compared to sending them directly. In this regime, the optimizer should never route tasks through the judge ( $\phi_i^* = 0$ ). Conversely, if  $q_{\text{acc},i} > (1 - \alpha_i)$ , the judge acts as a quality filter, and routing through the judge can be beneficial (subject to capacity constraints).

## 2.3. Stochastic Network Model and Control Problem

*A sequence of systems indexed by  $n$ .* We model a many-server regime via a sequence of systems indexed by  $n \in \mathbb{N}$ . The  $n$ th system has  $n_w^n, n_j^n$ , and  $n_h^n$  servers in the AI-Worker, Judge, and Human pools, respectively, with

$$n_w^n := n n_w, \quad n_j^n := n n_j, \quad n_h^n := n n_h, \quad (4)$$

and class- $i$  arrivals forming a Poisson process with rate

$$\lambda_i^n := n \lambda_i. \quad (5)$$

The primitive error parameters  $(\alpha_i, \beta_i^{(I)}, \beta_i^{(II)})$  and service rates  $(\mu_{w,i}, \mu_{j,i}, \mu_{h,i})$  do not scale with  $n$ .

*Primitives and service parameters.* External arrivals of class- $i$  tasks in system  $n$  form a Poisson process with rate  $\lambda_i^n$ . Service times are exponential and independent across tasks and stations: AI-Workers serve class  $i$  tasks at rate  $\mu_{w,i}$ , LLM-Judges at rate  $\mu_{j,i}$ , and Humans at rate  $\mu_{h,i}$ . AI-Worker, Judge, and Human capacities are  $n_w^n, n_j^n, n_h^n$ , respectively. Impatience is modeled at the worker queue: any waiting class- $i$  task abandons after an independent exponential patience time with rate  $\theta_i$ .

*State processes (uppercase notation).* Let the system state at time  $t$  be described by queue lengths and in-service counts. For each class  $i$ :

- $Q_{w,i}^n(t)$ : number of class- $i$  tasks waiting for AI-Workers;  $X_i^n(t)$ : number of class- $i$  tasks in AI-Worker service.
- $Q_{j,i}^n(t)$ : number of class- $i$  tasks waiting for the judge;  $Y_i^n(t)$ : number of class- $i$  tasks in judge service.
- $Q_{h,i,d}^n(t)$ : number of class- $i$  tasks waiting for human review on the direct path;  $Z_{i,d}^n(t)$ : number of class- $i$  tasks in human service on the direct path.
- $Q_{h,i,j}^n(t)$ : number of class- $i$  tasks waiting for human review on the judge path;  $Z_{i,j}^n(t)$ : number of class- $i$  tasks in human service on the judge path.

Capacity constraints impose

$$\sum_i X_i^n(t) \leq n_w^n, \quad \sum_i Y_i^n(t) \leq n_j^n, \quad \sum_i (Z_{i,d}^n(t) + Z_{i,j}^n(t)) \leq n_h^n, \quad \forall t \geq 0. \quad (6)$$

*Control (routing and scheduling).* Control actions determine (i) *admissions* from queues into service in each resource pool, and (ii) *routing* of AI-Worker outputs from the routing buffer to either the judge path or the direct human path. We encode these decisions through cumulative control processes:

- $U_{w,i}^n(t)$ : number of class- $i$  tasks admitted into AI-Worker service by time  $t$ .
- $U_{j,i}^n(t)$ : number of class- $i$  tasks admitted into judge service by time  $t$ .
- $U_{h,i,d}^n(t)$  and  $U_{h,i,j}^n(t)$ : numbers of class- $i$  tasks admitted into human service on the direct and judge paths by time  $t$ .

Routing of AI-Worker completions is encoded by controlled counting processes  $S_{w \rightarrow j,i}^n(t)$  and  $S_{w \rightarrow h,i}^n(t)$ , which count (respectively) the numbers of class- $i$  worker completions routed to the judge and routed directly to humans by time  $t$ . These routing processes can only increase at AI-Worker completion epochs and must satisfy

$$S_{w \rightarrow j,i}^n(t) + S_{w \rightarrow h,i}^n(t) = S_{w,i}^n(t), \quad \forall t \geq 0, \quad (7)$$

where  $S_{w,i}^n(t)$  is the total number of class- $i$  AI-Worker service completions by time  $t$  (defined below via a random time-change). Scheduling decisions specify how the available server capacity in each pool is allocated across classes, and are reflected in the evolution of the admission processes above.

*Flow counting processes and balance equations.* To formalize the dynamics, we define cumulative flow processes. Let  $A_i^n(t)$  be the cumulative number of exogenous class- $i$  arrivals by time  $t$ . Let  $B_{w,i}^n(t)$  be the cumulative number of abandonments from the worker queue.

Service completions are split by routing/outcomes:

- Total AI-Worker completions:  $S_{w,i}^n(t)$ ; routing splits:  $S_{w \rightarrow j,i}^n(t)$  and  $S_{w \rightarrow h,i}^n(t)$  satisfying (7).
- Judge completions that are rejected (rework) and accepted (sent to humans):  $S_{j \rightarrow w,i}^n(t)$  and  $S_{j \rightarrow h,i}^n(t)$ .
- Human completions on the direct path that fail and succeed:  $S_{h,d \rightarrow w,i}^n(t)$  and  $S_{h,d \rightarrow c,i}^n(t)$ .
- Human completions on the judge path that fail and succeed:  $S_{h,j \rightarrow w,i}^n(t)$  and  $S_{h,j \rightarrow c,i}^n(t)$ .

Define the cumulative number of successfully completed class- $i$  tasks as

$$C_i^n(t) := S_{h,d \rightarrow c,i}^n(t) + S_{h,j \rightarrow c,i}^n(t). \quad (8)$$

Under the exponential assumptions, these flows admit standard random time-change representations. Let  $\{N_{A,i}, N_{B,i}, N_{w,i}, N_{j \rightarrow w,i}, N_{j \rightarrow h,i}, N_{h,d \rightarrow w,i}, N_{h,d \rightarrow c,i}, N_{h,j \rightarrow w,i}, N_{h,j \rightarrow c,i}\}_{i \in \mathcal{I}}$  be mutually independent unit-rate Poisson processes. Then for each  $i \in \mathcal{I}$  and  $t \geq 0$ :

$$A_i^n(t) = N_{A,i}(\lambda_i^n t), \quad (9)$$

$$B_{w,i}^n(t) = N_{B,i} \left( \int_0^t \theta_i Q_{w,i}^n(s) ds \right), \quad (10)$$

$$S_{w,i}^n(t) = N_{w,i} \left( \int_0^t \mu_{w,i} X_i^n(s) ds \right), \quad (11)$$

$$S_{j \rightarrow w,i}^n(t) = N_{j \rightarrow w,i} \left( \int_0^t \mu_{j,i} Y_i^n(s) p_{\text{rej},i} ds \right), \quad (12)$$

$$S_{j \rightarrow h,i}^n(t) = N_{j \rightarrow h,i} \left( \int_0^t \mu_{j,i} Y_i^n(s) p_{\text{pass},i} ds \right), \quad (13)$$

where  $S_{j \rightarrow w,i}^n$  and  $S_{j \rightarrow h,i}^n$  are independent thinnings of the total judge completion process  $S_{j,i}^n(t) := N_{j,i} \left( \int_0^t \mu_{j,i} Y_i^n(s) ds \right)$ , satisfying  $S_{j \rightarrow w,i}^n(t) + S_{j \rightarrow h,i}^n(t) = S_{j,i}^n(t)$  almost surely. Analogous representations hold for the human completion splits given below. The worker-routing counts  $S_{w \rightarrow j,i}^n(t)$  and  $S_{w \rightarrow h,i}^n(t)$  are *policy-controlled* splitting processes constrained by (7); in particular, they are integer-valued, nondecreasing, and can only jump when  $S_{w,i}^n(t)$  jumps. In particular, for the direct human path, incorrect outputs occur with probability  $\alpha_i$ , so

$$S_{h,d \rightarrow w,i}^n(t) = N_{h,d \rightarrow w,i} \left( \int_0^t \mu_{h,i} Z_{i,d}^n(s) \alpha_i ds \right), \quad S_{h,d \rightarrow c,i}^n(t) = N_{h,d \rightarrow c,i} \left( \int_0^t \mu_{h,i} Z_{i,d}^n(s) (1 - \alpha_i) ds \right). \quad (14)$$

For the judge path, conditional on judge acceptance, the probability that an output is incorrect equals  $(1 - q_{\text{acc},i})$ , hence

$$S_{h,j \rightarrow w,i}^n(t) = N_{h,j \rightarrow w,i} \left( \int_0^t \mu_{h,i} Z_{i,j}^n(s) (1 - q_{\text{acc},i}) ds \right), \quad (15)$$

$$S_{h,j \rightarrow c,i}^n(t) = N_{h,j \rightarrow c,i} \left( \int_0^t \mu_{h,i} Z_{i,j}^n(s) q_{\text{acc},i} ds \right). \quad (16)$$

The state and flow processes satisfy the following balance equations for each class  $i$  and all  $t \geq 0$ :

$$Q_{w,i}^n(t) = Q_{w,i}^n(0) + A_i^n(t) + S_{j \rightarrow w,i}^n(t) + S_{h,d \rightarrow w,i}^n(t) + S_{h,j \rightarrow w,i}^n(t) - U_{w,i}^n(t) - B_{w,i}^n(t), \quad (17)$$

$$X_i^n(t) = X_i^n(0) + U_{w,i}^n(t) - (S_{w \rightarrow j,i}^n(t) + S_{w \rightarrow h,i}^n(t)), \quad (18)$$

$$Q_{j,i}^n(t) = Q_{j,i}^n(0) + S_{w \rightarrow j,i}^n(t) - U_{j,i}^n(t), \quad (19)$$

$$Y_i^n(t) = Y_i^n(0) + U_{j,i}^n(t) - (S_{j \rightarrow w,i}^n(t) + S_{j \rightarrow h,i}^n(t)), \quad (20)$$

$$Q_{h,i,d}^n(t) = Q_{h,i,d}^n(0) + S_{w \rightarrow h,i}^n(t) - U_{h,i,d}^n(t), \quad (21)$$

$$Z_{i,d}^n(t) = Z_{i,d}^n(0) + U_{h,i,d}^n(t) - (S_{h,d \rightarrow w,i}^n(t) + S_{h,d \rightarrow c,i}^n(t)), \quad (22)$$

$$Q_{h,i,j}^n(t) = Q_{h,i,j}^n(0) + S_{j \rightarrow h,i}^n(t) - U_{h,i,j}^n(t), \quad (23)$$

$$Z_{i,j}^n(t) = Z_{i,j}^n(0) + U_{h,i,j}^n(t) - (S_{h,j \rightarrow w,i}^n(t) + S_{h,j \rightarrow c,i}^n(t)), \quad (24)$$

where the cumulative admission processes  $U_{w,i}^n(t), U_{j,i}^n(t), U_{h,i,d}^n(t), U_{h,i,j}^n(t)$  are policy-controlled and must respect the capacity constraints.

*Admissible policies.* Following standard queueing-control conventions, we define a policy  $\pi^n$  as the collection of all non-primitive processes in the  $n$ th system: state processes (queues and in-service counts), cumulative flow processes (arrivals, abandonments, service completions, routing splits, and successful completions), and control processes (admissions and routing decisions), each indexed by class  $i \in \mathcal{I}$ . All control processes are adapted to the natural filtration generated by the primitive processes (arrivals, service completions, abandonments) and past control actions. Let  $\Pi^n$  denote the set of policies satisfying:

- (i) The resulting processes satisfy the capacity constraints and balance equations (17)–(24) for all  $t \geq 0$ .
- (ii) The policy is *event-driven*: each control process  $U_{\cdot,i}^n(t)$  and each routing process  $S_{w \rightarrow j,i}^n(t), S_{w \rightarrow h,i}^n(t)$  can change only at arrival epochs, abandonment epochs, service-completion epochs, or at  $t = 0$ .
- (iii) Service is non-preemptive and within each class queues are served in first-come-first-served order.

In Section 3 we replace these stochastic dynamics by a steady-state fluid approximation that yields a tractable optimization problem.

*Objective.* With reward weights  $r_i > 0$ , we consider the long-run average throughput objective

$$\max_{\pi^n \in \Pi^n} \liminf_{T \rightarrow \infty} \frac{1}{nT} \mathbb{E}^{\pi^n} \left[ \sum_{i \in \mathcal{I}} r_i C_i^n(T) \right], \quad (25)$$

over the admissible policy class  $\Pi^n$ . The remainder of the paper focuses on structural insights obtainable from the associated steady-state fluid model.

### 3. Fluid Model

The stochastic network in Section 2.3 is analytically intractable due to the high-dimensional state space and the feedback loops created by rework. We adopt a many-server fluid approximation that is justified by a fluid limit as the system scales. For any process  $W^n(t)$  in system  $n$ , define its fluid-scaled version  $\bar{W}^n(t) := W^n(t)/n$  and let  $n \rightarrow \infty$ . In the limit, stochastic fluctuations average out and the network is described by deterministic flow-balance equations and capacity constraints.

*Fluid model.* We write

$$(q_{w,i}(t), x_i(t), q_{j,i}(t), y_i(t), q_{h,i,d}(t), z_{i,d}(t), q_{h,i,j}(t), z_{i,j}(t))$$

for generic deterministic fluid trajectories that arise as subsequential limits of the fluid-scaled stochastic processes. These functions satisfy, for all  $t \geq 0$  and all  $i \in \mathcal{I}$ , the flow-balance equations

$$\begin{aligned} q_{w,i}(t) &= q_{w,i}(0) + a_i(t) + s_{j \rightarrow w,i}(t) + s_{h,d \rightarrow w,i}(t) + s_{h,j \rightarrow w,i}(t) - u_{w,i}(t) - b_{w,i}(t), \\ x_i(t) &= x_i(0) + u_{w,i}(t) - s_{w \rightarrow j,i}(t) - s_{w \rightarrow h,i}(t), \\ q_{j,i}(t) &= q_{j,i}(0) + s_{w \rightarrow j,i}(t) - u_{j,i}(t), \\ y_i(t) &= y_i(0) + u_{j,i}(t) - s_{j \rightarrow w,i}(t) - s_{j \rightarrow h,i}(t), \\ q_{h,i,d}(t) &= q_{h,i,d}(0) + s_{w \rightarrow h,i}(t) - u_{h,i,d}(t), \\ z_{i,d}(t) &= z_{i,d}(0) + u_{h,i,d}(t) - s_{h,d \rightarrow w,i}(t) - s_{h,d \rightarrow c,i}(t), \\ q_{h,i,j}(t) &= q_{h,i,j}(0) + s_{j \rightarrow h,i}(t) - u_{h,i,j}(t), \\ z_{i,j}(t) &= z_{i,j}(0) + u_{h,i,j}(t) - s_{h,j \rightarrow w,i}(t) - s_{h,j \rightarrow c,i}(t). \end{aligned} \quad (26)$$

Here  $u_{\cdot,i}(t)$  are cumulative admissions into service (policy controls),  $b_{w,i}(t)$  is cumulative abandonment from the work queue, and  $s_{\cdot \rightarrow \cdot,i}(t)$  are cumulative routing/service-completion flows between nodes.

*Mean-rate primitives.* Let  $v_i(t)$  denote the judge-routed worker service level: the instantaneous in-service mass of class  $i$  at workers whose completions are routed to the judge, satisfying  $0 \leq v_i(t) \leq x_i(t)$ . The primitive arrivals, abandonments, and service-driven routing flows evolve at their mean rates:

$$\begin{aligned} a_i(t) &= \lambda_i t, & b_{w,i}(t) &= \int_0^t \theta_i q_{w,i}(s) ds, \\ s_{w \rightarrow j,i}(t) &= \int_0^t \mu_{w,i} v_i(s) ds, & s_{w \rightarrow h,i}(t) &= \int_0^t \mu_{w,i} (x_i(s) - v_i(s)) ds, \\ s_{j \rightarrow w,i}(t) &= \int_0^t \mu_{j,i} y_i(s) p_{\text{rej},i} ds, & s_{j \rightarrow h,i}(t) &= \int_0^t \mu_{j,i} y_i(s) p_{\text{pass},i} ds, \\ s_{h,d \rightarrow w,i}(t) &= \int_0^t \mu_{h,i} z_{i,d}(s) \alpha_i ds, & s_{h,d \rightarrow c,i}(t) &= \int_0^t \mu_{h,i} z_{i,d}(s) (1 - \alpha_i) ds, \\ s_{h,j \rightarrow w,i}(t) &= \int_0^t \mu_{h,i} z_{i,j}(s) (1 - q_{\text{acc},i}) ds, & s_{h,j \rightarrow c,i}(t) &= \int_0^t \mu_{h,i} z_{i,j}(s) q_{\text{acc},i} ds. \end{aligned} \quad (27)$$

Equivalently,  $v_i(t) = \phi_i(t) x_i(t)$  for some  $\phi_i(t) \in [0, 1]$ .

*Capacity constraints.* Let  $x(t) := \sum_i x_i(t)$ ,  $y(t) := \sum_i y_i(t)$ , and  $z(t) := \sum_i (z_{i,d}(t) + z_{i,j}(t))$ . The fluid model enforces the normalized capacity constraints

$$0 \leq x(t) \leq n_w, \quad 0 \leq y(t) \leq n_j, \quad 0 \leq z(t) \leq n_h, \quad \forall t \geq 0. \quad (28)$$

**ASSUMPTION 1 (Convergence of initial state).** *The fluid-scaled initial states converge in probability to a deterministic limit: for each  $i \in \mathcal{I}$ ,*

$$\frac{1}{n} (Q_{w,i}^n(0), X_i^n(0), Q_{j,i}^n(0), Y_i^n(0), Q_{h,i,d}^n(0), Z_{i,d}^n(0), Q_{h,i,j}^n(0), Z_{i,j}^n(0)) \xrightarrow{P} \mathbf{z}_{0,i},$$

where  $\mathbf{z}_{0,i}$  is a deterministic vector.

**THEOREM 1 (Fluid limit).** *Fix any finite horizon  $T > 0$ . Under Assumption 1 and any admissible policy sequence  $\{\pi^n\}_{n \geq 1}$  with  $\pi^n \in \Pi^n$  for each  $n$ , the sequence of fluid-scaled processes is tight in  $\mathbb{D}([0, T], \mathbb{R}^d)$  under the Skorokhod  $J_1$  topology, where  $d$  is the total dimension of the process vector. Moreover, any subsequential weak limit is almost surely continuous and satisfies the fluid model equations (26)–(27) and the capacity constraints (28) on  $[0, T]$ , with initial state given by Assumption 1.*

*Steady-state fluid optimization.* We now focus on steady-state operating points of the fluid model above. Fix the exogenous parameters  $(\lambda_i, \theta_i, \mu_{w,i}, \mu_{j,i}, \mu_{h,i}, n_w, n_j, n_h)$  and the quality parameters summarized by  $p_{\text{pass},i}$ ,  $p_{\text{rej},i}$ , and  $q_{\text{acc},i}$  in (1)–(3). Let  $q_{w,i}$  be the steady-state work-queue mass, and let  $(x_i, y_i, z_{i,d}, z_{i,j})$  be the steady-state in-service masses at workers, judges, humans (direct), and humans (judge path), respectively. Introduce an auxiliary variable  $v_i$  representing the judge-routed worker service level, satisfying  $0 \leq v_i \leq x_i$  (equivalently,  $v_i = \phi_i x_i$  for some  $\phi_i \in [0, 1]$ ). The steady-state completion rate of class  $i$  equals  $\lambda_i - \theta_i q_{w,i}$  since abandonment occurs only at the work queue. We therefore solve:

$$\max_{\{q_{w,i}, x_i, y_i, z_{i,d}, z_{i,j}, v_i\}} \sum_{i=1}^I r_i (\lambda_i - \theta_i q_{w,i}) \quad (29a)$$

$$\text{s.t. } \mu_{w,i} v_i = \mu_{j,i} y_i, \quad \forall i \in \mathcal{I}, \quad (29b)$$

$$\mu_{w,i} (x_i - v_i) = \mu_{h,i} z_{i,d}, \quad \forall i \in \mathcal{I}, \quad (29c)$$

$$\mu_{j,i} y_i p_{\text{pass},i} = \mu_{h,i} z_{i,j}, \quad \forall i \in \mathcal{I}, \quad (29d)$$

$$\begin{aligned} \lambda_i + \mu_{j,i} y_i p_{\text{rej},i} + \mu_{h,i} z_{i,d} \alpha_i + \mu_{h,i} z_{i,j} (1 - q_{\text{acc},i}) \\ = \mu_{w,i} x_i + \theta_i q_{w,i}, \quad \forall i \in \mathcal{I}, \end{aligned} \quad (29e)$$

$$\sum_{i=1}^I x_i \leq n_w, \quad \sum_{i=1}^I y_i \leq n_j, \quad \sum_{i=1}^I (z_{i,d} + z_{i,j}) \leq n_h, \quad (29f)$$

$$0 \leq v_i \leq x_i, \quad q_{w,i}, x_i, y_i, z_{i,d}, z_{i,j} \geq 0, \quad \forall i \in \mathcal{I}. \quad (29g)$$

The optimization (29) is the steady-state specialization of the fluid model. The objective (29a) maximizes weighted throughput:  $\lambda_i - \theta_i q_{w,i}$  is the completion rate of class  $i$ , since tasks abandon only from the work queue at rate  $\theta_i q_{w,i}$ . Constraints (29b)–(29d) are flow-balance equations linking adjacent nodes. Constraint (29b) balances worker-to-judge flow: the rate at which workers complete tasks routed to judges ( $\mu_{w,i} v_i$ ) must equal the rate at which judges process them ( $\mu_{j,i} y_i$ ). Constraint (29c) balances the direct path:

the rate of worker completions sent directly to humans ( $\mu_{w,i}(x_i - v_i)$ ) equals the human processing rate on the direct path ( $\mu_{h,i}z_{i,d}$ ). Constraint (29d) balances the judge-to-human flow: the rate at which judges pass tasks ( $\mu_{j,i}y_i p_{\text{pass},i}$ ) equals the human processing rate on the judge path ( $\mu_{h,i}z_{i,j}$ ). Constraint (29e) is the work-queue balance. The inflow comprises fresh arrivals  $\lambda_i$ , judge rejections  $\mu_{j,i}y_i p_{\text{rej},i}$ , human failures on the direct path  $\mu_{h,i}z_{i,d}\alpha_i$ , and human failures on the judge path  $\mu_{h,i}z_{i,j}(1 - q_{\text{acc},i})$ . The outflow is worker service  $\mu_{w,i}x_i$  plus abandonment  $\theta_i q_{w,i}$ . Constraint (29f) enforces resource capacities: aggregate in-service mass at workers, judges, and humans cannot exceed  $n_w$ ,  $n_j$ , and  $n_h$ , respectively.

*Reduced multi-class LP.* Eliminating the intermediate variables ( $y_i, z_{i,d}, z_{i,j}, q_{w,i}$ ) via flow balance yields an equivalent LP in only  $(x_i, v_i)$ . Using  $y_i = (\mu_{w,i}/\mu_{j,i})v_i$ ,  $z_{i,d} = (\mu_{w,i}/\mu_{h,i})(x_i - v_i)$ , and  $z_{i,j} = (\mu_{w,i}/\mu_{h,i})p_{\text{pass},i}v_i$ , the human capacity constraint becomes  $\sum_i (\mu_{w,i}/\mu_{h,i})(x_i - p_{\text{rej},i}v_i) \leq n_h$ , where  $p_{\text{rej},i} = 1 - p_{\text{pass},i}$ . The objective simplifies via the identity  $p_{\text{pass},i}q_{\text{acc},i} = (1 - \alpha_i)(1 - \beta_i^{(I)})$  to  $\sum_i r_i \mu_{w,i}(1 - \alpha_i)(x_i - \beta_i^{(I)}v_i)$ . The reduced LP is:

$$\max_{(x_i, v_i)_{i \in \mathcal{I}}} \sum_{i \in \mathcal{I}} r_i \mu_{w,i}(1 - \alpha_i)(x_i - \beta_i^{(I)}v_i) \quad (30a)$$

$$\text{s.t. } 0 \leq v_i \leq x_i, \quad x_i - \beta_i^{(I)}v_i \leq \frac{\lambda_i}{\mu_{w,i}(1 - \alpha_i)}, \quad i \in \mathcal{I}, \quad (30b)$$

$$\sum_{i \in \mathcal{I}} x_i \leq n_w, \quad \sum_{i \in \mathcal{I}} \frac{\mu_{w,i}}{\mu_{j,i}}v_i \leq n_j, \quad (30c)$$

$$\sum_{i \in \mathcal{I}} \frac{\mu_{w,i}}{\mu_{h,i}}(x_i - p_{\text{rej},i}v_i) \leq n_h. \quad (30d)$$

Given an optimal solution, a corresponding judge-flow proportion can be recovered by  $\phi_i^* = v_i^*/x_i^*$  when  $x_i^* > 0$  (and  $\phi_i^* := 0$  when  $x_i^* = 0$ ).

## 4. Phase Transitions and Priority Reversal in Optimal Judge Allocation

The general formulation in Section 3 yields a tractable linear program, but the structural properties of the optimal allocation are not apparent from the LP alone. This section reveals that optimal judge allocation exhibits sharp *phase transitions*, that is, discrete structural changes at computable capacity thresholds where the system bottleneck shifts between resource types. We analyze two canonical cases. The single-class case (Section 4.1) establishes *how* to use the judge: a four-phase structure governs judge intensity and reveals a regime in which the system should reduce judge usage even when judge capacity is available, because rework crowds out new production. The two-class case (Section 4.2) establishes *who* gets the judge: optimal priority can *reverse* across bottleneck regimes, with a complementarity zone where both classes share judge capacity.

### 4.1. Single-Class System: The Four-Phase Structure

We begin with the single-class case ( $I = 1$ ), which reveals the fundamental trade-off governing judge allocation.

*The quality-quantity trade-off.* The judge serves as a quality filter: it screens worker outputs and rejects those it deems incorrect, reducing the burden on human reviewers. However, this filtering carries a cost. Type I errors (false rejections) send correct outputs back to workers for unnecessary rework, consuming worker capacity. When workers are abundant, this rework cost is negligible, and the system benefits from maximizing judge usage. When workers are scarce, rework competes with new production for limited capacity, and the system must balance filtering benefits against efficiency losses.

The optimal judge allocation  $\phi^*$  depends on which resource is the bottleneck. As human capacity varies from scarce to abundant, the bottleneck shifts, and the optimal allocation exhibits phase transitions: discrete changes at specific capacity thresholds.

Specializing the reduced multi-class LP (30) to  $I = 1$  yields a 2D LP; we state it in Appendix EC.1.3. To isolate the impact of resource scarcity, we assume an overloaded regime.

**ASSUMPTION 2 (Overloaded regime).** *Throughout this section, we assume the system is overloaded:  $\frac{\lambda}{\mu_w(1-\alpha)} \geq n_w$ , so that the arrival constraint in the single-class LP is slack and the work queue is always backlogged.*

*Normalized capacities.* To express results in comparable units, we normalize all capacities to worker-equivalent units:

$$H := \frac{\mu_h}{\mu_w} n_h, \quad J := \frac{\mu_j}{\mu_w} n_j, \quad J_{\text{eff}} := \min\{n_w, J\}. \quad (31)$$

Here  $H$  is the rate at which humans can process tasks in worker-output units,  $J$  is the nominal judge capacity, and  $J_{\text{eff}}$  is the effective judge capacity. The judge can only process tasks that workers have completed, so its effective capacity is bounded by worker output  $n_w$ ; hence  $J_{\text{eff}} = \min\{n_w, J\}$ .

We focus on the regime where the judge improves quality, i.e.,  $q_{\text{acc}} > 1 - \alpha$ . Otherwise the optimal allocation trivially has  $\phi^* = 0$ .

*Thresholds.* The four phases are separated by three thresholds:

$$n_h^{(1)} := \frac{\mu_w}{\mu_h} p_{\text{pass}} J_{\text{eff}}, \quad n_h^{(2)} := \frac{\mu_w}{\mu_h} (n_w - p_{\text{rej}} J_{\text{eff}}), \quad n_h^{(3)} := \frac{\mu_w}{\mu_h} n_w. \quad (32)$$

The threshold  $n_h^{(1)}$  is the minimum human capacity needed to absorb all judge-filtered output when  $\phi = 1$ . The threshold  $n_h^{(2)}$  is the human capacity at which workers first become saturated. The threshold  $n_h^{(3)}$  is the human capacity sufficient to absorb all worker output directly, making the judge unnecessary.

**LEMMA 1 (Threshold ordering).** *The thresholds satisfy  $n_h^{(1)} \leq n_h^{(2)} \leq n_h^{(3)}$ . If  $J_{\text{eff}} < n_w$ , then the inequalities are strict.*

**PROPOSITION 1 (Four-phase structure).** *Under Assumption 2, if  $q_{\text{acc}} > 1 - \alpha$  and  $J_{\text{eff}} < n_w$ , then the optimal judge allocation  $\phi^* = v^*/x^*$  exhibits four phases:*

1. If  $n_h \leq n_h^{(1)}$ , then  $\phi^* = 1$  (full screening).

2. If  $n_h^{(1)} \leq n_h \leq n_h^{(2)}$ , then  $\phi^* = \frac{J_{\text{eff}}}{H + p_{\text{rej}} J_{\text{eff}}}$  (judge saturation).
3. If  $n_h^{(2)} \leq n_h \leq n_h^{(3)}$ , then  $\phi^* = \frac{n_w - H}{p_{\text{rej}} n_w}$  (active reduction).
4. If  $n_h \geq n_h^{(3)}$ , then  $\phi^* = 0$  (judge bypass).

Each phase corresponds to a different binding constraint, and the optimal response differs accordingly.

In *Phase 1*, humans are the bottleneck. The judge converts one unit of worker output into  $p_{\text{pass}} < 1$  units of human workload, with the remainder rejected back to workers. This filtering amplifies the effective human capacity: the same number of humans can clear more tasks. The benefit outweighs the rework cost, so the system maximizes judge usage ( $\phi^* = 1$ ).

In *Phase 2*, the judge reaches its capacity limit at  $v^* = J_{\text{eff}}$ . Human capacity continues to grow beyond  $n_h^{(1)}$ , but the system cannot route more than  $J_{\text{eff}}$  through the judge. The additional human capacity must be filled via the direct path, so total worker output  $x^*$  increases while  $v^*$  stays fixed. The ratio  $\phi^* = v^*/x^*$  declines as  $n_h$  grows.

In *Phase 3*, workers become the bottleneck ( $x^* = n_w$ ). Each unit of judge usage now carries a direct opportunity cost: the  $p_{\text{rej}}$  units of rework compete with new arrivals for scarce worker capacity. To maximize throughput, the system reduces  $\phi^*$  below the judge-saturated level, trading filtering quality for worker efficiency.

In *Phase 4*, humans are abundant enough to handle all worker output directly. The judge's filtering benefit (reducing human load) is no longer needed, but its rework cost persists. The system bypasses the judge entirely.

*Illustration (Figure 2a).* Figure 2a plots  $\phi^*$  and resource utilizations as  $n_h$  varies. The four phases are clearly visible: full screening when humans are scarce ( $n_h \lesssim 6$ ), judge saturation ( $n_h \approx 6\text{--}7.5$ ), active reduction of judge usage despite spare capacity ( $n_h \approx 7.5\text{--}10$ ), and complete judge bypass when humans are abundant ( $n_h \gtrsim 10$ ).

*Special case: abundant workers.* When worker capacity is large enough to handle both direct flow and maximum rework, Phase 3 vanishes because workers never saturate. Concretely, this requires  $n_w \geq H + p_{\text{rej}} J$ , i.e., workers can absorb all direct human flow ( $H$ ) plus the maximum rework generated by judge rejections ( $p_{\text{rej}} J$ ). Under this condition, the four-phase structure simplifies to two phases.

**PROPOSITION 2 (Abundant workers).** *Under Assumption 2, if  $n_w \geq H + p_{\text{rej}} J$  and  $q_{\text{acc}} > 1 - \alpha$ , the optimal judge allocation  $\phi^* = v^*/x^*$  exhibits two regimes:*

1. If  $H \leq p_{\text{pass}} J$ , then  $\phi^* = 1$ .
2. If  $H \geq p_{\text{pass}} J$ , then  $\phi^* = \frac{J}{H + p_{\text{rej}} J}$ .

The transition occurs at threshold  $n_h^{(\text{aw})} := \frac{\mu_w}{\mu_h} p_{\text{pass}} J$ .

Below threshold  $n_h^{(aw)}$ , humans are scarce enough that the system maximizes judge usage ( $\phi^* = 1$ ). Beyond this threshold, the judge saturates at  $v^* = J$  while human capacity continues to grow. Total worker output  $x^*$  increases to fill additional human capacity via the direct path, so  $\phi^* = v^*/x^*$  declines hyperbolically as  $\phi^* \propto 1/n_h$ . Figure 2b confirms this: beyond threshold  $n_h^{(aw)} \approx 7$ ,  $\phi^*$  follows a smooth concave curve while all utilizations remain below 100%.

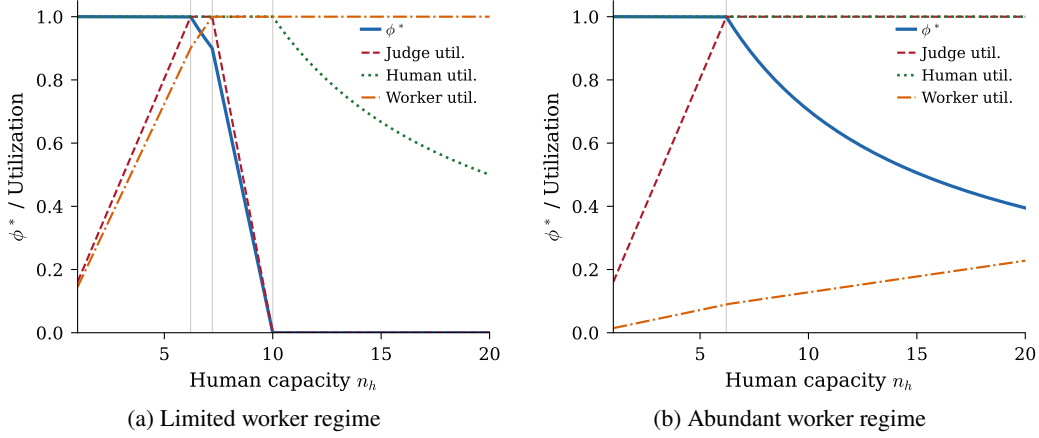


**Figure 2** Single-class optimal judge allocation  $\phi^*$  and resource utilizations as human capacity  $n_h$  varies. Parameters:  $\lambda = 75$ ,  $(\mu_w, \mu_j, \mu_h) = (20, 30, 10)$ ,  $n_w = 5$ ,  $n_j = 3$ ,  $\alpha = 0.3$ ,  $\beta^{(I)} = 0.1$ ,  $\beta^{(II)} = 0.2$ . Vertical lines mark theoretical thresholds.

In summary, the operational logic shifts from maximizing judge usage (Phases 1–2) to actively reducing it (Phase 3) to bypassing it entirely (Phase 4), as the bottleneck evolves from humans to workers. When workers are abundant, Phase 3 vanishes and judge usage declines smoothly once the judge saturates.

## 4.2. Two-Class System: Priority Reversal

Section 4.1 established *how* to use the judge: a four-phase structure governs the intensity of judge usage as the bottleneck shifts from humans to workers. When tasks are heterogeneous, differing in judge error rates ( $\beta_i^{(I)}, \beta_i^{(II)}$ ), a new question arises: *which class should receive judge capacity?* The single-class phase structure still determines aggregate judge utilization; what changes is the allocation of that capacity across classes. We show that the answer depends on which resource is scarce, and that optimal priority can *reverse*: the class that should receive judge priority under human scarcity differs from the class prioritized under worker scarcity.

*Priority indices.* The optimal class priority is governed by two indices, one for each scarcity regime:

$$q_{\text{acc},i} = \frac{(1 - \alpha_i)(1 - \beta_i^{(I)})}{p_{\text{pass},i}}, \quad \eta_i := \frac{\beta_i^{(I)}}{p_{\text{rej},i}}. \quad (33)$$

The index  $q_{\text{acc},i}$  is the probability that a judge-approved output is correct. When humans are the bottleneck, each unit of human time should yield the highest possible quality, so the system prioritizes the class with higher  $q_{\text{acc},i}$ .

The index  $\eta_i$  is the fraction of judge rejections that are false rejections. When workers are the bottleneck, rework is costly: each false rejection consumes worker capacity without correcting an actual error. The class with lower  $\eta_i$  generates less wasted rework per unit of judge usage, so it is preferred.

**ASSUMPTION 3 (Two-class overloaded regime).** *We assume symmetric worker parameters  $\mu_{w,1} = \mu_{w,2} =: \mu_w$  and  $\alpha_1 = \alpha_2 =: \alpha$ , and that the system is overloaded:  $\frac{\lambda_i}{\mu_w(1-\alpha)} \geq n_w$  for each  $i \in \{1, 2\}$ , so that per-class constraints (30b) are slack.*

Let  $k_q := \arg \max_{i \in \{1,2\}} q_{\text{acc},i}$  and  $k_\eta := \arg \min_{i \in \{1,2\}} \eta_i$  denote the classes favored under human scarcity and worker scarcity, respectively. The nontrivial regime arises when judge capacity is scarce ( $J_{\text{eff}} < n_w$ , so the system cannot screen all worker outputs and must choose which class to prioritize) and when the two priority indices rank the classes differently ( $k_q \neq k_\eta$ , so one class excels at producing high-quality approved outputs while the other excels at avoiding false rejections). Under these circumstances, the system faces a genuine trade-off between quality and rework as human capacity varies, giving rise to priority reversal. When  $k_q = k_\eta$ , the same class dominates both metrics and retains exclusive priority throughout, a degenerate case we set aside. The condition  $k_q \neq k_\eta$  arises naturally in practice: a class with a strict judge (low Type II error  $\beta^{(II)}$  but relatively high Type I error  $\beta^{(I)}$ ) may achieve high  $q_{\text{acc}}$  while simultaneously having high  $\eta$ ; conversely, a class with a lenient judge may have low  $q_{\text{acc}}$  but also low  $\eta$ .

**PROPOSITION 3 (Priority reversal).** *Under Assumption 3, if  $q_{\text{acc},i} > 1 - \alpha$  for both classes,  $J_{\text{eff}} < n_w$ , and  $k_q \neq k_\eta$ , the following holds. For  $k \in \{1, 2\}$ , let  $\ell := 3 - k$ .*

1. **Human-scarce priority.** *There exists a threshold  $\underline{n}_h > 0$  such that for all  $n_h \leq \underline{n}_h$ , every optimal solution satisfies  $v_{k_q}^* > 0$  and  $v_\ell^* = 0$ .*

2. **Worker-scarce priority.** *There exists a threshold  $\bar{n}_h$  such that for all  $n_h \geq \bar{n}_h$ , every optimal solution satisfies  $v_\ell^* = 0$ ; moreover  $v_{k_\eta}^* > 0$  whenever  $n_h < \frac{\mu_w}{\mu_h} n_w$ .*

3. **Complementarity.**  *$\underline{n}_h < \bar{n}_h$ , and there exists a non-degenerate interval  $I \subset (\underline{n}_h, \bar{n}_h)$  on which both classes receive strictly positive judge allocation ( $v_1^* > 0$  and  $v_2^* > 0$ ).*

*Both thresholds  $\underline{n}_h$  and  $\bar{n}_h$  admit closed-form expressions in terms of system parameters; see the proof in Appendix EC.1.5.*

The proposition distills optimal multi-class judge allocation into a clean separation of regimes. In the *human-scarce regime*, each unit of human time is precious, and the system routes judge capacity to the class whose approved outputs are most likely correct (highest  $q_{\text{acc}}$ ), ensuring that humans see the highest-quality work. In the *worker-scarce regime*, rework is the primary cost, and the system routes judge capacity to the class with the lowest false-rejection rate (lowest  $\eta$ ), preserving worker capacity for new production.

The complementarity zone reflects the fact that concentrating judge capacity on a single class is not always optimal. Suppose we allocate all judge capacity to class  $k_q$  (highest  $q_{\text{acc}}$ ), which produces the highest-quality screened outputs. Because judge capacity is limited, only a portion of tasks can be screened; the remainder bypass the judge and go directly to human review at lower quality. If human capacity is not fully utilized by the screened outputs from class  $k_q$  alone, the slack is filled by unscreened work. Now consider diverting some judge capacity to the other class, which has lower  $\eta$  (fewer false rejections). This class produces “medium-quality” screened outputs at a higher rate per unit of judge capacity. The result is a portfolio of “high-quality plus medium-quality” screened work, which can dominate the original “high-quality plus low-quality (unscreened)” mix. In the complementarity zone, this rebalancing strictly improves throughput: sharing judge capacity across both classes yields better overall performance than concentrating it on either one.

*Illustration (Figure 3).* Figure 3 plots the optimal judge allocation for two classes as  $n_h$  varies, with Class 1 having a lenient judge ( $\beta_1^{(I)} = 0.05$ ,  $\beta_1^{(II)} = 0.40$ ) and Class 2 having a stricter judge ( $\beta_2^{(I)} = 0.15$ ,  $\beta_2^{(II)} = 0.10$ ). Here Class 2 has higher  $q_{\text{acc}}$  (better quality conditioned on acceptance) but also higher  $\eta$  (more false rejections), so  $k_q = 2$  and  $k_\eta = 1$ : the two indices disagree, producing a priority reversal. As predicted by the proposition: for small  $n_h$ , all judge capacity goes to Class 2 (human-scarce priority); for large  $n_h$  approaching  $\frac{\mu_w}{\mu_h} n_w$ , judge capacity shifts entirely to Class 1 (worker-scarce priority). The reversal is not abrupt: the complementarity zone provides a smooth transition where Class 2’s allocation gradually decreases while Class 1’s allocation gradually increases, with both classes sharing judge capacity during this intermediate regime.

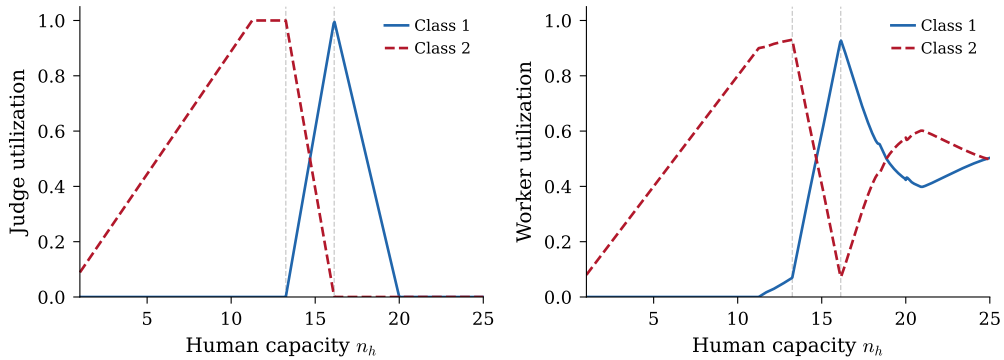


**Figure 3** Two-class judge allocation as  $n_h$  varies. Class 1:  $(\beta_1^{(I)}, \beta_1^{(II)}) = (0.05, 0.40)$  (lenient judge); Class 2:  $(\beta_2^{(I)}, \beta_2^{(II)}) = (0.15, 0.10)$  (strict judge). Class 2 has higher  $q_{\text{acc}}$  ( $k_q = 2$ , prioritized when humans are scarce), while Class 1 has lower  $\eta$  ( $k_\eta = 1$ , prioritized when workers are scarce). Priority reverses as  $n_h$  grows, with a complementarity zone where both classes share judge capacity. Other parameters:  $\lambda_i = 75$ ,  $(\mu_w, \mu_j, \mu_h) = (20, 30, 10)$ ,  $n_w = 10$ ,  $n_j = 6$ ,  $\alpha = 0.3$ .

In summary, optimal judge allocation in multi-class systems is governed by a simple structural principle: priority is determined by  $q_{\text{acc}}$  when humans are scarce and by  $\eta$  when workers are scarce. When these

two indices disagree on which class should be prioritized, the system must reverse its priority as operating conditions change, with a complementarity zone smoothing the transition. All thresholds are computable in closed form from system parameters (Proposition 3), enabling direct implementation.

## 5. Stochastic Control Policy

The steady-state analysis in Sections 3–4 characterizes optimal judge allocation and resource utilization for the fluid model. This section translates these insights into an implementable control policy for the stochastic  $n$ -system, establishing asymptotic optimality as the system scale grows.

### 5.1. The Fluid-Tracking Policy

The policy has two components: (i) an *inspection rule* that determines the probability of routing completed work to the judge, and (ii) an *admission rule* that regulates which tasks enter worker service. Both components are derived directly from the LP solution.

*Inspection rule.* Given an optimal solution  $(q_{w,i}^*, x_i^*, y_i^*, z_{i,d}^*, z_{i,j}^*, v_i^*)_{i \in \mathcal{I}}$  to the steady-state fluid LP (29), define the inspection rate for each class  $i$  as

$$\phi_i^* := v_i^*/x_i^* \quad \text{if } x_i^* > 0, \quad \phi_i^* := 0 \quad \text{if } x_i^* = 0. \quad (34)$$

Whenever an AI-Worker completes service on a class- $i$  task, route the output to the judge for screening with probability  $\phi_i^*$ ; otherwise, forward it directly to human review. This probabilistic routing ensures that the long-run fraction of class- $i$  outputs sent to the judge matches the fluid-optimal allocation  $v_i^*/x_i^*$ .

The inspection rate  $\phi_i^*$  encodes the trade-off identified in Section 4: higher  $\phi_i^*$  increases judge utilization and reduces human load through rejection filtering, but also increases Type I rework. The LP solution balances these effects optimally for each class.

*Admission rule.* Let  $Q_{w,i}^n(t)$  denote the number of class- $i$  tasks waiting in the work queue at time  $t$ , and let  $X_i^n(t)$  denote the number currently in AI-Worker service. When worker capacity becomes available, a class  $i$  is *admissible* at time  $t$  if

$$X_i^n(t^-) < n x_i^* \quad \text{and} \quad Q_{w,i}^n(t^-) > 0. \quad (35)$$

If multiple classes are admissible, select one according to any work-conserving rule (e.g., FCFS across classes, round-robin, or maximum queue deviation from target). The policy is work-conserving whenever  $\sum_i X_i^n(t^-) < n \sum_i x_i^*$  and  $\sum_i Q_{w,i}^n(t^-) > 0$ ; idling occurs only when all classes have reached their target in-service levels. The judge and human pools operate under work-conserving FCFS scheduling.

The threshold condition  $X_i^n(t) < n x_i^*$  is the key mechanism for achieving steady-state optimality. It prevents over-admission to any single class and ensures that worker capacity is reserved for rework traffic. Without this threshold, a naive policy might saturate workers with new arrivals, leaving no capacity for tasks that require reprocessing after judge rejection or human correction.

## 5.2. Asymptotic Optimality

We now establish that the Fluid-Tracking policy achieves the fluid-optimal throughput as the system scale grows. Let  $C_i^n(T)$  denote the cumulative number of class- $i$  tasks successfully completed (accepted by human reviewers) by time  $T$  in the  $n$ -system.

**THEOREM 2 (Asymptotic optimality).** *Let  $R^*$  denote the optimal value of the steady-state fluid LP (29), and let Assumption 1 hold. Under the Fluid-Tracking policy  $\pi^{n,*}$ :*

$$\liminf_{T \rightarrow \infty} \liminf_{n \rightarrow \infty} \frac{1}{nT} \mathbb{E}^{\pi^{n,*}} \left[ \sum_{i \in \mathcal{I}} r_i C_i^n(T) \right] = R^*. \quad (36)$$

The inner limit ( $n \rightarrow \infty$ ) invokes the fluid approximation on a fixed horizon  $[0, T]$ ; the outer limit ( $T \rightarrow \infty$ ) captures the long-run average. The proof follows the standard fluid-limit methodology: show that the stochastic system, when scaled by  $1/n$ , converges to the deterministic fluid model; then verify that the Fluid-Tracking policy drives the fluid trajectory to the optimal steady state. The threshold condition (35) ensures that binding capacity constraints are satisfied with equality in the limit, while the inspection rate (34) ensures optimal flow splitting between the judge and direct paths.

## 6. Extensions

The baseline model assumes that AI-Worker error rates remain constant and that AI capacities are exogenously fixed. This section relaxes both assumptions. Section 6.1 models how human feedback from rejected tasks improves the AI-Worker’s success probability on rework, altering the optimal routing policy. Section 6.2 treats AI-Worker and LLM-Judge capacities as decision variables subject to a budget constraint, enabling joint optimization of capacity allocation and operational control.

### 6.1. Human Feedback Improves Success Probability

When human review rejects a task, the accompanying feedback helps the AI-Worker improve upon rework. This section extends the baseline model to capture this learning effect. We proceed in four steps: (i) define the extended state space and flow dynamics, (ii) derive the steady-state LP for a single class, (iii) extend to multiple classes, and (iv) establish an asymptotically optimal control policy.

*Model setup.* We distinguish *fresh tasks*, which have failure rate  $\alpha$  and judge routing fraction  $\phi$ , from *feedback tasks*, which have reduced failure rate  $\kappa\alpha$  for some  $\kappa \in (0, 1)$  and routing fraction  $\phi_{fb}$ . Feedback tasks that fail a second time are removed from the system to ensure finite rework cycles, and judge-rejected tasks return to the fresh pool since no human feedback is received.

At the stochastic level, we duplicate all state processes for the two task types. For fresh tasks:  $Q_w^n(t)$  (work queue),  $X^n(t)$  (in worker service),  $Q_j^n(t)$  (judge queue),  $Y^n(t)$  (in judge service),  $Q_h^n(t)$  (human queue), and  $Z^n(t)$  (in human service). For feedback tasks, we use the subscript *fb*:  $Q_{w,fb}^n(t)$ ,  $X_{fb}^n(t)$ ,  $Q_{j,fb}^n(t)$ ,

$Y_{fb}^n(t)$ ,  $Q_{h,fb}^n(t)$ , and  $Z_{fb}^n(t)$ . Fresh tasks arrive exogenously and from judge rejections; feedback tasks arrive from human rejections of fresh tasks. At the fluid level, we use lowercase:  $(q_w, x, q_j, y, q_h, z)$  for fresh and  $(q_{w,fb}, x_{fb}, q_{j,fb}, y_{fb}, q_{h,fb}, z_{fb})$  for feedback. The judge-routed worker service levels are  $v := \phi x$  for fresh and  $v_{fb} := \phi_{fb} x_{fb}$  for feedback.

*Single-class steady-state LP.* The flow balance linking the two task types follows from the observation that feedback tasks are generated by human rejections of fresh tasks. Since  $p_{\text{pass}} = (1 - \alpha)(1 - \beta^{(I)}) + \alpha\beta^{(II)}$  and  $q_{\text{acc}} = (1 - \alpha)(1 - \beta^{(I)})/p_{\text{pass}}$ , we have  $p_{\text{pass}}(1 - q_{\text{acc}}) = p_{\text{pass}} - (1 - \alpha)(1 - \beta^{(I)}) = \alpha\beta^{(II)}$ . Using this identity, the feedback task service level satisfies  $x_{fb} = \alpha(x - (1 - \beta^{(II)})v)$ . The judge rejection probability for feedback tasks is  $p_{\text{rej},fb} := (1 - \kappa\alpha)\beta^{(I)} + \kappa\alpha(1 - \beta^{(II)})$ . Applying the same variable elimination as in Section 3, the steady-state LP becomes

$$\max_{x,v,x_{fb},v_{fb}} \mu_w \left[ (1 - \alpha)(x - \beta^{(I)}v) + (1 - \kappa\alpha)(x_{fb} - \beta^{(I)}v_{fb}) \right] \quad (37a)$$

$$\text{s.t. } x_{fb} = \alpha(x - (1 - \beta^{(II)})v), \quad 0 \leq v \leq x, \quad 0 \leq v_{fb} \leq x_{fb}, \quad (37b)$$

$$x + x_{fb} \leq n_w, \quad \frac{\mu_w}{\mu_j}(v + v_{fb}) \leq n_j, \quad (37c)$$

$$\frac{\mu_w}{\mu_h} \left[ (x - p_{\text{rej}}v) + (x_{fb} - p_{\text{rej},fb}v_{fb}) \right] \leq n_h. \quad (37d)$$

We next state two structural properties of LP (37). The first shows that feedback tasks do not build a steady-state queue at optimality. The second characterizes how scarce judge capacity is allocated between fresh and feedback tasks.

**PROPOSITION 4 (Feedback queue vanishes in steady state).** *In the feedback model (37), any optimal solution satisfies  $x_{fb}^* = \alpha(x^* - (1 - \beta^{(II)})v^*)$ ; that is, the feedback flow-balance constraint (37b) holds with equality, implying zero feedback-queue mass in steady state.*

The key point is that feedback arrivals are endogenous: feedback tasks are created only when humans reject fresh tasks. If a positive feedback queue formed in steady state, then some feedback tasks would abandon, reducing feedback throughput. Since the objective is strictly increasing in completed feedback tasks, any solution permitting such losses is suboptimal; the optimizer maintains  $q_{w,fb}^* = 0$ .

**PROPOSITION 5 (Judge priority under feedback).** *Consider the feedback model (37) with  $\kappa \in (0, 1)$  and  $q_{\text{acc}} > 1 - \alpha$ . Suppose the judge and human constraints bind while the worker constraint is slack ( $v^* + v_{fb}^* = J_{\text{eff}}, x^* + x_{fb}^* < n_w$ ). Then:*

(i) If

$$1 - \beta^{(II)} > (1 - \beta^{(I)} - \beta^{(II)})(\alpha^2\kappa + \alpha), \quad (38)$$

then fresh-first is optimal:  $v_{fb}^* > 0 \Rightarrow \phi^* = 1$ .

(ii) If the strict reverse of (38) holds, then feedback-first is optimal:  $v^* > 0 \Rightarrow \phi_{fb}^* = 1$ .

The intuition is as follows. The left-hand side of (38),  $1 - \beta^{(II)}$ , is the judge's probability of catching an incorrect output. The right-hand side has a concrete two-layer interpretation. The term  $(1 - \beta^{(I)} - \beta^{(II)}) = (1 - \beta^{(II)}) - \beta^{(I)}$  measures how informative a rejection decision is, because it is the excess probability of rejecting wrong outputs over mistakenly rejecting correct ones. The factor  $\alpha + \kappa\alpha^2 = \alpha(1 + \alpha\kappa)$  summarizes the strength of error propagation through the feedback loop: a fraction  $\alpha$  of fresh tasks are wrong, and feedback tasks are still wrong with probability  $\kappa\alpha$ , so the second-round error mass scales as  $\kappa\alpha^2$ .

When judge and human are both binding and worker capacity is slack, a marginal unit of judge capacity should be used where it reduces expected human workload the most. Condition (38) is both necessary and sufficient for fresh-first priority: when it holds, allocating judge capacity to fresh tasks yields a strictly larger net human-load reduction than allocating it to feedback tasks. When it fails (strict inequality reversed), the opposite is true: screening fresh tasks too aggressively reduces human rejections and thereby shrinks the supply of feedback tasks. In that regime, the optimal policy allocates judge capacity to feedback tasks first, letting some fresh tasks bypass the judge to generate feedback while using the judge to protect the human bottleneck from feedback errors.

Figure 4 illustrates these structural properties for  $\kappa = 0.5$ . The left panel decomposes judge utilization into the fresh and feedback components as  $n_h$  varies. It shows that the phase structure from the baseline model persists, but the two task types compete for the same judge capacity, so the composition of judge load matters. The right panel plots the optimal routing fractions ( $\phi^*, \phi_{fb}^*$ ) and provides a visual illustration of Proposition 5: when judge capacity saturates, fresh tasks keep full judge routing while feedback tasks begin to bypass the judge.

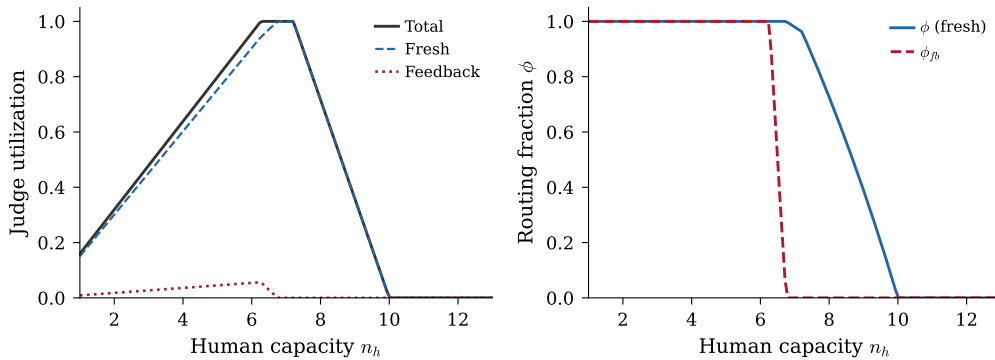


**Figure 4** Optimal judge routing with human feedback ( $\kappa = 0.5$ ). Left: judge utilization decomposed into fresh and feedback components as human capacity varies, showing that the baseline phase structure persists but composition changes due to resource competition. Right: routing fractions ( $\phi^*, \phi_{fb}^*$ ), illustrating that when judge capacity saturates, the system prioritizes fresh tasks.

*Multi-class steady-state LP.* The single-class analysis reveals two key structural properties: feedback queues vanish in steady state, and judge capacity prioritizes fresh tasks when judge and human are both binding and worker capacity is slack. We now generalize to multiple classes, where each class may have different feedback effectiveness.

We extend to multiple classes  $i \in \mathcal{I}$ , each with feedback effectiveness  $\kappa_i \in (0, 1)$ . The state processes are duplicated for fresh and feedback tasks within each class, following the single-class structure. Denoting the net completion rate of fresh and feedback tasks by  $T_i := (1 - \alpha_i)(x_i - \beta_i^{(I)} v_i)$  and  $T_{i,fb} := (1 - \kappa_i \alpha_i)(x_{i,fb} - \beta_i^{(I)} v_{i,fb})$ , the multi-class steady-state LP is:

$$\max_{\{x_i, v_i, x_{i,fb}, v_{i,fb}\}} \sum_{i \in \mathcal{I}} r_i \mu_{w,i} (T_i + T_{i,fb}) \quad (39a)$$

$$\text{s.t. } x_{i,fb} = \alpha_i (x_i - (1 - \beta_i^{(II)}) v_i), \quad 0 \leq v_i \leq x_i, \quad 0 \leq v_{i,fb} \leq x_{i,fb}, \quad \forall i \in \mathcal{I}, \quad (39b)$$

$$\sum_{i \in \mathcal{I}} (x_i + x_{i,fb}) \leq n_w, \quad \sum_{i \in \mathcal{I}} \frac{\mu_{w,i}}{\mu_{j,i}} (v_i + v_{i,fb}) \leq n_j, \quad (39c)$$

$$\sum_{i \in \mathcal{I}} \frac{\mu_{w,i}}{\mu_{h,i}} [(x_i - p_{\text{rej},i} v_i) + (x_{i,fb} - p_{\text{rej},i,fb} v_{i,fb})] \leq n_h. \quad (39d)$$

The structural insights from the single-class case extend naturally: within each class, feedback queues vanish in steady state, and judge capacity prioritizes fresh tasks over feedback tasks when judge and human are both binding and worker capacity is slack.

*Fluid-Tracking policy for feedback model.* We now translate the LP solution into an implementable stochastic control policy. Given an optimal solution  $(x_i^*, v_i^*, x_{i,fb}^*, v_{i,fb}^*)_{i \in \mathcal{I}}$  to LP (39), define the Fluid-Tracking policy  $\pi^{n,fb}$  as follows.

*Admission rule.* For each class  $i$ , define the aggregate worker threshold as  $n(x_i^* + x_{i,fb}^*)$ . A fresh task of class  $i$  is *admissible* at time  $t$  if

$$X_i^n(t^-) + X_{i,fb}^n(t^-) < n(x_i^* + x_{i,fb}^*) \quad \text{and} \quad Q_{w,i}^n(t^-) > 0.$$

A feedback task of class  $i$  is *admissible* if

$$X_i^n(t^-) + X_{i,fb}^n(t^-) < n(x_i^* + x_{i,fb}^*) \quad \text{and} \quad Q_{w,i,fb}^n(t^-) > 0.$$

When worker capacity becomes available, *feedback tasks have priority over fresh tasks*: among admissible tasks, admit feedback tasks first. This priority rule is consistent with Proposition 4: since  $q_{w,i,fb}^* = 0$  in the optimal fluid solution, the stochastic policy should ensure feedback tasks do not accumulate.

*Routing rule.* Define the inspection rates  $\phi_i^* := v_i^*/x_i^*$  for fresh tasks and  $\phi_{i,fb}^* := v_{i,fb}^*/x_{i,fb}^*$  for feedback tasks (with the convention  $0/0 := 0$ ). When a fresh task of class  $i$  completes worker service, route it to the judge with probability  $\phi_i^*$ ; otherwise route directly to human review. When a feedback task of class  $i$  completes worker service, route it to the judge with probability  $\phi_{i,fb}^*$ .

**THEOREM 3 (Asymptotic optimality under feedback).** Let  $R_{fb}^*$  denote the optimal value of LP (39), and let  $C_i^n(T)$  and  $C_{i,fb}^n(T)$  denote the cumulative completions of fresh and feedback tasks of class  $i$  by time  $T$ . Under the Fluid-Tracking policy  $\pi^{n,fb}$ :

$$\liminf_{T \rightarrow \infty} \liminf_{n \rightarrow \infty} \frac{1}{nT} \mathbb{E}^{\pi^{n,fb}} \left[ \sum_{i \in \mathcal{I}} r_i (C_i^n(T) + C_{i,fb}^n(T)) \right] = R_{fb}^*. \quad (40)$$

## 6.2. Capacity Planning for AI Resources

In practice, AI-Worker and LLM-Judge capacities are not fixed but can be scaled by allocating computational resources. This section studies the joint optimization of capacity allocation  $(n_w, n_j)$  and operational control  $(x_i, v_i)$  when the total AI resource budget  $\gamma_w n_w + \gamma_j n_j \leq B$  is constrained, where  $\gamma_w, \gamma_j > 0$  are unit costs and  $B > 0$  is the budget. Human capacity  $n_h$  is treated as fixed. Adding the budget constraint to the baseline LP yields:

$$\max_{n_w, n_j, \{x_i, v_i\}} \sum_{i \in \mathcal{I}} r_i \mu_{w,i} (1 - \alpha_i) (x_i - \beta_i^{(I)} v_i) \quad (41a)$$

$$\text{s.t. } \gamma_w n_w + \gamma_j n_j \leq B, \quad 0 \leq v_i \leq x_i \quad \forall i, \quad (41b)$$

$$\sum_i x_i \leq n_w, \quad \sum_i \frac{\mu_{w,i}}{\mu_{j,i}} v_i \leq n_j, \quad (41c)$$

$$\sum_i \frac{\mu_{w,i}}{\mu_{h,i}} (x_i - p_{\text{rej},i} v_i) \leq n_h. \quad (41d)$$

The key structural insight is that worker and judge capacities are coupled through the budget.

**PROPOSITION 6 (Worker-Judge coupling).** In LP (41) with  $q_{\text{acc},i} > 1 - \alpha_i$  for all  $i$ , if the human constraint binds, then there exists an optimal solution in which the worker and judge constraints are either both binding or both slack.

Intuitively, the budget constraint couples worker and judge capacities: spending more on one means spending less on the other. When humans are the bottleneck, the system invests in judge capacity to filter tasks and reduce human load; as humans become abundant, the system shifts budget from judges to workers to maximize throughput. Figure 5(a) illustrates this trade-off.

The right panel of Figure 5 demonstrates the value of capacity planning by comparing throughput against fixed allocation strategies. With capacity planning, throughput increases monotonically with  $n_h$  as the system dynamically reallocates budget from judges to workers. In contrast, fixed allocations perform well only in specific regimes: a balanced allocation  $(n_w, n_j) = (5, 5)$  works when humans are scarce but plateaus early; a worker-heavy allocation  $(7, 3)$  extends the range but still saturates; and a pure-worker allocation  $(10, 0)$  underperforms when humans are scarce (lacking filtering capability) but catches up when humans are abundant. Capacity planning dominates across all  $n_h$  by adapting the resource mix to the prevailing bottleneck.

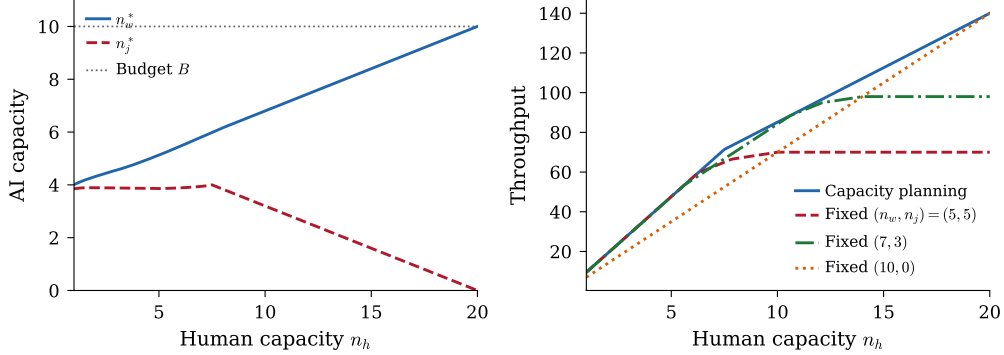


**Figure 5** Optimal capacity allocation and throughput comparison. (a) Capacity allocation: as  $n_h$  increases, budget shifts from judges to workers. (b) Throughput: capacity planning (solid blue) dominates fixed allocations across all  $n_h$  by adapting to the prevailing bottleneck. Parameters:  $B = 10$ ,  $(\beta_1^{(I)}, \beta_1^{(II)}) = (0.05, 0.40)$ ,  $(\beta_2^{(I)}, \beta_2^{(II)}) = (0.15, 0.10)$ ,  $\gamma_w = \gamma_j = 1$ .

For implementation, the capacity planning problem decouples into two stages: first solve LP (41) to obtain  $(n_w^*, n_j^*)$ , then apply the Fluid-Tracking policy from Section 5.1 with the planned capacities. We implement planned capacities as integers:  $n_w^n = \lfloor n \cdot n_w^* \rfloor$  and  $n_j^n = \lfloor n \cdot n_j^* \rfloor$ . This preserves feasibility of the fluid targets up to  $O(1)$  rounding error; stability is maintained by the admission control component of the Fluid-Tracking policy.

## 7. Numerical Experiments

This section validates the Fluid-Tracking policy through discrete-event simulation. We examine two aspects: (i) convergence to fluid-optimal throughput as system scale increases, and (ii) comparison with baseline policies that lack either admission control or optimal routing.

### 7.1. Asymptotic Optimality

We verify that the optimality gap between the Fluid-Tracking policy and the LP upper bound vanishes as the system scale  $n$  grows.

*Experimental setup.* We generate 20 random problem instances, each with 3–5 task classes. For each instance, the parameters are drawn independently: error rate  $\alpha_i \sim \text{Uniform}(0.20, 0.35)$ , Type I error  $\beta_i^{(I)} \sim \text{Uniform}(0.05, 0.15)$ , Type II error  $\beta_i^{(II)} \sim \text{Uniform}(0.10, 0.25)$ , service rates  $\mu_{w,i} \sim \text{Uniform}(18, 22)$ ,  $\mu_{j,i} \sim \text{Uniform}(28, 32)$ ,  $\mu_{h,i} \sim \text{Uniform}(9, 11)$ , arrival rate  $\lambda_i \sim \text{Uniform}(50, 70)$ , and abandonment rate  $\theta_i \sim \text{Uniform}(0.4, 0.6)$ . Base capacities are  $n_w \sim \text{Uniform}(4, 6)$ ,  $n_j \sim \text{Uniform}(2, 4)$ , and  $n_h \sim \text{Uniform}(5, 8)$ . Reward weights are  $r_i = 1$  for all classes. For each instance and scale factor  $n \in \{1, 2, 5, 10, 20, 50\}$ , we run 5 independent replications with different random seeds. Each replication simulates 500 time units with a 100-unit warmup period. We compute the optimality gap for each (instance, seed) pair and report the mean and standard deviation across all 100 runs at each scale  $n$ .

The optimality gap is defined as  $(R^* - R_{\text{sim}})/R^* \times 100\%$ , where  $R^*$  is the LP optimal value and  $R_{\text{sim}}$  is the simulated throughput.

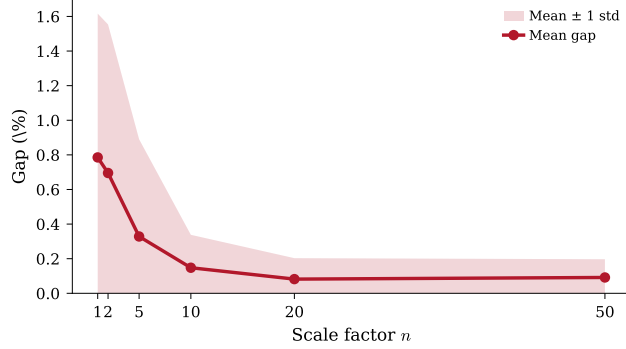


**Figure 6** Asymptotic optimality across 20 random instances ( $\times 5$  seeds each). The solid line shows the mean optimality gap, and the shaded band indicates  $\pm 1$  standard deviation. The gap decreases from 0.69% at  $n = 1$  to below 0.1% at  $n \geq 10$ , confirming convergence to fluid-optimal throughput.

*Results.* Figure 6 shows the optimality gap across all instances and seeds. The mean gap decreases from 0.69% at  $n = 1$  to below 0.1% for  $n \geq 10$ . The variance also decreases substantially: the standard deviation drops from 0.95% at  $n = 1$  to 0.08% at  $n = 50$ . This confirms the theoretical prediction that the Fluid-Tracking policy achieves asymptotic optimality. Even at the smallest scale ( $n = 1$ ), the mean gap remains below 1%, suggesting that the fluid-based policy provides reasonable guidance even for moderately sized systems. The small residual gap at large  $n$  reflects finite-horizon effects and discrete rounding in capacity allocation.

## 7.2. Policy Comparison

We compare the Fluid-Tracking policy against three baseline policies that represent common practical approaches. All baselines use greedy admission (admit any waiting task when capacity is available), but differ in routing:

- **Greedy + Optimal:** Uses the LP-optimal routing fractions  $\phi_i^*$ , but without admission control thresholds.
- **Greedy + Always-Judge:** Routes all tasks through the judge ( $\phi_i = 1$ ).
- **Greedy + Never-Judge:** Bypasses the judge entirely ( $\phi_i = 0$ ).

*Experimental setup.* We use the two-class instance from Section 4.2:  $\lambda_i = 75$ ,  $\alpha = 0.3$ ,  $(\beta_1^{(I)}, \beta_1^{(II)}) = (0.05, 0.40)$ ,  $(\beta_2^{(I)}, \beta_2^{(II)}) = (0.15, 0.10)$ ,  $(\mu_w, \mu_j, \mu_h) = (20, 30, 10)$ ,  $n_w = 10$ ,  $n_j = 6$ , and  $\theta_i = 0.5$ . Human capacity  $n_h$  varies from 3 to 22 to cover all four phases. The system is scaled by  $n = 10$ , and each configuration runs for 250 time units with a 50-unit warmup. We report the average over 3 seeds.

A policy is classified as *unstable* if the judge queue  $Q_j$  or human queue  $Q_h$  exhibits linear growth. Specifically, we fit a linear regression to the queue trajectory over the latter half of the simulation; if  $R^2 > 0.9$  and the slope exceeds 1.0 per unit time, the policy is deemed unstable. These thresholds are heuristic; qualitative conclusions are robust to moderate changes in the cutoff values.

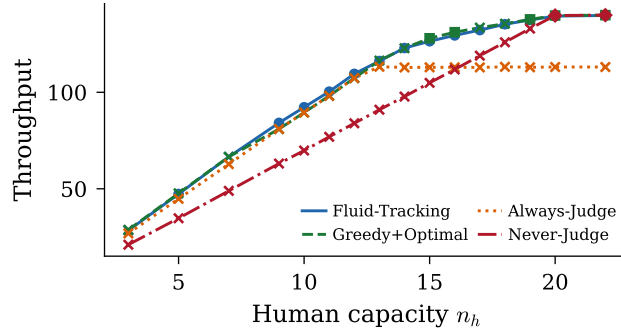


**Figure 7** Throughput comparison across policies. Circles indicate stable operation; crosses indicate instability (unbounded queue growth). Only Fluid-Tracking remains stable across all  $n_h$  values while achieving near-optimal throughput.

*Results: Throughput and stability.* Figure 7 compares throughput across policies as  $n_h$  varies. The Fluid-Tracking policy achieves the highest throughput and remains stable across all  $n_h$ . In contrast:

The Greedy + Optimal policy matches Fluid-Tracking throughput but is generically unstable across all values of  $n_h$ . Without admission control, it over-admits tasks, causing queues to grow unboundedly. This illustrates that optimal routing alone is insufficient; admission control is essential for stability.

The Always-Judge policy saturates at a lower throughput for  $n_h \geq 13$ . By routing all tasks through the judge, it creates a bottleneck at the judge queue, which grows without bound.

The Never-Judge policy performs poorly when humans are scarce ( $n_h < 10$ ) because it sends all worker outputs, including errors, directly to humans. As  $n_h$  increases, its throughput converges to the Fluid-Tracking level, since the optimal policy itself bypasses the judge when human capacity is abundant (Phase 4). However, greedy admission still causes instability at intermediate  $n_h$  values.

*Results: Queue trajectories.* Figure 8 shows queue trajectories at  $n_h = 14$ , a regime where human capacity is moderate. The Fluid-Tracking policy maintains bounded queues throughout the simulation, with both  $Q_j$  and  $Q_h$  fluctuating around low levels. All three baseline policies exhibit linear queue growth: Greedy + Optimal and Never-Judge cause human queue explosion, while Always-Judge causes judge queue explosion.

These trajectories illustrate the distinct failure modes. Greedy admission without thresholds admits tasks faster than the system can process them, leading to queue buildup at the downstream bottleneck. The routing choice determines *which* queue explodes: Always-Judge overloads the judge, while optimal routing and Never-Judge overload humans.

In summary, the Fluid-Tracking policy achieves near-optimal throughput with vanishing gap as scale increases, and both admission control and adaptive routing are necessary: policies using only one component fail to maintain stability across operating regimes.

## 8. Conclusion

The value of LLM-judge screening in AI-human workflows depends on which resource constrains the system, not on judge accuracy alone. This paper developed a framework for optimal judge allocation that

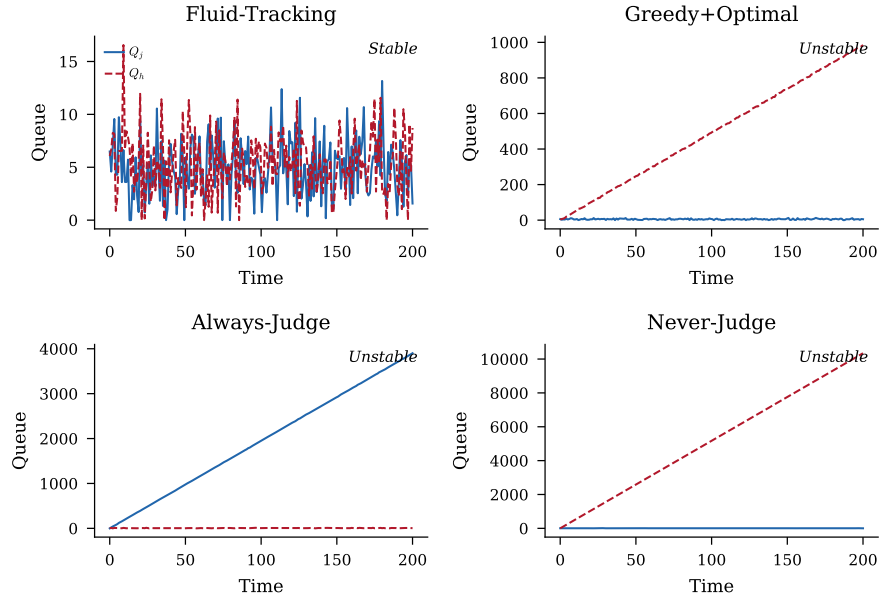


**Figure 8** Queue trajectories at  $n_h = 14$ . Fluid-Tracking maintains bounded queues; all baselines exhibit linear growth in either the judge queue ( $Q_j$ ) or human queue ( $Q_h$ ).

makes this precise: judge screening is neither universally beneficial nor universally harmful. When humans are scarce, screening amplifies their effective capacity. When workers are scarce, screening generates rework that crowds out new production. The closed-form thresholds we derive allow practitioners to determine which regime they operate in and to set routing policies accordingly.

The analysis reveals that optimal control of AI-human systems requires reasoning about feedback loops and capacity interactions, not just component-level accuracy metrics. A high-accuracy judge can reduce throughput if deployed in the wrong regime, while a moderate-accuracy judge can improve throughput if it relieves the binding constraint. This observation has broader implications for how organizations evaluate and deploy AI components: system-level performance depends on how components interact under resource constraints, not only on how each component performs in isolation.

Several directions remain open. First, extending the framework to *contextual routing*, where decisions condition on task-specific covariates rather than discrete classes, would enable finer-grained control, connecting to the contextual bandits literature. Second, allowing *heterogeneous resource pools*, where different agents have different error rates or specializations, would introduce assignment decisions alongside routing, potentially yielding richer structure when agent and task heterogeneity interact. Third, relaxing the binary quality model to *continuous quality scores* and the infallible human assumption to *imperfect human review* would create more realistic settings where screening stringency and cognitive load interact. Finally, modeling *learning judges* whose accuracy improves via operational feedback creates a joint learning-and-control problem, connecting to the growing literature on learning in service systems.

## References

- Adve VS, Nelson R (1994) The relationship between Bernoulli and fixed feedback policies for the M/G/1 queue. *Operations Research* 42(2):380–385.
- Ao R, Chen H, Gao S, Li H, Simchi-Levi D (2026) Best arm identification with LLM judges and limited human. URL <https://arxiv.org/abs/2601.21471>.
- Ata B (2006) Dynamic control of a multiclass queue with thin arrival streams. *Operations Research* 54(5):876–892.
- Atar R, Giat C, Shimkin N (2010) The  $c\mu/\theta$  rule for many-server queues with abandonment. *Operations Research* 58(5):1427–1439.
- Balakrishnan M, Ferreira KJ, Tong J (2026) Human-algorithm collaboration with private information: Naïve advice-weighting behavior and mitigation. *Management Science* 72(1):265–284.
- Bassamboo A, Randhawa RS (2010) On the accuracy of fluid models for capacity sizing in queueing systems with impatient customers. *Operations Research* 58(5):1398–1413.
- Bavaresco A, Bernardi R, Bertolazzi L, Elliott D, Fernández R, Gatt A, Ghaleb E, Giulianelli M, Hanna M, Koller A, et al. (2025) LLMs instead of human judges? a large scale empirical study across 20 NLP evaluation tasks. *Proceedings of the 63rd Annual Meeting of the Association for Computational Linguistics*, 238–255.
- Billingsley P (1999) *Convergence of Probability Measures* (Wiley).
- Chan CW, Yom-Tov G, Escobar G (2014) When to use speedup: An examination of service systems with returns. *Operations Research* 62(2):462–482.
- Chen D, Chen R, Zhang S, Liu Y, Wang Y, Zhou H, Zhang Q, Wan Y, Zhou P, Sun L (2024) MLLM-as-a-judge: Assessing multimodal LLM-as-a-judge with vision-language benchmark. *International Conference on Machine Learning (ICML)*, oral.
- Chen H, Harrison JM, Mandelbaum A, Van Ackere A, Wein LM (1988) Empirical evaluation of a queueing network model for semiconductor wafer fabrication. *Operations Research* 36(2):202–215.
- Dai JG (1995) On positive Harris recurrence of multiclass queueing networks: a unified approach via fluid limit models. *The Annals of Applied Probability* 5(1):49–77.
- Dai JG, Tezcan T (2011) State space collapse in many-server diffusion limits of parallel server systems. *Mathematics of Operations Research* 36(2):271–320.
- Dai T, Simchi-Levi D, Wu MX, Xie Y (2025) Assured autonomy: How operations research powers and orchestrates generative AI systems. URL <https://arxiv.org/abs/2512.23978>.
- Dong J, Feldman P, Yom-Tov GB (2015) Service systems with slowdowns: Potential failures and proposed solutions. *Operations Research* 63(2):305–324.
- Dong J, Hu Y, Wang S (2024) Value of sparse structures in dynamic reusable resource allocation with waiting. URL <http://dx.doi.org/10.2139/ssrn.4903557>, working paper.

- Fügener A, Grahl J, Gupta A, Ketter W (2022) Cognitive challenges in human–artificial intelligence collaboration: Investigating the path toward productive delegation. *Information Systems Research* 33(2):678–696.
- Fügener A, Walzner DD, Gupta A (2026) Roles of artificial intelligence in collaboration with humans: Automation, augmentation, and the future of work. *Management Science* 72(1):538–557.
- Furman E, Diamant A, Kristal M (2021) Customer acquisition and retention: A fluid approach for staffing. *Production and Operations Management* 30(11):4236–4257.
- Garipov R, Velikonitsev F, Ermakov I, Svirschevski R, Egiazarian V, Ryabinin M (2025) AutoJudge: Judge decoding without manual annotation. *Advances in Neural Information Processing Systems (NeurIPS)*.
- Goh YH, Li Z, Yan Z (2025) Strategic idling in appointment systems with sequential servers. *Manufacturing & Service Operations Management* 27(3):955–974.
- Greiner B, Grünwald P, Lindner T, Lintner G, Wiernsperger M (2026) Incentives, framing, and reliance on algorithmic advice: An experimental study. *Management Science* 72(1):302–322.
- Gu J, Jiang X, Shi Z, Tan H, Zhai X, Xu C, Li W, Shen Y, Ma S, Liu H, Wang S, Zhang K, Wang Y, Gao W, Ni L, Guo J (2024) A survey on LLM-as-a-judge. URL <https://arxiv.org/abs/2411.15594>.
- Guerdan L, Barocas S, Holstein K, Wallach H, Wu ZS, Chouldechova A (2025) Validating LLM-as-a-judge systems under rating indeterminacy. *Advances in Neural Information Processing Systems (NeurIPS)*.
- Gurvich I, Ward A (2014) On the dynamic control of matching queues. *Stochastic Systems* 4(2):479–523.
- Harrison JM, Zeevi A (2004) Dynamic scheduling of a multiclass queue in the Halfin-Whitt heavy traffic regime. *Operations Research* 52(2):243–257.
- Hu M, Zhang C (2023) The whiplash effect: Congestion dissipation in a disrupted circulatory system. URL <http://dx.doi.org/10.2139/ssrn.4429660>, minor revision at Management Science.
- Hu M, Zhou Y (2022) Dynamic type matching. *Manufacturing & Service Operations Management* 24(1):125–142.
- Ibrahim R (2018) Sharing delay information in service systems: a literature survey. *Queueing Systems* 89(1–2):49–79.
- Ibrahim R, Whitt W (2009) Real-time delay estimation in overloaded multiserver queues with abandonments. *Management Science* 55(10):1729–1742.
- Lee HW, Seo DW (1997) Design of a production system with a feedback buffer. *Queueing Systems* 26(1–2):187–202.
- Liu S, Gemp I, Marris L, Piliouras G, Heess N, Lanctot M (2025a) Re-evaluating open-ended evaluation of large language models. *International Conference on Learning Representations (ICLR)*.
- Liu Y, Liu P, Cohan A (2025b) On evaluating LLM alignment by evaluating LLMs as judges. *Advances in Neural Information Processing Systems (NeurIPS)*.
- Long Z, Shimkin N, Zhang H, Zhang J (2020) Dynamic scheduling of multiclass many-server queues with abandonment: the generalized  $c\mu/h$  rule. *Operations Research* 68(4):1218–1230.

- 
- Long Z, Zhang H, Zhang J, Zhang ZG (2024) The generalized  $c/\mu$  rule for queues with heterogeneous server pools. *Operations Research* 72(6):2488–2506.
- Lykouris T, Weng W (2024) Learning to defer in congested systems: The AI-human interplay. URL <https://arxiv.org/abs/2402.12237>.
- Puha AL, Ward AR (2019) Scheduling an overloaded multiclass many-server queue with impatient customers. *Tutorials in Operations Research* .
- Rafailov R, Sharma A, Mitchell E, Ermon S, Manning CD, Finn C (2023) Direct preference optimization: Your language model is secretly a reward model. *Advances in Neural Information Processing Systems (NeurIPS)*.
- So KC, Tang CS (1995) Optimal operating policy for a bottleneck with random rework. *Management Science* 41(4):620–636.
- Susarla A, Gopal R, Thatcher JB, Sarker S (2023) The Janus effect of generative AI: Charting the path for responsible conduct of scholarly activities in information systems. *Information Systems Research* 34(2):399–408.
- Tan S, Zhuang S, Montgomery K, Tang WY, Cuadron A, Wang C, Popa RA, Stoica I (2025) JudgeBench: A benchmark for evaluating LLM-based judges. *International Conference on Learning Representations (ICLR)*.
- Te’eni D, Yahav I, Zagalsky A, Schwartz D, Silverman G, Cohen D, Mann Y, Lewinsky D (2026) Reciprocal human-machine learning: A theory and an instantiation for the case of message classification. *Management Science* 72(1):167–192.
- Tong T, Wang F, Zhao Z, Chen M (2025) BadJudge: Backdoor vulnerabilities of LLM-as-a-judge. *International Conference on Learning Representations (ICLR)*.
- Wang H, Zhang Y, Lu T (2026) The power of disagreement: A field experiment to investigate human–algorithm collaboration in loan evaluations. *Management Science* 72(1):96–118.
- Wang Z, Yang L, Cui S, Ülkü S, Zhou YP (2023) Pooling agents for customer-intensive services. *Operations Research* 71(3):860–875.
- Whitt W (2006) Fluid models for multiserver queues with abandonments. *Operations Research* 54(1):37–54.
- Xu Y, Ruis L, Rocktäschel T, Kirk R (2025) Investigating non-transitivity in LLM-as-a-judge. *International Conference on Machine Learning (ICML)*, spotlight.
- Yang CL, Bauer K, Li X, Hinz O (2026) My advisor, her AI, and me: Evidence from a field experiment on human–AI collaboration and investment decisions. *Management Science* 72(1):242–264.
- Ye Z, Li X, Li Q, Ai Q, Zhou Y, Shen W, Yan D, Liu Y (2025) Learning LLM-as-a-judge for preference alignment. *International Conference on Learning Representations (ICLR)*.
- Yin J, Ngiam KY, Tan SSL, Teo HH (2025) Designing AI-based work processes: How the timing of AI advice affects diagnostic decision making. *Management Science* 71(11):9361–9383.
- Yom-Tov GB, Mandelbaum A (2014) Erlang-R: A time-varying queue with reentrant customers, in support of healthcare staffing. *Manufacturing & Service Operations Management* 16(2):283–299.

- Yuan W, Pang RY, Cho K, Li X, Sukhbaatar S, Xu J, Weston J (2024) Self-rewarding language models. *International Conference on Machine Learning (ICML)*.
- Zhang J (2013) Fluid models of many-server queues with abandonment. *Queueing Systems* 73(2):147–193.
- Zheng L, Chiang WL, Sheng Y, Zhuang S, Wu Z, Zhuang Y, Lin Z, Li Z, Li D, Xing EP, Zhang H, Gonzalez JE, Stoica I (2023) Judging LLM-as-a-judge with MT-Bench and Chatbot Arena. *Advances in Neural Information Processing Systems (NeurIPS)*, datasets and Benchmarks Track.
- Zhong H (2025) Optimal integration: Human, machine, and generative AI. *Management Science* .
- Zhou Y, Xu A, Wang P, Xiong C, Joty S (2025) Evaluating judges as evaluators: The JETTS benchmark of LLM-as-judges as test-time scaling evaluators. *International Conference on Machine Learning (ICML)*.
- Zhu L, Wang X, Wang X (2025) JudgeLM: Fine-tuned large language models are scalable judges. *International Conference on Learning Representations (ICLR)*, spotlight.

## Electronic Companion

### EC.1. Proofs of Main Results

#### EC.1.1. Proof of Theorem 1 (Fluid Limit)

*proof:* Fix  $T > 0$  and denote  $\bar{W}^n := W^n/n$  for any process  $W^n$ . The primitive counting processes are time-changed Poisson processes:

$$\begin{aligned} A_i^n(t) &= N_{a,i}(\lambda_i n t), & B_{w,i}^n(t) &= N_{b,i}\left(\int_0^t \theta_i Q_{w,i}^n(s) ds\right), \\ D_{w,i}^n(t) &= N_{d_w,i}\left(\int_0^t \mu_{w,i} X_i^n(s) ds\right), & D_{j,i}^n(t) &= N_{d_j,i}\left(\int_0^t \mu_{j,i} Y_i^n(s) ds\right), \\ D_{h,i}^n(t) &= N_{d_h,i}\left(\int_0^t \mu_{h,i}(Z_{i,d}^n(s) + Z_{i,j}^n(s)) ds\right), \end{aligned}$$

where  $\{N(\cdot)\}$  are independent unit-rate Poisson processes.

*Tightness.* Define the time-change functions  $\Lambda_{w,i}^n(t) := \int_0^t \mu_{w,i} X_i^n(s) ds$  and similarly for other service processes. The capacity constraints give  $\sum_i X_i^n(s) \leq n n_w$ ,  $\sum_i Y_i^n(s) \leq n n_j$ , and  $\sum_i (Z_{i,d}^n + Z_{i,j}^n)(s) \leq n n_h$ .

Hence

$$\frac{1}{n} \Lambda_{w,i}^n(t) \leq \mu_{w,i} n_w t, \quad \frac{1}{n} \Lambda_{j,i}^n(t) \leq \mu_{j,i} n_j t, \quad \frac{1}{n} \Lambda_{h,i}^n(t) \leq \mu_{h,i} n_h t.$$

For the abandonment time-change, since  $Q_{w,i}^n(s) \leq Q_{w,i}^n(0) + A_i^n(s)$ , we have  $\frac{1}{n} \int_0^t \theta_i Q_{w,i}^n(s) ds \leq \theta_i (t \bar{Q}_{w,i}^n(0) + t \bar{A}_i^n(t))$ . By the functional strong law of large numbers (FSLLN),  $\bar{A}_i^n(t) = N_{a,i}(\lambda_i n t)/n \rightarrow \lambda_i t$  uniformly on  $[0, T]$  almost surely. Combined with Assumption 1, the scaled time-changes are stochastically bounded on  $[0, T]$ .

For the scaled counting processes, since  $\Lambda_{w,i}^n(t) \leq \mu_{w,i} n n_w t$ , we have  $N_{d_w,i}(\Lambda_{w,i}^n(t))/n \leq N_{d_w,i}(\mu_{w,i} n n_w t)/n$ , and the latter is tight by FSLLN. The same bound applies to all other time-changed Poisson coordinates. The admission controls  $U_{\cdot,i}^n$  are nondecreasing with  $U_{w,i}^n(t) \leq Q_{w,i}^n(0) + A_i^n(t)$ , hence tight by monotonicity. By finite-dimensional tightness and the modulus-of-continuity criterion (Billingsley 1999, Theorem 13.2), the full vector  $\bar{X}^n$  is tight in  $\mathbb{D}([0, T], \mathbb{R}^d)$  under the  $J_1$  topology.

*Continuity of limits.* By Prohorov's theorem, extract a weakly convergent subsequence  $\bar{X}^{n_k} \Rightarrow \bar{X}$ . By the Skorokhod representation theorem, there exist versions of  $\bar{X}^{n_k}$  and  $\bar{X}$  defined on a common probability space such that  $\bar{X}^{n_k} \rightarrow \bar{X}$  almost surely in the  $J_1$  metric. Each coordinate of  $\bar{X}^n$  has jumps of size  $\pm 1/n$ . For any  $\epsilon > 0$ , the number of jumps exceeding  $\epsilon$  in  $\bar{X}^n$  is zero for  $n > 1/\epsilon$ . Hence the limit  $\bar{X}$  has no jumps exceeding  $\epsilon$  for any  $\epsilon > 0$ , implying  $\bar{X}$  is almost surely continuous.

*Identification of the limit.* For the arrival process, the FSLLN gives  $\bar{A}_i^n(t) \rightarrow \lambda_i t$  uniformly on compacts. For time-changed processes, if  $\bar{\Lambda}^n(t) \rightarrow \Lambda(t)$  uniformly on compacts with  $\Lambda$  continuous and strictly increasing, then  $N(n\bar{\Lambda}^n(\cdot))/n \rightarrow \Lambda(\cdot)$  uniformly on compacts by the continuous mapping theorem and FSLLN. Since  $\bar{X}_i^n \rightarrow x_i$  uniformly implies  $\frac{1}{n}\Lambda_{w,i}^n(t) = \int_0^t \mu_{w,i} \bar{X}_i^n(s) ds \rightarrow \int_0^t \mu_{w,i} x_i(s) ds$ , we obtain

$$\bar{D}_{w,i}^n(t) \rightarrow d_{w,i}(t) = \int_0^t \mu_{w,i} x_i(s) ds$$

uniformly on compacts. The same argument applies to  $\bar{D}_{j,i}^n$ ,  $\bar{D}_{h,i}^n$ , and  $\bar{B}_{w,i}^n$ . Taking limits in the flow-balance equations of the  $n$ -system yields (26)–(27). The capacity constraints (28) hold since  $\sum_i \bar{X}_i^n \leq n_w$ ,  $\sum_i \bar{Y}_i^n \leq n_j$ ,  $\sum_i (\bar{Z}_{i,d}^n + \bar{Z}_{i,j}^n) \leq n_h$  for all  $n$ , and weak inequalities are preserved under limits.

### EC.1.2. Proof of Lemma 1 (Single-Class Threshold Ordering)

Recall from (32):

$$n_h^{(1)} = \frac{\mu_w}{\mu_h} p_{\text{pass}} J_{\text{eff}}, \quad n_h^{(2)} = \frac{\mu_w}{\mu_h} (n_w - p_{\text{rej}} J_{\text{eff}}), \quad n_h^{(3)} = \frac{\mu_w}{\mu_h} n_w.$$

*Part (i): General ordering.* We prove  $n_h^{(1)} \leq n_h^{(2)} \leq n_h^{(3)}$  without any condition on  $J_{\text{eff}}$ .

For the first inequality  $n_h^{(1)} \leq n_h^{(2)}$ , we need to show

$$p_{\text{pass}} J_{\text{eff}} \leq n_w - p_{\text{rej}} J_{\text{eff}}.$$

Rearranging,

$$p_{\text{pass}} J_{\text{eff}} + p_{\text{rej}} J_{\text{eff}} \leq n_w \iff J_{\text{eff}} (p_{\text{pass}} + p_{\text{rej}}) \leq n_w.$$

Since  $p_{\text{pass}} + p_{\text{rej}} = 1$  (a task routed through the judge is either passed or rejected), this simplifies to  $J_{\text{eff}} \leq n_w$ , which always holds because  $J_{\text{eff}} = \min\{n_w, J\} \leq n_w$  by definition.

For the second inequality  $n_h^{(2)} \leq n_h^{(3)}$ , we need

$$n_w - p_{\text{rej}} J_{\text{eff}} \leq n_w \iff p_{\text{rej}} J_{\text{eff}} \geq 0.$$

Since  $p_{\text{rej}} \geq 0$  and  $J_{\text{eff}} \geq 0$ , this always holds. Therefore,  $n_h^{(1)} \leq n_h^{(2)} \leq n_h^{(3)}$  in general.

*Part (ii): Strict ordering under non-degeneracy.* Now assume  $J_{\text{eff}} < n_w$ . From Part (i),  $J_{\text{eff}} (p_{\text{pass}} + p_{\text{rej}}) = J_{\text{eff}} \leq n_w$ . Under  $J_{\text{eff}} < n_w$ , the inequality becomes strict, hence  $n_h^{(1)} < n_h^{(2)}$ . For the second inequality,  $n_h^{(2)} < n_h^{(3)}$  is equivalent to  $p_{\text{rej}} J_{\text{eff}} > 0$ . Under the standing assumption  $q_{\text{acc}} > 1 - \alpha$  (equivalently  $\beta^{(I)} + \beta^{(II)} < 1$ , which requires  $\alpha > 0$ ), we have  $p_{\text{rej}} \geq \alpha(1 - \beta^{(II)}) > 0$ . Moreover,  $J_{\text{eff}} < n_w$  with  $J_{\text{eff}} \geq 0$ ; we note that  $J_{\text{eff}} = 0$  is a degenerate case (no judge capacity) excluded by the four-phase analysis, so  $J_{\text{eff}} > 0$ . Therefore  $p_{\text{rej}} J_{\text{eff}} > 0$  and  $n_h^{(2)} < n_h^{(3)}$ .

### EC.1.3. Proof of Proposition 2

Specializing the reduced multi-class LP to  $I = 1$  yields the single-class 2D LP

$$\max_{x,v} x - \beta^{(I)}v \quad (\text{EC.1a})$$

$$\text{s.t. } 0 \leq v \leq x \leq n_w, \quad (\text{EC.1b})$$

$$v \leq \frac{\mu_j}{\mu_w} n_j, \quad (\text{EC.1c})$$

$$x - p_{\text{rej}}v \leq \frac{\mu_h}{\mu_w} n_h, \quad (\text{EC.1d})$$

$$x - \beta^{(I)}v \leq \frac{\lambda}{\mu_w(1-\alpha)}. \quad (\text{EC.1e})$$

Under the assumptions  $n_w \geq H + p_{\text{rej}}J$  and  $\frac{\lambda}{\mu_w(1-\alpha)} \geq n_w$ , we have  $x - \beta^{(I)}v \leq x \leq H + p_{\text{rej}}J \leq n_w \leq \frac{\lambda}{\mu_w(1-\alpha)}$  for every feasible  $(x, v)$  with binding human constraint, so both the worker constraint  $x \leq n_w$  and the arrival constraint (EC.1e) are slack. Dropping them, the LP (EC.1) reduces to

$$\begin{aligned} \max_{x,v} \quad & x - \beta^{(I)}v \\ \text{s.t.} \quad & 0 \leq v \leq x, \quad v \leq J, \quad x - p_{\text{rej}}v \leq H. \end{aligned}$$

Fix any  $v \in [0, J]$ . Since the objective is increasing in  $x$ , the optimal choice of  $x$  is the largest feasible one:

$$x(v) = H + p_{\text{rej}}v,$$

provided  $v \leq x(v)$ , which is equivalent to  $p_{\text{pass}}v \leq H$ , i.e.,  $v \leq H/p_{\text{pass}}$  (well-defined since  $q_{\text{acc}} > 1 - \alpha$  implies  $p_{\text{pass}} > 0$ ).

Therefore the problem reduces to a one-dimensional maximization over  $0 \leq v \leq \min\left\{J, \frac{H}{p_{\text{pass}}}\right\}$  of

$$x(v) - \beta^{(I)}v = H + (p_{\text{rej}} - \beta^{(I)})v.$$

Using  $q_{\text{acc}} = \frac{(1-\alpha)(1-\beta^{(I)})}{p_{\text{pass}}}$ , one checks the identity

$$p_{\text{rej}} - \beta^{(I)} = \frac{p_{\text{pass}}}{1-\alpha} (q_{\text{acc}} - (1-\alpha)),$$

so the objective is (strictly) increasing in  $v$  if  $q_{\text{acc}} > 1 - \alpha$ , (strictly) decreasing if  $q_{\text{acc}} < 1 - \alpha$ , and constant in  $v$  if  $q_{\text{acc}} = 1 - \alpha$ .

Hence:

- If  $q_{\text{acc}} > 1 - \alpha$ , the maximizer is  $v^* = \min\left\{J, \frac{H}{p_{\text{pass}}}\right\}$ .
  - If  $H \leq p_{\text{pass}}J$ , then  $v^* = H/p_{\text{pass}}$  and  $x^* = H + p_{\text{rej}}v^* = \frac{H}{p_{\text{pass}}}$ , hence  $\phi^* = \frac{v^*}{x^*} = 1$ .
  - Otherwise  $v^* = J$  and  $x^* = H + p_{\text{rej}}J$ , hence  $\phi^* = \frac{J}{H + p_{\text{rej}}J}$ .

- If  $q_{\text{acc}} < 1 - \alpha$ , the maximizer is  $v^* = 0$  and  $x^* = H$ , hence  $\phi^* = 0$ .
- If  $q_{\text{acc}} = 1 - \alpha$ , every  $v$  in the feasible interval attains the same objective value, and setting  $x^* = H + p_{\text{rej}}v^*$  yields a (generically) non-singleton optimal set.

This proves Proposition 2.

#### EC.1.4. Proof of Proposition 1

Assume  $\frac{\lambda}{\mu_w(1-\alpha)} \geq n_w$ , so constraint (EC.1e) is slack. Let

$$H := \frac{\mu_h}{\mu_w} n_h, \quad J := \frac{\mu_j}{\mu_w} n_j, \quad J_{\text{eff}} := \min\{n_w, J\}.$$

*Dual formulation.* Write the reduced 2D LP (EC.1a)–(EC.1e) in the standard form  $\max\{c^\top z : Az \leq b, z \geq 0\}$  with  $z = (x, v)$  and  $c = (1, -\beta^{(I)})$ . Let the dual variables  $(\eta, \nu_w, \nu_j, \nu_h, \nu_q) \geq 0$  correspond respectively to the constraints

$$v - x \leq 0, \quad x \leq n_w, \quad v \leq \frac{\mu_j}{\mu_w} n_j, \quad x - p_{\text{rej}}v \leq \frac{\mu_h}{\mu_w} n_h, \quad x - \beta^{(I)}v \leq \frac{\lambda}{\mu_w(1-\alpha)}.$$

Under the overloaded assumption (Assumption 2), constraint (EC.1e) is slack, so  $\nu_q = 0$  in any optimal dual solution.

*KKT conditions.* Since  $v \leq x \leq n_w$  (box constraint) and  $v \leq J$  (judge constraint), the effective bound is  $v \leq J_{\text{eff}} := \min\{n_w, J\}$ . Dropping the slack arrival constraint, the reduced LP is

$$\max_{x,v} x - \beta^{(I)}v \quad \text{s.t.} \quad v - x \leq 0, \quad x \leq n_w, \quad v \leq J_{\text{eff}}, \quad x - p_{\text{rej}}v \leq H, \quad x \geq 0, \quad v \geq 0.$$

Let  $(\eta, \nu_w, \nu_j, \nu_h) \geq 0$  be multipliers for  $v - x \leq 0$ ,  $x \leq n_w$ ,  $v \leq J_{\text{eff}}$ , and  $x - p_{\text{rej}}v \leq H$ . Dual feasibility and complementary slackness are

$$\begin{aligned} -\eta + \nu_w + \nu_h &\geq 1, \\ \eta + \nu_j - p_{\text{rej}}\nu_h &\geq -\beta^{(I)}, \\ \eta(v - x) &= 0, \quad \nu_w(x - n_w) = 0, \quad \nu_j(v - J_{\text{eff}}) = 0, \quad \nu_h(x - p_{\text{rej}}v - H) = 0, \\ (-\eta + \nu_w + \nu_h - 1)x &= 0, \quad (\eta + \nu_j - p_{\text{rej}}\nu_h + \beta^{(I)})v = 0. \end{aligned}$$

*A sign identity.* Using  $q_{\text{acc}} = \frac{(1-\alpha)(1-\beta^{(I)})}{p_{\text{pass}}}$ , we have

$$p_{\text{rej}} - \beta^{(I)} = \frac{p_{\text{pass}}}{1-\alpha} (q_{\text{acc}} - (1-\alpha)),$$

so  $\text{sign}(q_{\text{acc}} - (1-\alpha)) = \text{sign}(p_{\text{rej}} - \beta^{(I)})$  whenever  $\alpha \in (0, 1)$  and  $p_{\text{pass}} > 0$ .

Case A:  $q_{\text{acc}} > 1 - \alpha$ . Then  $p_{\text{rej}} - \beta^{(I)} > 0$ .

If  $H \leq p_{\text{pass}} J_{\text{eff}}$ , set

$$x^* = v^* = \frac{H}{p_{\text{pass}}}, \quad v_h^* = \frac{1 - \beta^{(I)}}{p_{\text{pass}}}, \quad \eta^* = v_h^* - 1, \quad v_w^* = v_j^* = 0.$$

Note that  $\eta^* = (1 - \beta^{(I)} - p_{\text{pass}})/p_{\text{pass}} = \alpha(1 - \beta^{(I)} - \beta^{(II)})/p_{\text{pass}} > 0$ , since  $q_{\text{acc}} > 1 - \alpha$  implies  $\beta^{(I)} + \beta^{(II)} < 1$ .

If  $p_{\text{pass}} J_{\text{eff}} \leq H \leq n_w - p_{\text{rej}} J_{\text{eff}}$ , set

$$v^* = J_{\text{eff}}, \quad x^* = H + p_{\text{rej}} J_{\text{eff}}, \quad v_h^* = 1, \quad v_j^* = p_{\text{rej}} - \beta^{(I)}, \quad \eta^* = v_w^* = 0.$$

If  $n_w - p_{\text{rej}} J_{\text{eff}} \leq H \leq n_w$ , set

$$x^* = n_w, \quad v^* = \frac{n_w - H}{p_{\text{rej}}}, \quad v_h^* = \frac{\beta^{(I)}}{p_{\text{rej}}}, \quad v_w^* = 1 - v_h^*, \quad \eta^* = v_j^* = 0.$$

If  $H \geq n_w$ , set

$$(x^*, v^*) = (n_w, 0), \quad (v_w^*, \eta^*, v_h^*, v_j^*) = (1, 0, 0, 0).$$

In each subcase, direct substitution verifies KKT; hence  $(x^*, v^*)$  is optimal and  $\phi^* = v^*/x^*$  matches Proposition 1.

Case B:  $q_{\text{acc}} < 1 - \alpha$ . Then  $p_{\text{rej}} - \beta^{(I)} < 0$ . If  $H \leq n_w$ , set  $(x^*, v^*) = (H, 0)$  and  $(\eta^*, v_w^*, v_j^*, v_h^*) = (0, 0, 0, 1)$ . If  $H \geq n_w$ , set  $(x^*, v^*) = (n_w, 0)$  and  $(\eta^*, v_w^*, v_j^*, v_h^*) = (0, 1, 0, 0)$ . In both subcases, KKT holds, so  $\phi^* = 0$ .

Case C:  $q_{\text{acc}} = 1 - \alpha$ . Then  $p_{\text{rej}} = \beta^{(I)}$ . For  $H < n_w$ , any  $v \in [0, J_{\text{eff}}]$  with  $vp_{\text{pass}} \leq H$ ,  $H + p_{\text{rej}}v \leq n_w$ , and  $x = H + p_{\text{rej}}v$  is primal feasible (the box constraint  $v \leq x$  follows from  $x - v = H - p_{\text{pass}}v \geq 0$ ) and satisfies  $x - \beta^{(I)}v = H$ . The dual certificate  $(\eta^*, v_w^*, v_j^*, v_h^*) = (0, 0, 0, 1)$  is feasible with dual objective  $H$ , hence the optimal value is  $H$  by strong duality and the optimal set is non-singleton (non-unique  $\phi^*$ ). For  $H \geq n_w$ , the certificate  $(0, 1, 0, 0)$  yields  $(x^*, v^*) = (n_w, 0)$ .

### EC.1.5. Proof of Proposition 3

We proceed by reduction to two 2D linear programs and verify optimality via KKT conditions. Throughout, let

$$H = \frac{\mu_h}{\mu_w} n_h, \quad J_{\text{eff}} = \min\{n_w, J\}.$$

Define, for  $i \in \{1, 2\}$ ,

$$c_i := p_{\text{rej},i} - \beta_i^{(I)}.$$

By (3),

$$c_i = p_{\text{rej},i} - \beta_i^{(I)} = \frac{p_{\text{pass},i}}{1 - \alpha} (q_{\text{acc},i} - (1 - \alpha)),$$

so  $c_i > 0$  under the standing assumption  $q_{\text{acc},i} > 1 - \alpha$ .

*Reduction to  $v$ .* Under Assumption 3, the reduced LP is equivalent, up to a positive constant, to

$$\max_{x_1, x_2, v_1, v_2} (x_1 - \beta_1^{(I)} v_1) + (x_2 - \beta_2^{(I)} v_2)$$

subject to

$$0 \leq v_i \leq x_i, \quad i = 1, 2, \quad x_1 + x_2 \leq n_w, \quad v_1 + v_2 \leq J_{\text{eff}}, \quad (x_1 - p_{\text{rej},1} v_1) + (x_2 - p_{\text{rej},2} v_2) \leq H.$$

Fix any  $v = (v_1, v_2)$  with  $v \geq 0$  and  $v_1 + v_2 \leq J_{\text{eff}}$ . Consider the subproblem of maximizing over  $x = (x_1, x_2)$ :

$$\max_{x_1, x_2} (x_1 + x_2) \quad \text{s.t.} \quad x_i \geq v_i, \quad i = 1, 2, \quad x_1 + x_2 \leq n_w, \quad x_1 + x_2 \leq H + p_{\text{rej},1} v_1 + p_{\text{rej},2} v_2.$$

Since the objective is  $x_1 + x_2$ , the optimal value is

$$x_1 + x_2 = \min\{n_w, H + p_{\text{rej},1} v_1 + p_{\text{rej},2} v_2\}.$$

If the minimum is attained by the second term (so  $x_1 + x_2 < n_w$ ), then we may set  $x_1 + x_2 = H + p_{\text{rej},1} v_1 + p_{\text{rej},2} v_2$ . The feasibility conditions  $x \geq v$  reduce to  $x_1 + x_2 \geq v_1 + v_2$ , i.e.,

$$H + p_{\text{rej},1} v_1 + p_{\text{rej},2} v_2 \geq v_1 + v_2 \quad \iff \quad p_{\text{pass},1} v_1 + p_{\text{pass},2} v_2 \leq H.$$

If the minimum is attained by  $n_w$  (so  $x_1 + x_2 = n_w$ ), then the human constraint is equivalent to

$$n_w - (p_{\text{rej},1} v_1 + p_{\text{rej},2} v_2) \leq H \quad \iff \quad p_{\text{rej},1} v_1 + p_{\text{rej},2} v_2 \geq n_w - H.$$

In that case we may take any  $x$  with  $x_i \geq v_i$  and  $x_1 + x_2 = n_w$  (possible since  $v_1 + v_2 \leq J_{\text{eff}} \leq n_w$ ).

*Two reduced 2D problems.* We use the reduction derived above. If an optimal solution satisfies  $x_1^* + x_2^* < n_w$  (worker-slack), then necessarily the human constraint binds (otherwise one could increase  $x_1 + x_2$  without affecting  $v$ ), and feasibility of  $x \geq v$  is equivalent to  $p_{\text{pass},1} v_1 + p_{\text{pass},2} v_2 \leq H$ . In that regime, the problem reduces to the 2D LP

$$\max_{v_1, v_2} c_1 v_1 + c_2 v_2 \quad \text{s.t.} \quad v_1 \geq 0, \quad v_2 \geq 0, \quad v_1 + v_2 \leq J_{\text{eff}}, \quad p_{\text{pass},1} v_1 + p_{\text{pass},2} v_2 \leq H.$$

Introduce dual multipliers  $\lambda \geq 0$  and  $\mu \geq 0$  for the last two constraints. The Lagrangian is

$$L(v; \lambda, \mu) = c_1 v_1 + c_2 v_2 + \lambda(J_{\text{eff}} - v_1 - v_2) + \mu(H - p_{\text{pass},1} v_1 - p_{\text{pass},2} v_2).$$

For fixed  $(\lambda, \mu)$ , the supremum of  $L$  over  $v \geq 0$  is finite iff  $c_i - \lambda - \mu p_{\text{pass},i} \leq 0$  for  $i = 1, 2$ , in which case  $\sup_{v \geq 0} L(v; \lambda, \mu) = \lambda J_{\text{eff}} + \mu H$ . Thus the dual is

$$\min_{\lambda, \mu} \lambda J_{\text{eff}} + \mu H \quad \text{s.t.} \quad \lambda \geq 0, \quad \mu \geq 0, \quad \lambda + \mu p_{\text{pass},i} \geq c_i, \quad i = 1, 2.$$

Since both primal and dual are feasible, strong duality holds, and KKT conditions are necessary and sufficient. Equivalently,  $(v^*, \lambda^*, \mu^*)$  is optimal iff:

$$\begin{aligned} v^* &\geq 0, \quad v_1^* + v_2^* \leq J_{\text{eff}}, \quad p_{\text{pass},1}v_1^* + p_{\text{pass},2}v_2^* \leq H, \\ \lambda^*, \mu^* &\geq 0, \quad \lambda^* + \mu^* p_{\text{pass},i} \geq c_i, \quad i = 1, 2, \\ \lambda^*(v_1^* + v_2^* - J_{\text{eff}}) &= 0, \quad \mu^*(p_{\text{pass},1}v_1^* + p_{\text{pass},2}v_2^* - H) = 0, \\ v_i^*(\lambda^* + \mu^* p_{\text{pass},i} - c_i) &= 0, \quad i = 1, 2. \end{aligned}$$

*Human-scarce priority (explicit  $\underline{n}_h$ ).* Let  $k_q \in \arg \max_{i \in \{1,2\}} \frac{c_i}{p_{\text{pass},i}}$  (equivalently  $k_q \in \arg \max_i q_{\text{acc},i}$ ). Define the explicit threshold

$$\underline{n}_h := \frac{\mu_w}{\mu_h} p_{\text{pass},k_q} J_{\text{eff}}.$$

Assume  $n_h \leq \underline{n}_h$ , i.e.,  $H \leq p_{\text{pass},k_q} J_{\text{eff}}$ . Define

$$v_{k_q}^* = \frac{H}{p_{\text{pass},k_q}}, \quad v_\ell^* = 0, \quad \lambda^* = 0, \quad \mu^* = \frac{c_{k_q}}{p_{\text{pass},k_q}}, \quad (\ell = 3 - k_q).$$

Then  $v^* \geq 0$  and  $p_{\text{pass},1}v_1^* + p_{\text{pass},2}v_2^* = H$ , and  $v_1^* + v_2^* \leq J_{\text{eff}}$  holds by  $H \leq p_{\text{pass},k_q} J_{\text{eff}}$ . Also  $\lambda^*, \mu^* \geq 0$  and for  $\ell \neq k_q$ ,

$$\lambda^* + \mu^* p_{\text{pass},\ell} = \frac{c_{k_q}}{p_{\text{pass},k_q}} p_{\text{pass},\ell} \geq c_\ell \iff \frac{c_{k_q}}{p_{\text{pass},k_q}} \geq \frac{c_\ell}{p_{\text{pass},\ell}},$$

which holds by definition of  $k_q$ . All complementary slackness equalities hold by construction, hence KKT holds and  $v^*$  is optimal.

*Complementarity in the worker-slack reduced LP.* Let  $k_c \in \arg \max_{i \in \{1,2\}} c_i$ .

*Corner solution.* If  $H \geq p_{\text{pass},k_c} J_{\text{eff}}$ , set

$$v_{k_c}^* = J_{\text{eff}}, \quad v_\ell^* = 0, \quad \lambda^* = c_{k_c}, \quad \mu^* = 0.$$

Then  $v_1^* + v_2^* = J_{\text{eff}}$  and  $p_{\text{pass},1}v_1^* + p_{\text{pass},2}v_2^* = p_{\text{pass},k_c} J_{\text{eff}} \leq H$ . Dual feasibility holds since  $\lambda^* = \max_i c_i \geq c_i$  for each  $i$ . Complementary slackness holds ( $\lambda^* > 0$  implies the judge constraint is tight, and  $\mu^* = 0$ ). Thus KKT holds and  $v^*$  is optimal.

*Interior (complementarity) solution.* If  $p_{\text{pass},k_q} J_{\text{eff}} < H < p_{\text{pass},k_c} J_{\text{eff}}$  and  $k_q \neq k_c$ , define  $v^*$  as the unique solution to

$$v_1^* + v_2^* = J_{\text{eff}}, \quad p_{\text{pass},1}v_1^* + p_{\text{pass},2}v_2^* = H.$$

Explicitly, if  $p_{\text{pass},1} \neq p_{\text{pass},2}$ ,

$$v_1^* = \frac{H - p_{\text{pass},2} J_{\text{eff}}}{p_{\text{pass},1} - p_{\text{pass},2}}, \quad v_2^* = J_{\text{eff}} - v_1^*.$$

The inequalities  $p_{\text{pass},k_q} J_{\text{eff}} < H < p_{\text{pass},k_c} J_{\text{eff}}$  imply  $0 < v_1^* < J_{\text{eff}}$  and  $0 < v_2^* < J_{\text{eff}}$ . Now define  $(\lambda^*, \mu^*)$  as the unique solution to the two linear equations

$$\lambda^* + \mu^* p_{\text{pass},i} = c_i, \quad i = 1, 2.$$

Namely, if  $p_{\text{pass},1} \neq p_{\text{pass},2}$ ,

$$\mu^* = \frac{c_1 - c_2}{p_{\text{pass},1} - p_{\text{pass},2}}, \quad \lambda^* = c_1 - \mu^* p_{\text{pass},1}.$$

Then  $v_i^* > 0$  forces the reduced-cost equalities  $\lambda^* + \mu^* p_{\text{pass},i} - c_i = 0$  for both  $i$ . Since  $k_q \neq k_c$  and there are only two classes, we have  $c_{k_c} > c_{k_q}$  and, by definition of  $k_q$ ,  $c_{k_q}/p_{\text{pass},k_q} > c_{k_c}/p_{\text{pass},k_c}$ , implying  $p_{\text{pass},k_c} > p_{\text{pass},k_q}$ . Plugging into the explicit formulas yields  $\mu^* \geq 0$ , and

$$\lambda^* = \frac{c_{k_q} p_{\text{pass},k_c} - c_{k_c} p_{\text{pass},k_q}}{p_{\text{pass},k_c} - p_{\text{pass},k_q}} \geq 0$$

by  $c_{k_q}/p_{\text{pass},k_q} \geq c_{k_c}/p_{\text{pass},k_c}$ . Hence KKT holds and  $v^*$  is optimal, with  $v_1^* + v_2^* = J_{\text{eff}}$ . In particular, both classes receive strictly positive judge allocation.

In this case, setting

$$\bar{n}_h := \frac{\mu_w}{\mu_h} p_{\text{pass},k_c} J_{\text{eff}}$$

gives a closed-form upper threshold for which the complementarity interval is  $(\underline{n}_h, \bar{n}_h)$ . (When  $k_q \neq k_\eta$ , the condition  $k_q \neq k_c$  is equivalent to  $k_c = k_\eta$  since there are only two classes.)

If instead  $k_q = k_c$ , then the worker-slack reduced LP has no interior (complementarity) region; complementarity, when it occurs, arises in the worker-binding reduced LP below.

**LEMMA EC.1 (When workers must bind).** *If  $H \geq n_w - p_{\text{rej},k_c} J_{\text{eff}}$  and  $H < n_w$ , then every optimal solution satisfies  $x_1^* + x_2^* = n_w$ .*

*proof:* Suppose, to the contrary, that there is an optimal solution with  $x_1^* + x_2^* < n_w$ . Then by the reduction above, the corresponding  $v^*$  must be optimal for the worker-slack 2D LP, i.e., it maximizes  $c_1 v_1 + c_2 v_2$  subject to  $v_1 + v_2 \leq J_{\text{eff}}$  and  $p_{\text{pass},1} v_1 + p_{\text{pass},2} v_2 \leq H$ . Since  $H \geq n_w - p_{\text{rej},k_c} J_{\text{eff}} \geq p_{\text{pass},k_c} J_{\text{eff}}$  (because  $n_w \geq J_{\text{eff}}$ ), the human constraint is slack at  $v = J_{\text{eff}} e_{k_c}$ , and the worker-slack 2D LP reduces to maximizing  $c_1 v_1 + c_2 v_2$  over  $v \geq 0$  with  $v_1 + v_2 \leq J_{\text{eff}}$ . Hence there exists an optimal solution with  $v_{k_c}^* = J_{\text{eff}}$  and  $v_\ell^* = 0$ . But then

$$x_1^* + x_2^* = H + p_{\text{rej},k_c} J_{\text{eff}} \geq n_w,$$

contradicting  $x_1^* + x_2^* < n_w$ . Therefore every optimal solution must have  $x_1^* + x_2^* = n_w$ .

*Worker-binding reduced LP.* We now consider the case in which an optimal solution satisfies  $x_1^* + x_2^* = n_w$  (worker-binding). By the reduction above, the remaining feasibility condition is  $p_{\text{rej},1}v_1 + p_{\text{rej},2}v_2 \geq R$ , where we define  $R := n_w - H$ . In that regime, the  $v$ -subproblem reduces to the LP

$$\min_{v_1, v_2} \beta_1^{(I)} v_1 + \beta_2^{(I)} v_2 \quad \text{s.t.} \quad v_1 \geq 0, v_2 \geq 0, v_1 + v_2 \leq J_{\text{eff}}, p_{\text{rej},1}v_1 + p_{\text{rej},2}v_2 \geq R,$$

Introduce dual multipliers  $\lambda \geq 0$  for  $v_1 + v_2 \leq J_{\text{eff}}$  and  $\mu \geq 0$  for  $R - p_{\text{rej},1}v_1 - p_{\text{rej},2}v_2 \leq 0$ . The Lagrangian is

$$L(v; \lambda, \mu) = \beta_1^{(I)} v_1 + \beta_2^{(I)} v_2 + \lambda(v_1 + v_2 - J_{\text{eff}}) + \mu(R - p_{\text{rej},1}v_1 - p_{\text{rej},2}v_2).$$

For fixed  $(\lambda, \mu)$ , the infimum of  $L$  over  $v \geq 0$  is finite iff  $\beta_i^{(I)} + \lambda - \mu p_{\text{rej},i} \geq 0$  for  $i = 1, 2$ , in which case  $\inf_{v \geq 0} L(v; \lambda, \mu) = \mu R - \lambda J_{\text{eff}}$ . Thus the dual is

$$\max_{\lambda, \mu} \mu R - \lambda J_{\text{eff}} \quad \text{s.t.} \quad \lambda \geq 0, \mu \geq 0, \beta_i^{(I)} + \lambda - \mu p_{\text{rej},i} \geq 0, i = 1, 2.$$

Again, strong duality holds and KKT is necessary and sufficient. Equivalently,  $(v^*, \lambda^*, \mu^*)$  is optimal iff:

$$\begin{aligned} v^* &\geq 0, & v_1^* + v_2^* &\leq J_{\text{eff}}, & p_{\text{rej},1}v_1^* + p_{\text{rej},2}v_2^* &\geq R, \\ \lambda^*, \mu^* &\geq 0, & \beta_i^{(I)} + \lambda^* - \mu^* p_{\text{rej},i} &\geq 0, & i = 1, 2, \\ \lambda^*(v_1^* + v_2^* - J_{\text{eff}}) &= 0, & \mu^*(R - p_{\text{rej},1}v_1^* - p_{\text{rej},2}v_2^*) &= 0, \\ v_i^*(\beta_i^{(I)} + \lambda^* - \mu^* p_{\text{rej},i}) &= 0, & i = 1, 2. \end{aligned}$$

*Worker-scarce priority (explicit upper threshold in the worker-binding LP).* Let  $k_\eta \in \arg \min_{i \in \{1,2\}} \frac{\beta_i^{(I)}}{p_{\text{rej},i}}$  (equivalently  $k_\eta \in \arg \min_i \eta_i$ ). Define

$$\bar{n}_h^{(\text{wb})} := \frac{\mu_w}{\mu_h} (n_w - p_{\text{rej},k_\eta} J_{\text{eff}}).$$

Assume  $n_h \geq \bar{n}_h^{(\text{wb})}$ . If  $n_h \geq \frac{\mu_w}{\mu_h} n_w$ , then the judge is bypassed (see below) and  $v_\ell^* = 0$  holds trivially. Otherwise  $H < n_w$ . Since  $k_c$  maximizes  $c_i$  while  $k_\eta$  minimizes  $\eta_i = \beta_i^{(I)} / p_{\text{rej},i}$  (equivalently maximizes  $c_i / p_{\text{rej},i}$ ), we have  $p_{\text{rej},k_\eta} \leq p_{\text{rej},k_c}$  (indeed, if  $k_\eta \neq k_c$  then  $c_{k_c} > c_{k_\eta}$  and  $c_{k_c} / p_{\text{rej},k_c} \leq c_{k_\eta} / p_{\text{rej},k_\eta}$  imply  $p_{\text{rej},k_c} > p_{\text{rej},k_\eta}$ ), hence

$$H \geq n_w - p_{\text{rej},k_\eta} J_{\text{eff}} \implies H \geq n_w - p_{\text{rej},k_c} J_{\text{eff}}.$$

Therefore Lemma EC.1 implies the worker constraint binds, so  $0 < R \leq p_{\text{rej},k_\eta} J_{\text{eff}}$  and the worker-binding reduced LP applies. Define

$$v_{k_\eta}^* = \frac{R}{p_{\text{rej},k_\eta}}, \quad v_\ell^* = 0, \quad \lambda^* = 0, \quad \mu^* = \frac{\beta_{k_\eta}^{(I)}}{p_{\text{rej},k_\eta}}, \quad (\ell = 3 - k_\eta).$$

Then  $p_{\text{rej},1}v_1^* + p_{\text{rej},2}v_2^* = R$  and  $v_1^* + v_2^* \leq J_{\text{eff}}$  holds because  $R \leq p_{\text{rej},k_\eta} J_{\text{eff}}$ . Dual feasibility for  $\ell \neq k_\eta$  is

$$\beta_\ell^{(I)} - \mu^* p_{\text{rej},\ell} \geq 0 \iff \frac{\beta_\ell^{(I)}}{p_{\text{rej},\ell}} \geq \frac{\beta_{k_\eta}^{(I)}}{p_{\text{rej},k_\eta}},$$

which holds by definition of  $k_\eta$ . Complementary slackness holds ( $\mu^* > 0$  implies the rejection constraint is tight;  $\lambda^* = 0$ ). Thus KKT holds and  $v^*$  is optimal.

*Complementarity in the worker-binding reduced LP.* Assume  $k_q = k_c$  (and hence  $k_q \neq k_\eta$ ). Note that

$$\eta_i = \frac{\beta_i^{(I)}}{p_{\text{rej},i}} = 1 - \frac{c_i}{p_{\text{rej},i}},$$

so  $k_\eta$  maximizes  $c_i/p_{\text{rej},i}$ . With only two classes and  $k_q = k_c \neq k_\eta$ , we have  $c_{k_q} > c_{k_\eta}$  and  $c_{k_q}/p_{\text{rej},k_q} < c_{k_\eta}/p_{\text{rej},k_\eta}$ , which implies  $p_{\text{rej},k_q} > p_{\text{rej},k_\eta}$ . Hence the interval

$$p_{\text{rej},k_\eta} J_{\text{eff}} < R < p_{\text{rej},k_q} J_{\text{eff}}$$

is non-degenerate. For any such  $R$ , define  $v^*$  as the unique solution to

$$v_1^* + v_2^* = J_{\text{eff}}, \quad p_{\text{rej},1} v_1^* + p_{\text{rej},2} v_2^* = R.$$

If  $p_{\text{rej},1} \neq p_{\text{rej},2}$ , this gives

$$v_1^* = \frac{R - p_{\text{rej},2} J_{\text{eff}}}{p_{\text{rej},1} - p_{\text{rej},2}}, \quad v_2^* = J_{\text{eff}} - v_1^*,$$

and the inequalities  $p_{\text{rej},k_\eta} J_{\text{eff}} < R < p_{\text{rej},k_q} J_{\text{eff}}$  imply  $v_1^*, v_2^* > 0$ .

Now define  $(\lambda^*, \mu^*)$  as the unique solution to

$$\beta_i^{(I)} + \lambda^* = \mu^* p_{\text{rej},i}, \quad i = 1, 2.$$

Namely, if  $p_{\text{rej},1} \neq p_{\text{rej},2}$ ,

$$\mu^* = \frac{\beta_1^{(I)} - \beta_2^{(I)}}{p_{\text{rej},1} - p_{\text{rej},2}}, \quad \lambda^* = \mu^* p_{\text{rej},1} - \beta_1^{(I)}.$$

Then  $v_i^* > 0$  forces the reduced-cost equalities  $\beta_i^{(I)} + \lambda^* - \mu^* p_{\text{rej},i} = 0$  for both  $i$ . Let  $a := k_\eta$  and  $b := k_q$ ; since  $p_{\text{rej},b} > p_{\text{rej},a}$  and  $\beta_b^{(I)}/p_{\text{rej},b} \geq \beta_a^{(I)}/p_{\text{rej},a}$ , we have  $\beta_b^{(I)} p_{\text{rej},a} \geq \beta_a^{(I)} p_{\text{rej},b}$  and hence  $\mu^* = (\beta_b^{(I)} - \beta_a^{(I)})/(p_{\text{rej},b} - p_{\text{rej},a}) \geq 0$  and

$$\lambda^* = \frac{\beta_b^{(I)} p_{\text{rej},a} - \beta_a^{(I)} p_{\text{rej},b}}{p_{\text{rej},b} - p_{\text{rej},a}} \geq 0.$$

Thus KKT holds and  $v^*$  is optimal, with  $v_1^*, v_2^* > 0$  (complementarity). In terms of  $n_h$ , this gives a non-degenerate interval

$$I := \left( \frac{\mu_w}{\mu_h} (n_w - p_{\text{rej},k_q} J_{\text{eff}}), \frac{\mu_w}{\mu_h} (n_w - p_{\text{rej},k_\eta} J_{\text{eff}}) \right)$$

on which both classes receive strictly positive judge allocation.

*Conclusion (explicit thresholds).* Under the standing assumptions of Proposition 3 and  $k_q \neq k_\eta$ , there are only two possibilities: either  $k_q \neq k_c$  (in which case the worker-slack reduced LP has an interior region with complementarity), or  $k_q = k_c$  (in which case complementarity arises in the worker-binding reduced LP as above). In either case, the thresholds  $\underline{n}_h$  and  $\bar{n}_h$  admit closed-form expressions (given above), and there exists a non-degenerate interval  $I \subset (\underline{n}_h, \bar{n}_h)$  on which  $v_1^* > 0$  and  $v_2^* > 0$ .

*Judge bypass.* If  $n_h \geq \frac{\mu_w}{\mu_h} n_w$ , then  $H \geq n_w$  and hence  $R \leq 0$ . Taking  $v^* = (0, 0)$  is feasible, and since  $\beta_i^{(I)} \geq 0$  and  $v \geq 0$ , it is optimal to bypass the judge.

This completes the proof.

### EC.1.6. Proof of Theorem 2 (Asymptotic Optimality)

We first establish convergence of the fluid model under the Fluid-Tracking policy.

LEMMA EC.2. *There exists  $t_0$  such that  $x_i(t) \leq x_i^*$  for all  $t \geq t_0$  and  $i \in \mathcal{I}$ .*

*proof:* Suppose not. Then for some  $i$  and arbitrarily large  $t$ , we have  $x_i(t) > x_i^*$ . Pick such a  $t_1$  and let  $\tilde{t} = \sup\{t < t_1 : x_i(t) \leq x_i^*\}$ . By continuity,  $x_i(\tilde{t}) = x_i^*$  and  $x_i(t) > x_i^*$  for  $t \in (\tilde{t}, t_1]$ . When  $x_i(t) > x_i^*$ , admission is blocked, so  $\dot{x}_i(t) = -\mu_{w,i}x_i(t) < 0$ . Hence  $x_i(t_1) < x_i(\tilde{t}) = x_i^*$ , contradiction.

LEMMA EC.3. *For each  $i$  with  $q_{w,i}^* > 0$ , there exists  $t_i$  such that  $q_{w,i}(t) > 0$  for all  $t \geq t_i$ .*

*proof:* Suppose  $q_{w,i}(t) = 0$  for all  $t$ . The admission condition requires  $q_{w,i}(t) > 0$ , so admission is blocked. By Lemma EC.2,  $x_i(t) \leq x_i^*$  eventually. Since no admission occurs,  $\dot{x}_i(t) = -\mu_{w,i}x_i(t)$ , giving  $x_i(t) \rightarrow 0$ . But the queue receives arrivals at rate  $\lambda_i > 0$ , so  $q_{w,i}(t)$  must become positive, contradiction.

Now suppose  $q_{w,i}(\tilde{t}) = 0$  for some  $\tilde{t}$  after  $q_{w,i}$  becomes positive. By continuity, there exists an interval  $(\tilde{t} - \epsilon, \tilde{t})$  where  $q_{w,i}(t) > 0$  and decreasing. In this interval, if  $x_i(t) < x_i^*$ , admission is allowed and  $\dot{x}_i > 0$ ; by Lemma EC.2,  $x_i(t) \rightarrow x_i^*$ . Once  $x_i(t) = x_i^*$ , the admission rate equals the service rate  $\mu_{w,i}x_i^*$ . By the steady-state flow balance  $\lambda_i + (\text{rework}) = \mu_{w,i}x_i^* + \theta_i q_{w,i}^*$ , the queue dynamics become  $\dot{q}_{w,i}(t) = \theta_i(q_{w,i}^* - q_{w,i}(t)) > 0$  when  $q_{w,i}(t) < q_{w,i}^*$ , contradicting that  $q_{w,i}$  is decreasing.

LEMMA EC.4. *Under the Fluid-Tracking policy,  $x_i(t) \rightarrow x_i^*$  and  $q_{w,i}(t) \rightarrow q_{w,i}^*$  as  $t \rightarrow \infty$ .*

*proof:* By Lemma EC.3,  $q_{w,i}(t) > 0$  for  $t$  large. When  $q_{w,i}(t) > 0$  and  $x_i(t) < x_i^*$ , admission is allowed, so  $\dot{x}_i(t) > 0$ . Combined with Lemma EC.2, this forces  $x_i(t) \rightarrow x_i^*$ .

Once  $x_i(t) = x_i^*$ , the queue dynamics become

$$\dot{q}_{w,i}(t) = \theta_i(q_{w,i}^* - q_{w,i}(t)).$$

This linear ODE has solution  $q_{w,i}(t) - q_{w,i}^* = (q_{w,i}(t_0) - q_{w,i}^*)e^{-\theta_i(t-t_0)} \rightarrow 0$ .

*Proof of Theorem 2 Upper bound.* The fluid LP (29) is a relaxation: any admissible stochastic policy yields a fluid trajectory satisfying the capacity constraints (28). Hence the long-run average reward is bounded by  $R^*$ .

*Lower bound.* By Lemma EC.4, the fluid trajectory under the Fluid-Tracking policy converges to  $(x_i^*, q_{w,i}^*)$ . The reward rate converges to

$$\sum_{i \in \mathcal{I}} r_i \mu_{w,i} (1 - \alpha_i) (x_i^* - \beta_i^{(I)} v_i^*) = R^*.$$

Fix  $T > 0$  and define the total class- $i$  population in the  $n$ th system as

$$W_i^n(t) := Q_{w,i}^n(t) + X_i^n(t) + Q_{j,i}^n(t) + Y_i^n(t) + Q_{h,i,d}^n(t) + Z_{i,d}^n(t) + Q_{h,i,j}^n(t) + Z_{i,j}^n(t).$$

Summing the balance equations (17)–(24) cancels all internal routing terms and yields, for all  $t \geq 0$ ,

$$W_i^n(t) = W_i^n(0) + A_i^n(t) - B_{w,i}^n(t) - C_i^n(t). \quad (\text{EC.2})$$

Rearranging and taking expectations at time  $T$  gives

$$\begin{aligned} \frac{1}{nT} \mathbb{E}^{\pi^{n,*}}[C_i^n(T)] &= \frac{1}{nT} \mathbb{E}[A_i^n(T)] - \frac{1}{nT} \mathbb{E}[B_{w,i}^n(T)] + \frac{1}{nT} \mathbb{E}[W_i^n(0) - W_i^n(T)] \\ &= \lambda_i - \frac{1}{T} \mathbb{E} \left[ \int_0^T \theta_i \bar{Q}_{w,i}^n(s) ds \right] + \frac{1}{T} \mathbb{E}[\bar{W}_i^n(0) - \bar{W}_i^n(T)], \end{aligned} \quad (\text{EC.3})$$

where we used  $\mathbb{E}[A_i^n(T)] = \lambda_i^n T = n\lambda_i T$  and  $\mathbb{E}[B_{w,i}^n(T)] = \mathbb{E} \left[ \int_0^T \theta_i Q_{w,i}^n(s) ds \right]$  from the random time-change (10), and  $\bar{W}_i^n := W_i^n/n$ .

Let  $\{n_k\}$  be a subsequence such that

$$\frac{1}{n_k T} \mathbb{E}^{\pi^{n_k,*}} \left[ \sum_{i \in \mathcal{I}} r_i C_i^{n_k}(T) \right] \longrightarrow \liminf_{n \rightarrow \infty} \frac{1}{nT} \mathbb{E}^{\pi^{n,*}} \left[ \sum_{i \in \mathcal{I}} r_i C_i^n(T) \right].$$

By Theorem 1,  $\{\bar{X}^{n_k}\}$  is tight on  $[0, T]$ , hence along a further subsequence (not relabeled) we have  $\bar{X}^{n_k} \Rightarrow \bar{X}$  on  $[0, T]$ , where  $\bar{X}$  is a (continuous) fluid trajectory satisfying (26)–(27). In particular,  $\bar{Q}_{w,i}^{n_k}(\cdot) \Rightarrow q_{w,i}(\cdot)$  and  $\bar{W}_i^{n_k}(T) \Rightarrow w_i(T)$ , where

$$w_i(t) := q_{w,i}(t) + x_i(t) + q_{j,i}(t) + y_i(t) + q_{h,i,d}(t) + z_{i,d}(t) + q_{h,i,j}(t) + z_{i,j}(t).$$

Since  $C_i^n(T) \geq 0$  and  $\bar{W}_i^n(T) \geq 0$ , (EC.3) implies

$$\mathbb{E} \left[ \int_0^T \theta_i \bar{Q}_{w,i}^{n_k}(s) ds \right] \leq \lambda_i T + \mathbb{E}[\bar{W}_i^{n_k}(0)].$$

By the Skorokhod representation theorem, there exist versions of  $\bar{Q}_{w,i}^{n_k}$ ,  $q_{w,i}$ ,  $\bar{W}_i^{n_k}(T)$ , and  $w_i(T)$  defined on a common probability space such that  $\bar{Q}_{w,i}^{n_k} \rightarrow q_{w,i}$  almost surely uniformly on  $[0, T]$  and  $\bar{W}_i^{n_k}(T) \rightarrow w_i(T)$  almost surely, and therefore

$$\int_0^T \theta_i \bar{Q}_{w,i}^{n_k}(s) ds \rightarrow \int_0^T \theta_i q_{w,i}(s) ds, \quad \bar{W}_i^{n_k}(T) \rightarrow w_i(T), \quad \text{a.s.}$$

Taking limits in (EC.3) along the subsequence yields

$$\lim_{k \rightarrow \infty} \frac{1}{n_k T} \mathbb{E}^{\pi^{n_k,*}}[C_i^{n_k}(T)] = \lambda_i - \frac{1}{T} \int_0^T \theta_i q_{w,i}(s) ds + \frac{1}{T} (w_i(0) - w_i(T)). \quad (\text{EC.4})$$

Summing (EC.4) over  $i$  with weights  $r_i$  yields the corresponding identity for the total reward.

Finally, under the Fluid-Tracking policy, Lemma EC.4 gives  $q_{w,i}(t) \rightarrow q_{w,i}^*$  as  $t \rightarrow \infty$ , and the fluid trajectory remains bounded so  $w_i(T)$  stays finite; hence

$$\frac{1}{T} \int_0^T \theta_i q_{w,i}(s) ds \rightarrow \theta_i q_{w,i}^*, \quad \frac{w_i(0) - w_i(T)}{T} \rightarrow 0 \quad \text{as } T \rightarrow \infty.$$

Taking  $\liminf_{T \rightarrow \infty}$  on both sides and using that  $R^* = \sum_i r_i (\lambda_i - \theta_i q_{w,i}^*)$  by (29) completes the lower bound in (36).

### EC.1.7. Proof of Theorem 3 (Asymptotic Optimality under Feedback)

*proof:* For each  $i \in \mathcal{I}$  define

$$C_i^n(t) := S_{h, \rightarrow c, i}^n(t), \quad C_{i, fb}^n(t) := S_{h, fb, \rightarrow c, i}^n(t), \quad (\text{EC.5})$$

where  $S_{h, \rightarrow c, i}^n(t)$  and  $S_{h, fb, \rightarrow c, i}^n(t)$  are the cumulative numbers of human-accepted completions of fresh and feedback class- $i$  tasks by time  $t$  (aggregated over all paths into human service).

**LEMMA EC.5 (Time-averaged constraints).** Fix  $T > 0$ . Under any admissible policy define

$$\begin{aligned} \hat{x}_i^n(T) &:= \frac{1}{T} \int_0^T \frac{X_i^n(s)}{n} ds, & \hat{x}_{i, fb}^n(T) &:= \frac{1}{T} \int_0^T \frac{X_{i, fb}^n(s)}{n} ds, \\ \hat{v}_i^n(T) &:= \frac{1}{\mu_{w, i} T} \frac{S_{w \rightarrow j, i}^n(T)}{n}, & \hat{v}_{i, fb}^n(T) &:= \frac{1}{\mu_{w, i} T} \frac{S_{w \rightarrow j, i, fb}^n(T)}{n}. \end{aligned} \quad (\text{EC.6})$$

Let  $\hat{x}_{i, +}^n(T) := \hat{x}_i^n(T) + \hat{x}_{i, fb}^n(T)$ ,  $\hat{v}_{i, +}^n(T) := \hat{v}_i^n(T) + \hat{v}_{i, fb}^n(T)$ , and

$$\hat{h}_i^n(T) := (\hat{x}_i^n(T) - p_{\text{rej}, i} \hat{v}_i^n(T)) + (\hat{x}_{i, fb}^n(T) - p_{\text{rej}, i, fb} \hat{v}_{i, fb}^n(T)).$$

Then, for any subsequential limit point as  $n \rightarrow \infty$ ,

$$0 \leq v_i \leq x_i, \quad 0 \leq v_{i, fb} \leq x_{i, fb}. \quad (\text{EC.7})$$

Moreover, for all  $n$ ,

$$\sum_{i \in \mathcal{I}} \hat{x}_{i, +}^n(T) \leq \frac{n_w^n}{n}, \quad (\text{EC.8a})$$

$$\sum_{i \in \mathcal{I}} \frac{\mu_{w, i}}{\mu_{j, i}} \hat{v}_{i, +}^n(T) \leq \frac{n_j^n}{n}, \quad (\text{EC.8b})$$

$$\sum_{i \in \mathcal{I}} \frac{\mu_{w, i}}{\mu_{h, i}} \hat{h}_i^n(T) \leq \frac{n_h^n}{n}. \quad (\text{EC.8c})$$

Finally, defining

$$\hat{x}_{i, fb}^{n, \text{gen}}(T) := \alpha_i \left( \hat{x}_i^n(T) - (1 - \beta_i^{(II)}) \hat{v}_i^n(T) \right), \quad (\text{EC.9})$$

we have

$$0 \leq \hat{x}_{i, fb}^n(T) \leq \hat{x}_{i, fb}^{n, \text{gen}}(T). \quad (\text{EC.10})$$

*proof:* Fix  $i$ . We have  $0 \leq S_{w \rightarrow j, i}^n(T) \leq S_{w, i}^n(T)$  and the random time-change representation

$$S_{w, i}^n(T) = N_{w, i} \left( \int_0^T \mu_{w, i} X_i^n(s) ds \right),$$

where  $N_{w, i}$  is a unit-rate Poisson process. Hence,

$$0 \leq \hat{v}_i^n(T) \leq \frac{1}{\mu_{w, i} T} \frac{S_{w, i}^n(T)}{n} = \frac{1}{T} \int_0^T \frac{X_i^n(s)}{n} ds + o(1) = \hat{x}_i^n(T) + o(1),$$

and passing to a subsequential limit yields  $0 \leq v_i \leq x_i$ . The feedback-type inequality  $0 \leq v_{i,fb} \leq x_{i,fb}$  is identical. For all  $t \geq 0$ , the feedback network satisfies the pointwise capacity constraints

$$\begin{aligned} \sum_{i \in \mathcal{I}} (X_i^n(t) + X_{i,fb}^n(t)) &\leq n_w^n, \\ \sum_{i \in \mathcal{I}} (Y_i^n(t) + Y_{i,fb}^n(t)) &\leq n_j^n, \\ \sum_{i \in \mathcal{I}} (Z_i^n(t) + Z_{i,fb}^n(t)) &\leq n_h^n, \end{aligned} \tag{EC.11}$$

We now derive (EC.8a)–(EC.8c) line by line. Integrating the worker constraint in (EC.11) over  $[0, T]$ , dividing by  $nT$ , and using (EC.6) gives

$$\sum_{i \in \mathcal{I}} \hat{x}_{i,+}^n(T) = \frac{1}{T} \int_0^T \sum_{i \in \mathcal{I}} \frac{X_i^n(s) + X_{i,fb}^n(s)}{n} ds \leq \frac{n_w^n}{n},$$

which is (EC.8a). The judge and human constraints (EC.8b)–(EC.8c) follow by the same time-averaging argument applied to the second and third inequalities in (EC.11) (with the normalizations chosen so that all constraints are written in AI-Worker service units, matching the LP).

To justify (EC.10) without circularity, we compute the feedback-generation rate explicitly. Feedback tasks have no exogenous arrivals: they are created only when a *fresh* class- $i$  task is rejected by a human. In AI-Worker service units, fresh class- $i$  output is produced at rate  $\mu_{w,i}x_i$ , of which a fraction  $v_i/x_i$  is routed to the judge. Thus:

- **Direct-to-human fresh flow:** rate  $\mu_{w,i}(x_i - v_i)$ . Each such task is rejected by a human with probability  $\alpha_i$ , generating feedback at rate  $\mu_{w,i}\alpha_i(x_i - v_i)$ .
- **Judge-to-human fresh flow:** among the judge-routed fresh flow (rate  $\mu_{w,i}v_i$ ), only judge-accepted tasks reach humans; conditional on judge acceptance, a human rejection occurs with probability  $\alpha_i\beta_i^{(II)}/p_{\text{pass},i}$ , hence the feedback-generation rate contributed by this path equals

$$\mu_{w,i}v_i \cdot p_{\text{pass},i} \cdot \frac{\alpha_i\beta_i^{(II)}}{p_{\text{pass},i}} = \mu_{w,i}\alpha_i\beta_i^{(II)}v_i.$$

Summing the two contributions gives the total feedback-generation rate (in tasks/time)

$$\mu_{w,i}\alpha_i(x_i - v_i) + \mu_{w,i}\alpha_i\beta_i^{(II)}v_i = \mu_{w,i}\alpha_i(x_i - (1 - \beta_i^{(II)})v_i).$$

Dividing by  $\mu_{w,i}$  converts this to an AI-Worker *service level* upper bound, yielding the fluid balance inequality

$$x_{i,fb} \leq \alpha_i(x_i - (1 - \beta_i^{(II)})v_i),$$

and the corresponding time-averaged generation term (EC.9). Since feedback tasks may additionally be lost via worker-queue abandonment before entering AI-Worker service, the time-averaged feedback service level cannot exceed the time-averaged generation, which is exactly (EC.10).

**LEMMA EC.6 (Relaxed LP and reward bound).** Fix  $T > 0$ . Let  $(x_i, v_i, x_{i,fb}, v_{i,fb})$  be any subsequential limit point of  $(\hat{x}_i^n(T), \hat{v}_i^n(T), \hat{x}_{i,fb}^n(T), \hat{v}_{i,fb}^n(T))$  as  $n \rightarrow \infty$ . Then  $(x_i, v_i, x_{i,fb}, v_{i,fb})$  is feasible for the relaxed LP obtained from (39) by replacing the feedback flow-balance equality with the inequality

$$x_{i,fb} \leq \alpha_i(x_i - (1 - \beta_i^{(T)})v_i), \quad i \in \mathcal{I}. \quad (\text{EC.12})$$

Moreover,

$$\limsup_{n \rightarrow \infty} \frac{1}{nT} \mathbb{E} \left[ \sum_i r_i (C_i^n(T) + C_{i,fb}^n(T)) \right] \leq \sum_i r_i \mu_{w,i} \left[ (1 - \alpha_i)(x_i - \beta_i^{(T)}v_i) + (1 - \kappa_i \alpha_i)(x_{i,fb} - \beta_i^{(T)}v_{i,fb}) \right]. \quad (\text{EC.13})$$

*proof:* We establish feasibility and the reward bound in turn.

*Feasibility.* By Lemma EC.5, any subsequential limit point satisfies the box constraints (EC.7), the time-averaged capacity constraints (EC.8), and the feedback-generation inequality (EC.10). Taking  $n \rightarrow \infty$  along the subsequence yields feasibility of  $(x_i, v_i, x_{i,fb}, v_{i,fb})$  for the relaxed LP (EC.12) together with the remaining constraints in (39).

*Reward bound.* Fix  $i$  and  $T$ . A human-accepted completion of a *fresh* task of class  $i$  can occur only if the AI-Worker output is correct. Consider the two routing outcomes for each fresh worker completion:

- If it is routed directly to humans, then it can contribute at most one completion by time  $T$ , and only if it is correct. Since each fresh worker completion is routed either to the judge or to the direct human path, the number routed directly to humans by time  $T$  equals  $S_{w,i}^n(T) - S_{w \rightarrow j,i}^n(T)$ . Hence the expected number of such completions is bounded by  $(1 - \alpha_i) \mathbb{E}[S_{w,i}^n(T) - S_{w \rightarrow j,i}^n(T)]$ .
- If it is routed to the judge, then it can contribute at most one completion by time  $T$ , and only if it is correct *and* the judge does not falsely reject it. The probability of this event is  $(1 - \alpha_i)(1 - \beta_i^{(T)})$ . Hence the expected number of such completions is bounded by  $(1 - \alpha_i)(1 - \beta_i^{(T)}) \mathbb{E}[S_{w \rightarrow j,i}^n(T)]$ .

Adding the two bounds yields

$$\mathbb{E}[C_i^n(T)] \leq (1 - \alpha_i) \mathbb{E}[S_{w,i}^n(T)] - (1 - \alpha_i)\beta_i^{(T)} \mathbb{E}[S_{w \rightarrow j,i}^n(T)].$$

Dividing by  $nT$  and using the random time-change law of large numbers for  $S_{w,i}^n(T)$  together with (EC.6) yields

$$\limsup_{n \rightarrow \infty} \frac{1}{nT} \mathbb{E}[C_i^n(T)] \leq \mu_{w,i}(1 - \alpha_i)(x_i - \beta_i^{(T)}v_i).$$

The same argument applies to feedback tasks, replacing the fresh error rate  $\alpha_i$  by the feedback error rate  $\kappa_i \alpha_i$ , which yields

$$\limsup_{n \rightarrow \infty} \frac{1}{nT} \mathbb{E}[C_{i,fb}^n(T)] \leq \mu_{w,i}(1 - \kappa_i \alpha_i)(x_{i,fb} - \beta_i^{(T)}v_{i,fb}).$$

Summing over  $i$  and weighting by  $r_i$  yields (EC.13).

**LEMMA EC.7 (Relaxation is tight).** Let  $\widetilde{R}_{fb}^*$  be the optimal value of the relaxed LP (i.e., (39) with (EC.12) in place of the equality). Then  $\widetilde{R}_{fb}^* = R_{fb}^*$ .

*proof:* Clearly  $\widetilde{R}_{fb}^* \geq R_{fb}^*$ . We show that every optimal solution of the relaxed LP satisfies the feedback flow-balance with equality, hence is feasible for the original LP.

Suppose for contradiction that  $(x_i^*, v_i^*, x_{i,fb}^*, v_{i,fb}^*)$  is optimal for the relaxed LP with slack  $s_i := \alpha_i(x_i^* - (1 - \beta_i^{(II)})v_i^*) - x_{i,fb}^* > 0$  for some  $i$ . Since  $s_i > 0$  and  $x_{i,fb}^* \geq 0$ , we have  $\alpha_i > 0$  and  $x_i^* > 0$ .

*Case 1:*  $v_i^* < x_i^*$ . Choose  $\epsilon \in (0, \min\{s_i/(1 + \alpha_i), x_i^* - v_i^*\})$  and define

$$(\tilde{x}_i, \tilde{v}_i, \tilde{x}_{i,fb}, \tilde{v}_{i,fb}) := (x_i^* - \epsilon, v_i^*, x_{i,fb}^* + \epsilon, v_{i,fb}^*).$$

Since  $v_i$  and  $v_{i,fb}$  are unchanged, the judge constraint is unaffected. The worker load satisfies  $\tilde{x}_i + \tilde{x}_{i,fb} = x_i^* + x_{i,fb}^*$ , and the human load satisfies  $(\tilde{x}_i - p_{rej,i}\tilde{v}_i) + (\tilde{x}_{i,fb} - p_{rej,i,fb}\tilde{v}_{i,fb}) = (x_i^* - p_{rej,i}v_i^*) + (x_{i,fb}^* - p_{rej,i,fb}v_{i,fb}^*)$ , so both are preserved. The box constraints hold because  $\tilde{v}_i = v_i^* < x_i^* - \epsilon = \tilde{x}_i$  and  $\tilde{v}_{i,fb} = v_{i,fb}^* \leq x_{i,fb}^* < \tilde{x}_{i,fb}$ . The feedback inequality holds because  $\epsilon < s_i/(1 + \alpha_i)$  implies  $\tilde{x}_{i,fb} = x_{i,fb}^* + \epsilon \leq \alpha_i(\tilde{x}_i - (1 - \beta_i^{(II)})\tilde{v}_i)$ . The objective changes by  $r_i\mu_{w,i}[-(1 - \alpha_i) + (1 - \kappa_i\alpha_i)]\epsilon = r_i\mu_{w,i}\alpha_i(1 - \kappa_i)\epsilon > 0$ , contradicting optimality.

*Case 2:*  $v_i^* = x_i^*$ . Then  $s_i = \alpha_i\beta_i^{(II)}x_i^* - x_{i,fb}^* > 0$ , so  $\beta_i^{(II)} > 0$ . Let

$$A_i := (1 - \alpha_i)(1 - \beta_i^{(I)}) + \alpha_i\beta_i^{(II)} = 1 - p_{rej,i}, \quad B_i := (1 - \kappa_i\alpha_i)(1 - \beta_i^{(I)}) + \kappa_i\alpha_i\beta_i^{(II)} = 1 - p_{rej,i,fb}.$$

If  $\beta_i^{(I)} < 1$ , set  $\delta := \epsilon$  when  $B_i \leq A_i$  and  $\delta := (B_i/A_i)\epsilon$  when  $B_i > A_i$ , and define

$$(\tilde{x}_i, \tilde{v}_i, \tilde{x}_{i,fb}, \tilde{v}_{i,fb}) := (x_i^* - \delta, x_i^* - \delta, x_{i,fb}^* + \epsilon, v_{i,fb}^* + \epsilon).$$

Feasibility follows exactly as in Proposition 4 (Subcase 2a), applied componentwise to class  $i$ , and the objective change is  $\Delta = r_i\mu_{w,i}(1 - \beta_i^{(I)})\alpha_i(1 - \kappa_i)\epsilon > 0$  when  $B_i \leq A_i$ , and  $\Delta = r_i\mu_{w,i}(1 - \beta_i^{(I)})\alpha_i\beta_i^{(II)}(1 - \kappa_i)\epsilon/A_i > 0$  when  $B_i > A_i$ . If  $\beta_i^{(I)} = 1$ , the same argument as Proposition 4 (Subcase 2b) applies. In all subcases,  $\Delta > 0$ , contradicting optimality.

Hence  $s_i = 0$  for every  $i$ , so  $\widetilde{R}_{fb}^* = R_{fb}^*$ .

*Upper bound.* By Lemma EC.6, for each fixed  $T$ ,

$$\limsup_{n \rightarrow \infty} \frac{1}{nT} \mathbb{E} \left[ \sum_i r_i (C_i^n(T) + C_{i,fb}^n(T)) \right] \leq R_{fb}^*,$$

and therefore

$$\liminf_{T \rightarrow \infty} \liminf_{n \rightarrow \infty} \frac{1}{nT} \mathbb{E} \left[ \sum_i r_i (C_i^n(T) + C_{i,fb}^n(T)) \right] \leq R_{fb}^*. \quad (\text{EC.14})$$

**LEMMA EC.8 (Fluid convergence under feedback Fluid-Tracking).** Let  $(x_i(\cdot), x_{i,fb}(\cdot))$  be any feedback fluid limit under  $\pi^{n,fb}$ . Then, for each  $i \in \mathcal{I}$ ,

$$x_i(t) \rightarrow x_i^*, \quad x_{i,fb}(t) \rightarrow x_{i,fb}^*, \quad v_i(t) \rightarrow v_i^*, \quad v_{i,fb}(t) \rightarrow v_{i,fb}^*. \quad (\text{EC.15})$$

*proof:* Fix  $i$ . Under  $\pi^{n,fb}$ , each *fresh* class- $i$  worker completion is routed to the judge with probability  $\phi_i^* := v_i^*/x_i^*$  (and to the direct human path otherwise), and each *feedback* class- $i$  worker completion is routed to the judge with probability  $\phi_{i,fb}^* := v_{i,fb}^*/x_{i,fb}^*$  (with the convention  $0/0 := 0$ ). Equivalently, there exist i.i.d. Bernoulli routing indicators  $\{\xi_{i,k}\}_{k \geq 1}$  with  $\mathbb{P}(\xi_{i,k} = 1) = \phi_i^*$  and  $\{\xi_{i,fb,k}\}_{k \geq 1}$  with  $\mathbb{P}(\xi_{i,fb,k} = 1) = \phi_{i,fb}^*$  such that, for all  $t \geq 0$ ,

$$S_{w \rightarrow j,i}^n(t) = \sum_{k=1}^{S_{w,i}^n(t)} \xi_{i,k}, \quad S_{w \rightarrow j,i,fb}^n(t) = \sum_{k=1}^{S_{w,i,fb}^n(t)} \xi_{i,fb,k}.$$

By the strong law of large numbers for Bernoulli thinnings (applied to these random sums) and the fluid scaling, along any fluid-limit subsequence we have

$$v_i(t) = \phi_i^* x_i(t), \quad v_{i,fb}(t) = \phi_{i,fb}^* x_{i,fb}(t), \quad \text{for a.e. } t \geq 0.$$

Let  $x_i^+(t) := x_i(t) + x_{i,fb}(t)$  and  $x_i^{+,*} := x_i^* + x_{i,fb}^*$ . If  $x_i^+(t) > x_i^{+,*}$ , admissions are blocked and  $\dot{x}_i^+(t) = -\mu_{w,i} x_i^+(t) < 0$ . If  $x_i^+(t) < x_i^{+,*}$  and the class- $i$  worker queue is nonempty, admissions occur and  $\dot{x}_i^+(t) > 0$ . Hence  $x_i^+(t) \rightarrow x_i^{+,*}$ . To make the drift statement explicit, note that in any feedback fluid limit  $x_i^+(\cdot)$  satisfies a.e.

$$\dot{x}_i^+(t) = u_i^+(t) - \mu_{w,i} x_i^+(t),$$

where  $u_i^+(t)$  is the (fluid) admission rate of class- $i$  jobs into AI-Worker service (fresh plus feedback). Under the admission rule,  $u_i^+(t) = 0$  whenever  $x_i^+(t) \geq x_i^{+,*}$ , which yields  $\dot{x}_i^+(t) = -\mu_{w,i} x_i^+(t)$  on  $\{x_i^+(t) > x_i^{+,*}\}$ . When  $x_i^+(t) < x_i^{+,*}$  and the worker queue for class  $i$  is positive, the policy admits class- $i$  jobs whenever worker capacity becomes available, implying  $u_i^+(t) > \mu_{w,i} x_i^+(t)$  and hence  $\dot{x}_i^+(t) > 0$ . This yields a one-dimensional monotonicity/Lyapunov drift argument for  $|x_i^+(t) - x_i^{+,*}|$  and implies  $x_i^+(t) \rightarrow x_i^{+,*}$ .

Let  $q_{w,i,fb}(t)$  be the feedback worker-queue fluid mass. By Theorem 1 applied to the feedback state vector (the proof uses only the Poisson/exponential primitives and random time-change representations, hence extends verbatim to the duplicated feedback network), any fluid limit satisfies the corresponding mean-rate flow equations; in particular the feedback arrival rate equals the fresh human-rejection rate  $\mu_{w,i} \alpha_i(x_i(t) - (1 - \beta_i^{(II)})v_i(t))$  and the abandonment rate is  $\theta_i q_{w,i,fb}(t)$ . Hence the feedback-queue dynamics satisfy

$$\dot{q}_{w,i,fb}(t) = \mu_{w,i} \alpha_i(x_i(t) - (1 - \beta_i^{(II)})v_i(t)) - \mu_{w,i} x_{i,fb}(t) - \theta_i q_{w,i,fb}(t)$$

whenever  $q_{w,i,fb}(t) > 0$ . Under admission priority to feedback tasks, the equilibrium satisfies  $q_{w,i,fb}^* = 0$  and  $x_{i,fb}^* = \alpha_i(x_i^* - (1 - \beta_i^{(II)})v_i^*)$ . Together with  $x_i^+(t) \rightarrow x_i^{+,*}$ , this yields  $x_{i,fb}(t) \rightarrow x_{i,fb}^*$  and  $x_i(t) \rightarrow x_i^*$ , and thus  $v_i(t) \rightarrow v_i^*$  and  $v_{i,fb}(t) \rightarrow v_{i,fb}^*$ .

*Lower bound.* By Lemma EC.8, the feedback fluid reward rate converges to  $R_{fb}^*$ , i.e.,

$$\sum_i r_i \mu_{w,i} \left[ (1 - \alpha_i)(x_i(t) - \beta_i^{(I)} v_i(t)) + (1 - \kappa_i \alpha_i)(x_{i,fb}(t) - \beta_i^{(I)} v_{i,fb}(t)) \right] \rightarrow R_{fb}^*.$$

Applying Theorem 1 to the enlarged feedback state vector is valid: the feedback model preserves the same Poisson/exponential primitives and random time-change representations, with all  $fb$ -type processes being duplicates of the baseline ones, and the endogenous feedback generation being an internal flow count. Moreover, the routing rule is implemented by i.i.d. thinnings with fixed probabilities  $(\phi_i^*, \phi_{i,fb}^*)$ , which is compatible with the fluid-scaling law of large numbers. Using standard long-run averaging (Dai 1995),

$$\liminf_{T \rightarrow \infty} \liminf_{n \rightarrow \infty} \frac{1}{nT} \mathbb{E}^{\pi^{n,fb}} \left[ \sum_i r_i (C_i^n(T) + C_{i,fb}^n(T)) \right] \geq R_{fb}^*. \quad (\text{EC.16})$$

Combining (EC.14) and (EC.16) proves the theorem.

### EC.1.8. Proof of Proposition 5 (Judge Priority under Feedback)

*proof:* We work under the hypothesis that both the judge and human constraints bind while the worker constraint is slack. Since  $v + v_{fb} \leq x + x_{fb} < n_w$ , the judge constraint  $(\mu_w/\mu_j)(v + v_{fb}) \leq n_j$  can bind only when  $J := (\mu_j/\mu_w)n_j < n_w$ , so  $J_{\text{eff}} = J$ . Set  $H := (\mu_h/\mu_w)n_h$ .

*Step 1: Reduction to a single free variable.* Substitute the flow balance  $x_{fb} = \alpha(x - (1 - \beta^{(II)})v)$  into the objective (37a) and divide by the positive constant  $\mu_w$ . The reduced objective is  $Ax - Bv - Cv_{fb}$ , where

$$A := 1 - \kappa\alpha^2, \quad B := (1 - \alpha)\beta^{(I)} + (1 - \kappa\alpha)\alpha(1 - \beta^{(II)}), \quad C := (1 - \kappa\alpha)\beta^{(I)}.$$

(Here  $A = (1 - \alpha) + (1 - \kappa\alpha)\alpha$  is simplified by expanding and collecting terms.) On the face where the judge and human constraints bind, we have  $v = J - v_{fb}$  and the human constraint (37d) reads

$$(1 + \alpha)x - (p_{\text{rej}} + \alpha(1 - \beta^{(II)}))(J - v_{fb}) - p_{\text{rej},fb} v_{fb} = H.$$

Solving for  $x$  yields

$$x(v_{fb}) = \frac{H + (p_{\text{rej}} + \alpha(1 - \beta^{(II)}))J - \Delta_p v_{fb}}{1 + \alpha}, \quad (\text{EC.17})$$

where  $\Delta_p := p_{\text{rej}} - p_{\text{rej},fb} + \alpha(1 - \beta^{(II)})$ . To determine its sign, note that expanding the definitions of  $p_{\text{rej}}$  and  $p_{\text{rej},fb}$  gives

$$p_{\text{rej}} - p_{\text{rej},fb} = (1 - \kappa)\alpha(1 - \beta^{(I)} - \beta^{(II)}),$$

so that  $\Delta_p = \alpha[(1 - \kappa)(1 - \beta^{(I)} - \beta^{(II)}) + (1 - \beta^{(II)})]$ . Since  $q_{\text{acc}} > 1 - \alpha$  is equivalent to  $\beta^{(I)} + \beta^{(II)} < 1$  and  $\kappa < 1$ , both summands inside the brackets are strictly positive, hence  $\Delta_p > 0$ .

*Step 2: Sign of  $\gamma$ .* Substituting  $v = J - v_{fb}$  and  $x = x(v_{fb})$  from (EC.17) into  $Ax - Bv - Cv_{fb}$  yields

$$\text{Obj}(v_{fb}) = \text{const} + \gamma v_{fb}, \quad \gamma := B - C - \frac{A \Delta_p}{1 + \alpha}. \quad (\text{EC.18})$$

We now compute  $\gamma$  in closed form. First,

$$B - C = [(1 - \alpha) - (1 - \kappa\alpha)]\beta^{(I)} + (1 - \kappa\alpha)\alpha(1 - \beta^{(II)}) = \alpha(\kappa - 1)\beta^{(I)} + (1 - \kappa\alpha)\alpha(1 - \beta^{(II)}).$$

Combining with  $A = 1 - \kappa\alpha^2$  and clearing the denominator  $1 + \alpha$ , the numerator  $(1 + \alpha)\gamma$  equals

$$(1 + \alpha)[\alpha(\kappa - 1)\beta^{(I)} + (1 - \kappa\alpha)\alpha(1 - \beta^{(II)})] - (1 - \kappa\alpha^2)\alpha[(1 - \kappa)(1 - \beta^{(I)} - \beta^{(II)}) + (1 - \beta^{(II)})].$$

Collecting the  $(1 - \beta^{(II)})$  terms gives  $(1 + \alpha)(1 - \kappa\alpha)\alpha(1 - \beta^{(II)}) - (1 - \kappa\alpha^2)\alpha(1 - \beta^{(II)}) = \alpha^2(1 - \kappa)(1 - \beta^{(II)})$ , and the remaining terms are  $\alpha(\kappa - 1)[(1 + \alpha)\beta^{(I)} + (1 - \kappa\alpha^2)(1 - \beta^{(I)} - \beta^{(II)})]$  (using  $-(1 - \kappa) = \kappa - 1$  to factor). Writing  $1 - \kappa\alpha^2 = (1 - \alpha)(1 + \alpha) + \alpha^2(1 - \kappa)$ , expanding, and combining with the  $(1 - \beta^{(II)})$  contribution, one obtains

$$\gamma = \frac{\alpha(\kappa - 1)}{1 + \alpha} \left[ (1 - \beta^{(II)}) - (1 - \beta^{(I)} - \beta^{(II)})\alpha(1 + \alpha\kappa) \right]. \quad (\text{EC.19})$$

Since  $\alpha > 0$  and  $\kappa \in (0, 1)$ , the prefactor  $\alpha(\kappa - 1)/(1 + \alpha)$  is strictly negative. Condition (38) states precisely that the bracketed term is strictly positive. Hence  $\gamma < 0$ .

*Step 3: Perturbation argument.* Because  $\gamma < 0$ , the objective on the face defined by the binding judge and human constraints is strictly decreasing in  $v_{fb}$ . Let  $(x^*, v^*, v_{fb}^*)$  be an optimal solution with  $v_{fb}^* > 0$ . We show  $v^* = x^*$  by contradiction.

Suppose  $v^* < x^*$ . For  $\epsilon \in (0, v_{fb}^*]$ , define the perturbation

$$v'_{fb} := v_{fb}^* - \epsilon, \quad v' := v^* + \epsilon, \quad x' := x^* + \frac{\Delta_p}{1 + \alpha} \epsilon, \quad x'_{fb} := \alpha(x' - (1 - \beta^{(II)})v').$$

We verify that  $(x', v', x'_{fb}, v'_{fb})$  is feasible for all sufficiently small  $\epsilon > 0$ .

*Judge constraint:*  $v' + v'_{fb} = (v^* + \epsilon) + (v_{fb}^* - \epsilon) = v^* + v_{fb}^* = J$ .

*Human constraint:* By construction,  $x' = x(v'_{fb})$  as given by (EC.17), so the human constraint holds at equality.

*Flow balance:*  $x'_{fb}$  is defined via the flow balance, so (37b) holds.

*Box constraint  $v' \leq x'$ :* The condition  $v^* + \epsilon \leq x^* + (\Delta_p/(1 + \alpha))\epsilon$  rearranges to  $\epsilon(1 - \Delta_p/(1 + \alpha)) \leq x^* - v^*$ .

Since  $x^* - v^* > 0$ , this holds for all  $\epsilon > 0$  sufficiently small (if  $\Delta_p/(1 + \alpha) \geq 1$  it holds trivially).

*Box constraint  $v'_{fb} \leq x'_{fb}$ :* A direct computation yields

$$x'_{fb} - v'_{fb} = (x_{fb}^* - v_{fb}^*) + \frac{1 + \alpha\beta^{(II)} + \alpha^2(1 - \kappa)(1 - \beta^{(I)} - \beta^{(II)})}{1 + \alpha} \epsilon.$$

Since  $\beta^{(I)} + \beta^{(II)} < 1$  and  $\kappa < 1$ , the coefficient of  $\epsilon$  is strictly positive, so the gap  $x'_{fb} - v'_{fb}$  exceeds  $x_{fb}^* - v_{fb}^* \geq 0$ .

*Worker constraint:* Substituting the flow balance gives

$$x' + x'_{fb} = x^* + x_{fb}^* + (p_{\text{rej}} - p_{\text{rej},fb})\epsilon,$$

where  $p_{\text{rej}} - p_{\text{rej},fb} = (1 - \kappa)\alpha(1 - \beta^{(I)} - \beta^{(II)}) > 0$ . The worker load increases, but since  $x^* + x_{fb}^* < n_w$ , the constraint  $x' + x'_{fb} \leq n_w$  holds for  $\epsilon$  small enough.

*Nonnegativity:* Each of  $v'_{fb} \geq 0$ ,  $v' \geq 0$ ,  $x' \geq 0$  is immediate. For  $x'_{fb} \geq 0$ , note  $x' \geq v' \geq 0$  and  $1 - \beta^{(II)} \leq 1$ , so  $x' - (1 - \beta^{(II)})v' \geq 0$ .

The perturbed solution is therefore feasible, and the objective changes by  $\gamma(v'_{fb} - v_{fb}^*) = -\gamma\epsilon > 0$ , contradicting the optimality of  $(x^*, v^*, v_{fb}^*)$ . Hence  $v^* = x^*$  whenever  $v_{fb}^* > 0$ , i.e.,  $\phi^* = v^*/x^* = 1$ .

*Step 4: Converse (necessity and reverse direction).* From (EC.19), the sign of  $\gamma$  is determined entirely by the bracketed term, since the prefactor  $\alpha(\kappa - 1)/(1 + \alpha) < 0$  is fixed. Therefore:

- If (38) holds (bracket  $> 0$ ), then  $\gamma < 0$ , and Steps 2–3 show fresh-first is optimal.
- If (38) holds with equality (bracket  $= 0$ ), then  $\gamma = 0$ , and the objective is constant in  $v_{fb}$  on the binding face; neither fresh-first nor feedback-first is uniquely optimal.
- If the strict reverse of (38) holds (bracket  $< 0$ ), then  $\gamma > 0$ , and the objective is *strictly increasing* in  $v_{fb}$ . A symmetric perturbation argument applies: given an optimal solution with  $v^* > 0$ , define  $v' := v^* - \epsilon$ ,  $v'_{fb} := v_{fb}^* + \epsilon$ , and  $x' := x^* - \frac{\Delta_p}{1+\alpha}\epsilon$ ,  $x'_{fb} := \alpha(x' - (1 - \beta^{(II)})v')$ . Feasibility of this perturbation for small  $\epsilon > 0$  follows by the same verification as in Step 3 with all signs reversed (the worker load *decreases*, so the worker constraint remains slack; the gap  $x' - v' = x^* - v^* - \epsilon(1 - \Delta_p/(1 + \alpha))$  is nonnegative for  $\epsilon$  small since  $x^* - v^* > 0$  when  $v^* < x^*$ ). The objective changes by  $\gamma\epsilon > 0$ , contradicting optimality. Hence  $v_{fb}^* = x_{fb}^*$  (i.e.,  $\phi_{fb}^* = 1$ ) whenever  $v^* > 0$ : the optimal policy allocates judge capacity to feedback tasks before fresh tasks.

This establishes the “if and only if” characterization: condition (38) is both necessary and sufficient for fresh-first priority on the face where judge and human bind and worker is slack.

### EC.1.9. Proof of Proposition 4 (Feedback Queue Vanishes)

*proof:* Consider the relaxed formulation obtained from (37) by replacing the feedback flow-balance equality with the inequality

$$x_{fb} \leq \alpha(x - (1 - \beta^{(II)})v). \quad (\text{EC.20})$$

When feedback queue buildup is permitted, the flow balance becomes  $x_{fb} + (\theta/\mu_w)q_{w,fb} = \alpha(x - (1 - \beta^{(II)})v)$ , so the slack  $s := \alpha(x - (1 - \beta^{(II)})v) - x_{fb}$  satisfies  $q_{w,fb} = (\mu_w/\theta)s$ . Hence  $q_{w,fb}^* = 0$  if and only if (EC.20) binds at optimality.

Suppose for contradiction that  $(x^*, v^*, x_{fb}^*, v_{fb}^*)$  is optimal for the relaxed LP with slack  $s > 0$ . Since  $s > 0$  and  $x_{fb}^* \geq 0$ , we have  $\alpha(x^* - (1 - \beta^{(II)})v^*) \geq s > 0$ , which requires  $\alpha > 0$  and  $x^* > 0$ .

*Case 1:*  $v^* < x^*$ . Choose  $\epsilon > 0$  such that  $\epsilon < \min\{s/(1+\alpha), x^* - v^*\}$ . Define

$$(\tilde{x}, \tilde{v}, \tilde{x}_{fb}, \tilde{v}_{fb}) := (x^* - \epsilon, v^*, x_{fb}^* + \epsilon, v_{fb}^*).$$

Since  $v$  and  $v_{fb}$  are unchanged, the judge constraint is unaffected. The worker constraint satisfies  $\tilde{x} + \tilde{x}_{fb} = x^* + x_{fb}^*$ , and the human constraint satisfies  $(\tilde{x} - p_{rej}\tilde{v}) + (\tilde{x}_{fb} - p_{rej,fb}\tilde{v}_{fb}) = (x^* - p_{rej}v^*) + (x_{fb}^* - p_{rej,fb}v_{fb}^*)$ , so both are preserved. The box constraints hold because  $\tilde{v} = v^* < x^* - \epsilon = \tilde{x}$  and  $\tilde{v}_{fb} = v_{fb}^* \leq x_{fb}^* < \tilde{x}_{fb}$ . The feedback inequality holds because  $\epsilon < s/(1+\alpha)$  implies  $\tilde{x}_{fb} = x_{fb}^* + \epsilon \leq x_{fb}^* + s - \alpha\epsilon = \alpha(\tilde{x} - (1 - \beta^{(II)})\tilde{v})$ . Nonnegativity is immediate from  $\epsilon < x^* - v^* \leq x^*$ .

The objective change is

$$\mu_w \left[ -(1-\alpha) + (1-\kappa\alpha) \right] \epsilon = \mu_w \alpha (1-\kappa) \epsilon > 0,$$

where the strict positivity uses  $\alpha > 0$  and  $\kappa \in (0, 1)$  (a standing model assumption). This contradicts optimality.

*Case 2:*  $v^* = x^*$ . Then  $s = \alpha(x^* - (1 - \beta^{(II)})x^*) - x_{fb}^* = \alpha\beta^{(II)}x^* - x_{fb}^* > 0$ , so  $\beta^{(II)} > 0$ . Define

$$A := 1 - p_{rej} = (1 - \alpha)(1 - \beta^{(I)}) + \alpha\beta^{(II)}, \quad B := 1 - p_{rej,fb} = (1 - \kappa\alpha)(1 - \beta^{(I)}) + \kappa\alpha\beta^{(II)}.$$

Since  $\beta^{(II)} > 0$  and  $\alpha, \kappa\alpha \in (0, 1)$ , both  $A$  and  $B$  are strictly positive (each is a sum of two non-negative terms with the second strictly positive).

*Subcase 2a:*  $\beta^{(I)} < 1$ . Fix  $\epsilon > 0$  sufficiently small and set  $\delta := \epsilon$  if  $B \leq A$ , and  $\delta := (B/A)\epsilon$  if  $B > A$ . Define

$$(\tilde{x}, \tilde{v}, \tilde{x}_{fb}, \tilde{v}_{fb}) := (x^* - \delta, x^* - \delta, x_{fb}^* + \epsilon, v_{fb}^* + \epsilon).$$

We verify feasibility. If  $B \leq A$ , then  $\delta = \epsilon$ , the worker and judge loads are unchanged, and the human load changes by  $(\mu_w/\mu_h)(B - A)\epsilon \leq 0$ . If  $B > A$ , then  $\delta = (B/A)\epsilon > \epsilon$ , the human load change is  $(\mu_w/\mu_h)(-A\delta + B\epsilon) = 0$ , and the worker and judge loads each change by  $\epsilon - \delta < 0$ . In either case, all three resource constraints remain feasible. The box constraint  $\tilde{v} = \tilde{x}$  holds by construction. The constraint  $\tilde{v}_{fb} \leq \tilde{x}_{fb}$  holds because  $v_{fb}^* + \epsilon \leq x_{fb}^* + \epsilon$ . Nonnegativity of  $\tilde{x} = x^* - \delta > 0$  holds for  $\epsilon$  small enough (since  $x^* > 0$ ). The feedback inequality requires  $x_{fb}^* + \epsilon \leq \alpha\beta^{(II)}(x^* - \delta)$ , i.e.,  $\epsilon + \alpha\beta^{(II)}\delta \leq s$ , which holds for sufficiently small  $\epsilon$  since  $s > 0$  and  $\delta$  is proportional to  $\epsilon$ .

The objective change is

$$\Delta = \mu_w(1 - \beta^{(I)}) \left[ (1 - \kappa\alpha)\epsilon - (1 - \alpha)\delta \right].$$

In the subcase  $B \leq A$  (so  $\delta = \epsilon$ ):  $\Delta = \mu_w(1 - \beta^{(I)})\alpha(1 - \kappa)\epsilon > 0$ , using  $\alpha > 0$ ,  $\kappa < 1$ , and  $\beta^{(I)} < 1$ . In the subcase  $B > A$  (so  $\delta = (B/A)\epsilon$ ):

$$\Delta = \frac{\mu_w(1 - \beta^{(I)})}{A} \left[ (1 - \kappa\alpha)A - (1 - \alpha)B \right] \epsilon.$$

Expanding  $A$  and  $B$  yields  $(1 - \kappa\alpha)A - (1 - \alpha)B = \alpha\beta^{(II)}(1 - \kappa) > 0$ , so  $\Delta > 0$ . In either subcase,  $\Delta > 0$ , contradicting optimality.

*Subcase 2b:*  $\beta^{(I)} = 1$ . In this subcase,  $A = \alpha\beta^{(II)} > 0$ . Fix  $\delta > 0$  small enough that  $\delta \leq x^*$  and  $2A\delta \leq s$ , and define

$$(\tilde{x}, \tilde{v}, \tilde{x}_{fb}, \tilde{v}_{fb}) := (x^* - \delta, x^* - \delta, x_{fb}^* + A\delta, v_{fb}^*).$$

The human load changes by  $(\mu_w/\mu_h)(-A\delta + A\delta) = 0$ , so the human constraint is preserved. The worker load changes by  $A\delta - \delta = (A - 1)\delta = -p_{\text{rej}}\delta < 0$ , and the judge load changes by  $-\delta < 0$ ; both constraints remain feasible. The box constraints hold:  $\tilde{v} = \tilde{x}$  by construction, and  $\tilde{v}_{fb} = v_{fb}^* \leq x_{fb}^* < \tilde{x}_{fb}$ . The feedback inequality requires  $x_{fb}^* + A\delta \leq \alpha\beta^{(II)}(x^* - \delta) = A(x^* - \delta)$ , i.e.,  $2A\delta \leq Ax^* - x_{fb}^* = s$ , which holds by the choice of  $\delta$ . Nonnegativity holds for small  $\delta$  since  $x^* > 0$ .

Since  $\beta^{(I)} = 1$ , the fresh objective contribution is  $(1 - \alpha)(x - \beta^{(I)}v) = (1 - \alpha)(x - v) = 0$  at any point with  $v = x$ , so the objective change comes entirely from the feedback term  $(1 - \kappa\alpha)(x_{fb} - \beta^{(I)}v_{fb})$ . Because  $\tilde{v}_{fb} = v_{fb}^*$ , the change is

$$\Delta = \mu_w(1 - \kappa\alpha) \left[ (\tilde{x}_{fb} - \beta^{(I)}\tilde{v}_{fb}) - (x_{fb}^* - \beta^{(I)}v_{fb}^*) \right] = \mu_w(1 - \kappa\alpha) A\delta = \mu_w(1 - \kappa\alpha)\alpha\beta^{(II)}\delta > 0.$$

This contradicts optimality.

In both cases, the assumption  $s > 0$  leads to a contradiction. Therefore  $s^* = 0$ , which yields  $q_{w,fb}^* = 0$  and the flow balance  $x_{fb}^* = \alpha(x^* - (1 - \beta^{(II)})v^*)$  stated in LP (37).

### EC.1.10. Proof of Proposition 6 (Worker-Judge Coupling)

*proof:* Let  $(n_w, n_j, \{x_i, v_i\})$  be any optimal solution for (41) at which the human constraint binds. Since the objective depends only on  $(x_i, v_i)$  and not directly on  $(n_w, n_j)$ , we may modify the capacities while keeping  $(x_i, v_i)$  fixed, provided feasibility is preserved.

Define the *used* worker and judge capacities by

$$\hat{n}_w := \sum_i x_i, \quad \hat{n}_j := \sum_i \frac{\mu_{w,i}}{\mu_{j,i}} v_i.$$

Because  $(n_w, n_j, \{x_i, v_i\})$  is feasible, we have  $\hat{n}_w \leq n_w$  and  $\hat{n}_j \leq n_j$ . Hence

$$\gamma_w \hat{n}_w + \gamma_j \hat{n}_j \leq \gamma_w n_w + \gamma_j n_j \leq B,$$

so  $(\hat{n}_w, \hat{n}_j, \{x_i, v_i\})$  is also feasible for (41). It attains the same objective value, since  $(x_i, v_i)$  is unchanged.

By construction, the worker and judge constraints are both binding at this new optimal solution:

$$\sum_i x_i = \hat{n}_w, \quad \sum_i \frac{\mu_{w,i}}{\mu_{j,i}} v_i = \hat{n}_j.$$

Now suppose moreover that the budget is slack at the original optimal solution, i.e.,

$$\gamma_w n_w + \gamma_j n_j < B.$$

Choose any  $\epsilon_w, \epsilon_j > 0$  small enough that

$$\gamma_w(\hat{n}_w + \epsilon_w) + \gamma_j(\hat{n}_j + \epsilon_j) \leq B.$$

Then  $(\hat{n}_w + \epsilon_w, \hat{n}_j + \epsilon_j, \{x_i, v_i\})$  is feasible and has the same objective value as before, while now both capacity constraints are strict:

$$\sum_i x_i = \hat{n}_w < \hat{n}_w + \epsilon_w, \quad \sum_i \frac{\mu_{w,i}}{\mu_{j,i}} v_i = \hat{n}_j < \hat{n}_j + \epsilon_j.$$

Thus there exists an optimal solution in which both the worker and judge constraints are slack.

Therefore, if the human constraint binds, there exists an optimal solution in which the worker and judge constraints are either both binding or both slack.